AFML-TR-68-334
Part I

MECHANISMS OF DEGRADATION OF POLYMERIC THERMAL CONTROL COATINGS

Part I. Investigation On Degradation of Thermal Control Coating Materials

D. M. J. Compton
T. E. Firle
Gulf General Atomic Incorporated

J. T. Neu
General Dynamics Convair

TECHNICAL REPORT AFML-TR-68-334, PART I
January 1969

**Air Force Materials Laboratory
Air Force Systems Command
Wright-Patterson Air Force Base, Ohio 45433**

NOTICE

When Government drawings, specifications, or other data are used for any purpose other than in connection with a definitely related Government procurement operation, the United States Government thereby incurs no responsibility nor any obligation whatsoever; and the fact that the Government may have formulated, furnished, or in any way supplied the said drawings, specifications, or other data, is not to be regarded by implication or otherwise as in any manner licensing the holder or any other person or corporation, or conveying any rights or permission to manufacture, use, or sell any patented invention that may in any way be related thereto.

This document has been approved for public release and sale; its distribution is unlimited.

Copies of this report should not be returned unless return is required by security considerations, contractual obligations, or notice on a specific document.

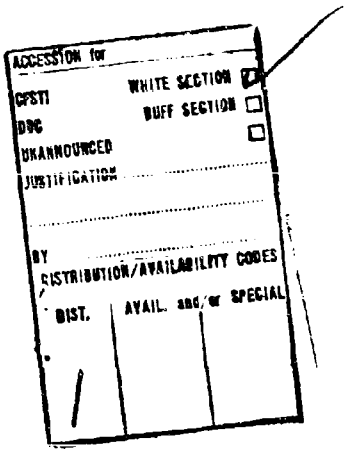

AFML-TR-68-334
Part I

MECHANISMS OF DEGRADATION OF POLYMERIC THERMAL CONTROL COATINGS

Part I. Investigation On Degradation Of Thermal Control Coating Materials

D. M. J. Compton
T. E. Firle
J. T. Neu

FOREWORD

This report was prepared by Gulf General Atomic, Incorporated, and the Space Sciences Laboratory of General Dynamics' Convair Division, under Air Force Contract F33615-67-C-1810. The contract was initiated under Project No. 7342, "Fundamental Research on Macromolecular Materials and Lubrication Phenomena," Task No. 734202, "Studies on the Structure-Property Relationship of Polymer Materials." The work was administered under the direction of the Elastomers and Coatings Branch, Nonmetallic Materials Division, Air Force Materials Laboratory, with Mr. C. P. Boebel serving as Project Engineer. This report describes work conducted between 1 June 1967 and 3 September 1968.

This report was released by the authors in October 1968 for publication as a Technical Report.

This technical report has been reviewed and is approved.

WARREN P. JOHNSON, Chief
Elastomers and Coatings Branch
Nonmetallic Materials Division
Air Force Materials Laboratory

ABSTRACT

Progress of an investigation on the mechanisms of degradiation of white pigments used in polymeric thermal control coatings by ultraviolet radiation is reported. The materials investigated were rutile (TiO_2) with different controlled impurity levels and surface treatments and high-purity strontium titanate ($SrTiO_3$). Apparatus combining a gas chromatograph with means for measuring optical reflectance and electrical conductivity enables samples of pigments to be investigated in a controlled environment. Changes in optical properties, produced by exposure to ultraviolet light, are correlated with gas evolution or adsorption. Some optical changes were correlated with gas evolution and electrical conductivity. The gas evolved in all cases was CO_2, with no O_2 being observed. Carbonaceous impurities found in these materials are believed to play a role in the damage process. Instrumentation and test techniques were developed, including a recently completed reflectometer of novel design.

A comparison was made between chemical reduction of various rutile pigments and the effects of uv light: Chemical reduction produces changes in optical and other properties that correlate with one of the two types of effects produced by uv light (reduction of reflectance near one micron) and the relative susceptibility of different pigments to chemical reductions similar to their relative susceptibility to uv degradation. Comparison with the effects of charged particle radiation is in progress. Also, a study of radiation effects and mechanisms of degradation of polymeric coatings pigmented with TiO_2 and $SrTiO_3$ is in progress.

CONTENTS

CONTENTS (cont'd)

FIGURES

FIGURES (cont'd)

FIGURES (cont'd)

FIGURES (cont'd)

TABLE

SECTION 1

INTRODUCTION

The objective of this program is to investigate the mechanisms by which polymeric thermal control coatings are degraded by the space environment, i.e., by exposure to ultraviolet (uv) light and charged particle irradiation in vacuum. One of the aims of the program is the development of a model for the damage process, both in microscopic terms, i.e., considering the nature and behavior of the defects formed in the pigment crystallites, and in parameter form, i.e., relating the effects produced on the observable parameters (reflectance, electrical conductivity, gas evolution, etc.) to dose, dose rate, and type of irradiation.

Such a model will be of great use in the correlation of data, providing a scientific framework for the interpretation of test results, indicating where further measurements are needed, making possible more reliable simulation procedures for the space environment, and leading to control of the damage mechanisms and thus improved performance. In addition, it will be useful in the prediction of the damage to be expected from types, energies, dose rates, and combinations of radiations other than those actually measured. These predictions will have a greater reliability for predicting performance than is now available. Previous work on damage mechanisms in rutile pgiments has been performed at Lockheed and is described in Ref. 1.

In the present program rutile was again studied since it would constitute a good pigment (high index of refraction) if the degradation in the space environment could be made less severe. In addition, strontium titanate was investigated. This material was chosen because many of its fundamental properties are known[2] and because it has good optical properties.

The basis of the present program is the use of a combined gas chromatograph—reflectance—electrical conductivity facility that enables measurements to be made on pigments in a controlled atmosphere. In addition, measurements of reflectance changes are made by the Convair Division of General Dynamics in-situ in a special reflectometer which enables irradiation to be performed with either uv or charged particles or both.

SECTION 2

SAMPLE PREPARATION

2.1 SOURCE MATERIALS

The materials studied in this program have been rutile (TiO_2) and strontium titanate ($SrTiO_3$), both in single crystal and powder form. The single crystals were from stock already at Gulf General Atomic, obtained from National Lead Company in the form of boules from which slices were cut and polished. Crystallographic orientation is accomplished by x-ray diffraction and impurity analysis by solid source mass spectrometry. Typical impurity levels for rutile crystals are: aluminum, 1.8 ppm; silicon, 4 ppm; chlorine, 1 ppm; and potassium, 0.3 ppm. The strontium titanate crystals were not analyzed.

Powder (pigmentary) rutile was obtained from a number of sources. A small sample of "very high purity" (99.9 percent) was obtained in England, having been manufactured by British Titan Products Ltd. The chief impurities found were chlorine (800 ppm) and silicon (270 ppm), with the chlorine presumably coming from the chloride process used. A 1-lb sample of high purity rutile made by a proprietary colloidal process was supplied at no cost by the W. R. Grace and Company, Research Division. A spectrographic analysis of this sample (experimental lot No. 5037-30A) showed 220 ppm silicon, 60 ppm aluminum, 100 ppm nickel, and 10 ppm magnesium. The specific surface area, determined using a BET method with nitrogen is ~1 m^2/g. X-ray diffraction analysis was carried out and showed the powder to be of rutile phase with a crystalline size greater than ~1150 Å, approaching the limit of this method using KCl for comparison. The appearance of this material is slightly off-white (yellow tinged) to the eye. This qualitative coloration does not change on heating to 100° to 125°C. Stabilized rutile pigments were obtained from several manufacturers. The one used in most of the work reported here was Ti-Pure, type R-910, produced by E. I. DuPont. This pigment (Lot 4392) was analyzed by emission spectroscopy and showed ~4000 ppm aluminum, 1000 ppm silicon, and 10 ppm magnesium. An additional analysis was made for carbon, in view of the possible importance of carbonaceous impurities in the oxygen loss process, and 87 ppm were found. A similar analysis of the W. R. Grace material showed 21 ppm of carbon. This is organic carbon (determined by total

oxidation and subtracting a value for the inorganic carbonate CO_2 released on acidification).

Strontium titanate pigment was also supplied at no cost by W. R. Grace. This material (experimental lot No. 5069-10) has particles 0.2 to 3μ in size and a surface area, determined by the BET method, of ~22 m^2/g. Principal impurities are silicon in the 1000-ppm range and lower concentrations of aluminum, barium, copper, iron, and magnesium. The material was not calcined.

2.2 REMOVAL OF CARBONACEOUS IMPURITIES

In some experiments, removal of carbonaceous material from the surface of the pigment was attempted. Simple heating in an oxygen stream causes sintering at temperatures below those at which oxidation of carbonaceous material occurs. Removal appears to occur as a result of exposure to uv light and oxygen gas flow at room temperature. Another technique that has been considered, but not yet tried, is exposure to oxygen in an atomic or excited form produced by a radio frequency discharge in oxygen at low pressure. This "plasma oxidation" has been found to remove graphite and similar materials at room temperature, and this should be useful as a treatment for pigments or even coatings.

2.3 QUARTZ DISPERSANT

To make if possible to vary flow conditions in the gas chromatograph, and to vary the degree of uv penetration throughout a powdered sample, quartz dispersant powder was prepared. The quartz was first crushed with a steel mortar and pestle and then further reduced with a ceramic mortar and pestle to an average of 70 mesh. Chemical cleaning was achieved in boiling HNO_3 followed by a distilled water rinse (10 times). The last water traces were evaporated, and the quartz powder was then kept in a clean container. This material appears to be a useful inert diluent.

2.4 METHODS OF PREPARING ADHERENT SAMPLES FROM POWDERS

Various methods were tried for the preparation of adherent discs, that can be handled, from powdered material. Compression in a hydraulic press, in a die usually used to prepare samples for infrared spectroscopy by compaction with KBr, proved successful. Some discoloration occurred, but this could be diminished by using an oxygen atmosphere, with slow compression. At the suggestion of Carl Boebel of AFML, water spraying was also tried. A suspension of TiO_2 in distilled water was sprayed through an atomizer

onto a metal plate maintained at ~120°C. For some pigments on some metal plates, this method works very well. For other pigments, it is very difficult to obtain dispersion in pure water, even using ultrasonic agitation, and it was also found difficult to obtain adherent coatings on the stainless steel discs used in the Convair in-situ reflectometer. Dispersion in alcohols or Freon was usually good, and these materials can be used at lower temperatures. Because of the possible effects of organic materials retained by the pigments, it was not desired to use detergent or other dispersive agents.

Several other methods of preparing layers were also tried. These included casting, i.e., allowing a slurry to dry, and hot dipping, i.e., warming a metal sample plate and dipping it into a slurry of the proper consistency. These methods produced reasonably coherent layers, but with a somewhat coarse surface appearance.

To obtain sufficient adhesion, the first samples run using the Convair in-situ reflectometer employed a binder, Sylvania's well-established PS-7 potassium silicate, used in a 50 percent mixture by weight. The material was applied by spraying and was allowed to cure at room temperature.

SECTION 3

EXPERIMENTAL APPARATUS

This section describes the apparatus developed and used for the present program. This apparatus consists of two facilities: 1. A combined facility at Gulf General Atomic for gas-chromatographic, optical, and electrical measurements on pigments enables measurement of their reactions and properties to be made while they are in a stream of ultrapure helium gas; this permits close control of their surface condition; 2. A facility at General Dynamics/Convair makes possible the irradiation in vacuum of coatings with combined uv light and particulate radiation, and the in-situ measurement of their reflectance properties without removal from the vacuum system.

3.1 GAS CHROMATOGRAPH

3.1.1 General Objectives

A gas chromatograph is used to identify and measure the gas or gases evolved when pigments are irradiated with uv light or charged particles. The powdered material is permeated by a flow of ultrapure helium gas, which is used as the carrier gas for the chromatograph. Electrical and optical measurements can be made on the sample while it is in the apparatus. The system can also be used to expose a sample to short-duration pulses of other gases, such as oxygen, so that the changes produced in the electrical and optical properties can be measured.

3.1.2 Apparatus

The gas chromatograph apparatus is shown schematically in Figure 1. The basic instrument is a Loenco Model 15, with interchangeable columns to provide different lengths and column materials. For the present application, the columns are packed with a molecular sieve. Various modifications have been made for the purposes of this study. Helium is used as a carrier gas and is purified to a few parts per billion by passage through a cooled molecular sieve trap. A gas sample injection loop provides for the injection of a controlled volume of a desired gas. This may be a premeasured "standard" mixture,

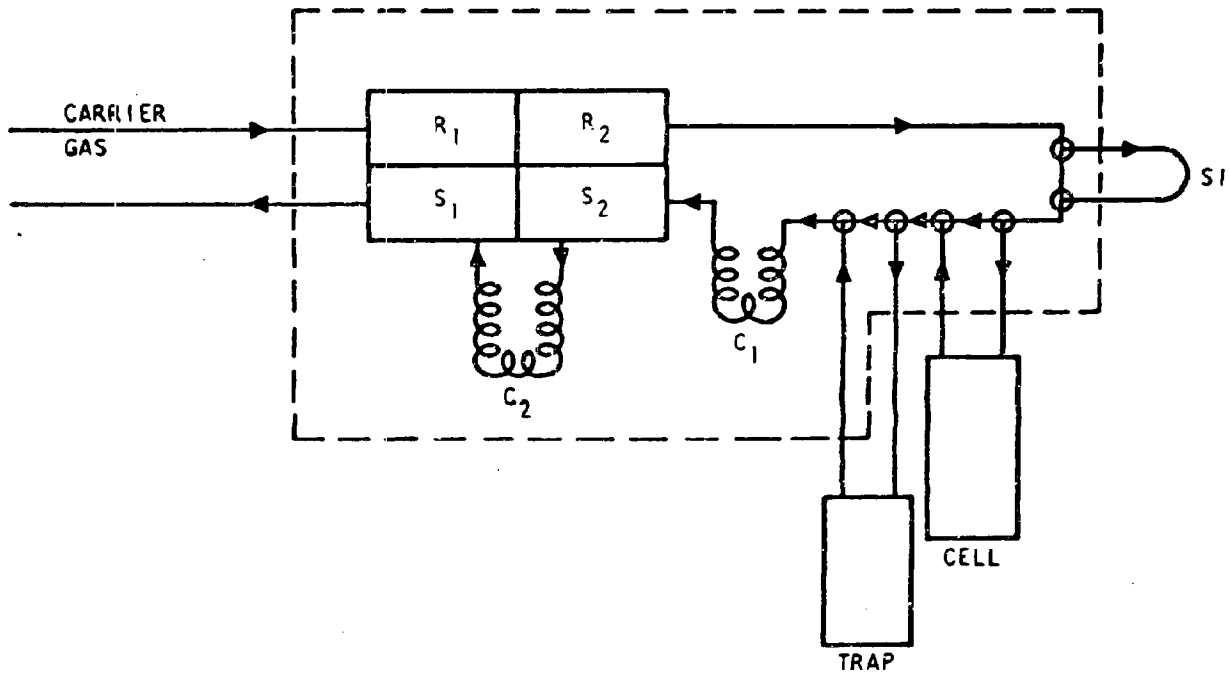

R_1, R_2	REFERENCE CELLS OF GAS CHROMATOGRAPH (GC SHOWN ENCLOSED BY DOTTED LINES)
S_1, S_2	DETECTOR CELLS OF GAS CHROMATOGRAPH
C_1, C_2	ANALYTICAL COLUMNS OF GC
SI	GAS SAMPLE INJECTION LOOP OF GC
CELL	SOLID SAMPLE CELL
TRAP	TRAP FOR DETECTION OF SLOWLY DESORBED GASES

Fig. 1 - Diagram of Flow Systems of Gas Chromatograph Assembly

used for calibration purposes, or a gas such as oxygen so that the interaction with the sample can be studied. In the latter case, the gas chromatograph is itself used to measure the uptake of oxygen by the sample, by comparing the oxygen signal found when a volume of oxygen is injected with the sample cell bypassed with that found when the sample cell is in the stream. The solid sample cell is arranged, as shown, so that it can be bypassed. Suitable cells are available for the measurement of optical and electrical properties while the sample is in the helium stream.

If gas is evolved from the sample in a fairly short burst (~1 sec), the evolved gases are carried by the helium stream to the columns, where they pass through at different rates and yield separated peaks on a recorder chart. If the evolution of gas is slow, as in most of the work performed on pigments, a different method is used, in which the evolved gases are accumulated over a period of time in a nonreactive trap. The helium stream passes through this trap after passing through the sample, although the trap can be bypassed if desired. The trap presently in use consists of silica gel, previously baked at 180°C, cooled to liquid nitrogen temperatures. The trapped gases can be very rapidly released by heating the silica gel to ~125°C in a few seconds, and they then enter the gas chromatograph for analysis. This arrangement works well for H_2, O_2, N_2, CO, and CO_2, for which calibration measurements have shown that trapping and release are both complete.

3.1.3 Experimental Procedures

After a sample has been placed in the cell, the apparatus is purged with helium (generally overnight) and the trap is baked out. Bypassing the sample cell and trap, a sample gas mixture is injected to give a quantitative calibration of the gas chromatograph. The trap is then placed on stream and cooled to liquid nitrogen temperatures, and the background impurities in the helium gas stream are condensed for a suitable time, typically 30 min. Typical background concentrations are: O_2, 18 parts per billion (ppb); N_2, 20 ppb; CO_2, not measurable (<1 ppb); CO, not measurable (<2 ppb). Background concentrations are repeatable but appear to arise from small leaks. They can be reduced to very small values by using an additional trap (of molecular sieve cooled with liquid nitrogen) just ahead of the sample cell. Typical concentrations of O_2 and N_2 are then <2 ppb. The sample cell is then introduced into the line, and a check is made to determine that the background with the sample in the line is the same as that without the sample. The sample may then be irradiated (with uv light, for example); and the evolved gases are collected for 30 min in the cooled trap, then dumped and measured by the gas chromatograph. Typical readily available sensitivities are 10^{-8} moles of most gases. Since a 0.1- or 0.01-mole sample can be used, a gas evolution of 10^{-6} or 10^{-7} of the sample weight can be studied.

3.2 ELECTRICAL CONDUCTIVITY

3.2.1 Fundamental Considerations

Changes in the electrical conductivity of pigments are associated with the changes produced in the optical properties by irradiation and are expected to be a very sensitive and useful technique for the study of the fundamental changes produced in thermal coating materials by irradiation. By inducing changes by different but controlled means--as, for instance, chemical reduction or through irradiation by uv light or charged particles--response can be measured and compared to give a clue to the determining primary mechanisms. Measurements on powders using DC techniques are, however, complicated by such effects as packing of the powder and are difficult to reproduce or interpret. Measurements using AC make it possible to separate out contact effects, and also yield additional information. Apparatus for these measurements will be described here.

The perturbation of the periodic potential of a crystalline solid, such as occurs in a finite crystal at a surface, leads, within the band approximation, to the appearance of new energy levels within the band gap in the region of the surface. Such intrinsic surface states can serve as acceptors or donors when gas is adsorbed or desorbed, and such charge transfer leads to a change in the conductivity of the surface region relative to that of bulk, and, in some cases, an extensive electrical double layer may be formed. This situation obtains in both single-crystal and polycrystalline specimens, although a much more complicated behavior is to be expected in powdered specimens.

Within the framework of the simple band description, one can attempt to describe the system in terms of an equivalent electrical circuit. This suggests that a study of the conductivity of powdered specimens as a function of frequency should permit discrimination between the various regions of conductivity resulting, in part, from the intrinsic surface and bulk conductivities of individual crystallites.

That such a discrimination is possible may be seen from the following general considerations. The measured conductivity is a volume average of the various relevant local conductivities, weighted by the magnitude of the electric field at each point. At low frequencies, the current and hence the electric field is determined by the conductivity. The measured conductivity will at these frequencies be weighted in favor of the low-conductivity regions, where the electric field is large. Therefore, if the surface region is that of lowest conductivity, one measures at low frequencies essentially the surface conductivity

(weighted by appropriate volume factors related to the apparent powder density).

At high frequencies, the current is determined by the dielectric constant. The variation of the dielectric constant over the sample is usually much smaller than that of the conductivity, and thus the electric field will be more uniform throughout the sample at these frequencies. The measured high-frequency conductivity will therefore be closer to a simple volume average. For the case of a low-conductivity surface region on a high-conductivity interior, one thus measures at high frequencies essentially the bulk conductivity (again weighted by appropriate volume factors).

Thus, as the frequency is varied, one probes regions of differing conductivity. The more general case, which includes other contributions to local conductivity variation (grain boundaries, interparticle contacts, etc.), is, of course, much more complicated, but in principle the discrimination between regions still obtains.

3.2.2 Setup and Technique

The technique which is utilized on this program involves the measurement of the conductivity of either a powdered specimen or single-crystal samples as a function of frequency over the range 10^3 to 10^{10} Hz and of the changes in conductivity, again as a function of frequency, resulting from ultraviolet or particle irradiation.

An important consideration is the desirability of being able to quantitatively monitor chemical changes which result in the evolution of one or more gaseous reaction products from the specimen. By incorporating the specimen cell used for the measurement of electrical conductivity into the stream of a gas chromatograph, both qualitative and quantitative studies can be carried out. The gas chromatograph is described separately.

A schematic diagram of the conductivity apparatus used for the range 10^3 to 10^8 Hz is shown in Figure 2. A Marconi Instruments Ltd. type TF 1245 "Q" meter in conjunction with a type TF 1246 matched wide-band, stabilized oscillator is used as the basic setup. In order to measure the conductivity of the powdered samples, a single conductivity cell had been designed[3] to permit measurements over a very wide frequency range (Figure 3). A stainless steel chamber with a coaxial center electrode was constructed so that the ratio of the diameters of the inner and outer conductors causes the cell to form a coaxial line with the characteristic impedance of 50 Ω. Electrical connection is made at the upper end of the chamber, where the outer

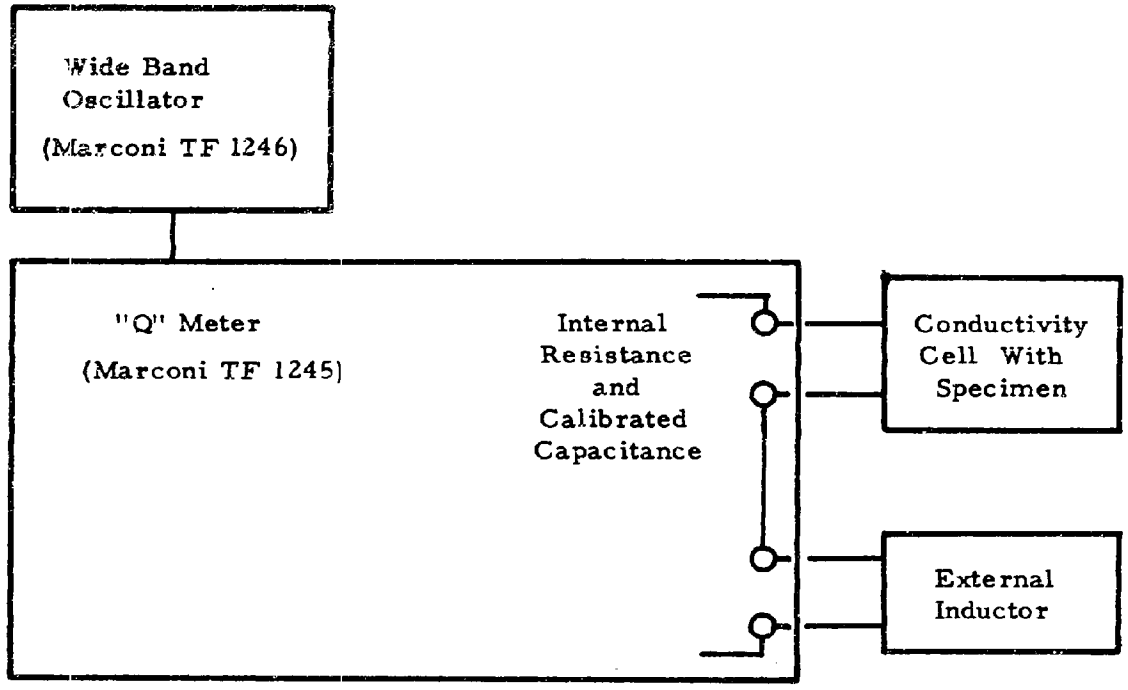

Fig. 2 - Schematic Diagram for Electrical Conductivity Measurement

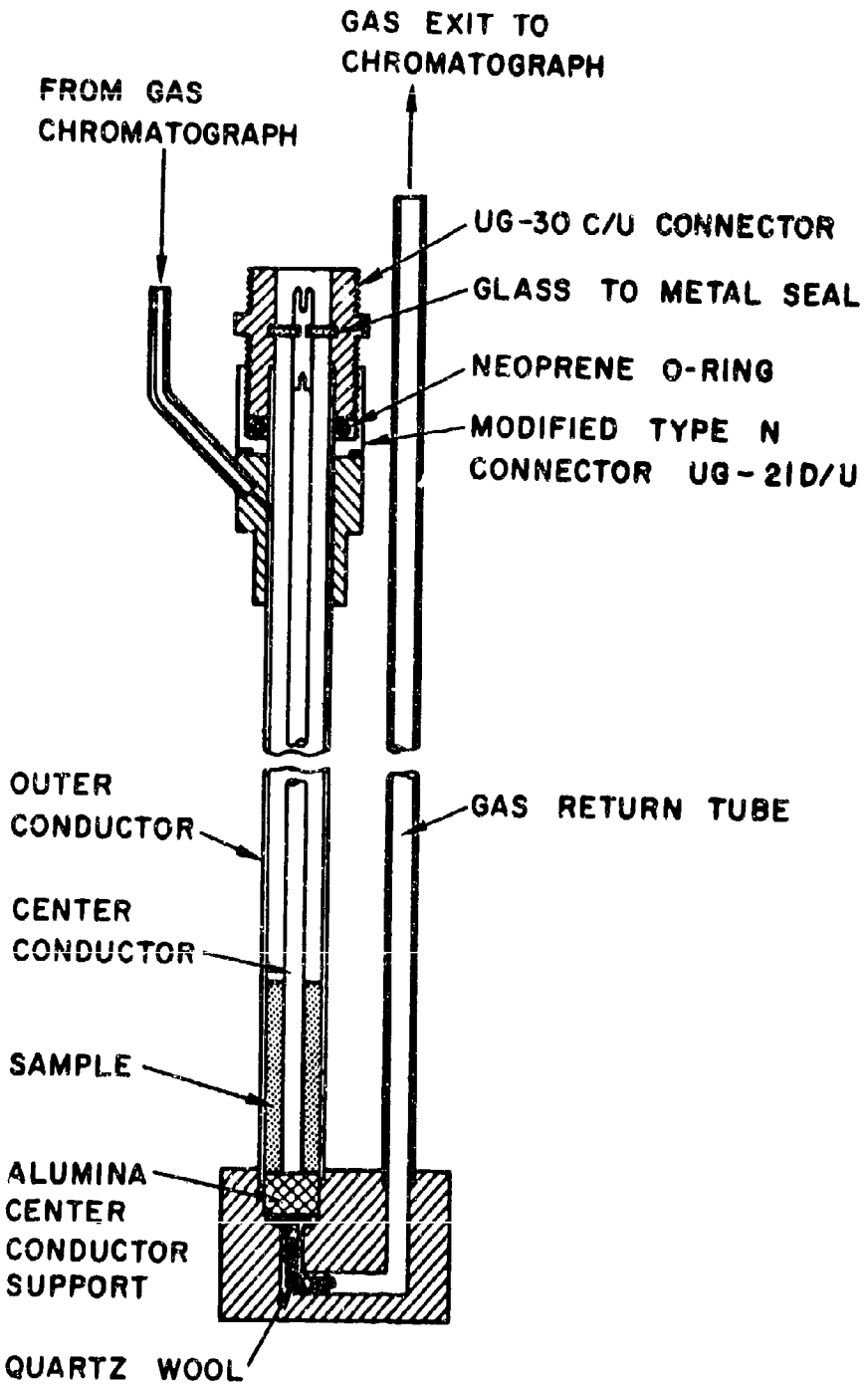

Fig. 3 - Conductivity Cell

part of a "Series N" plug mates with an "improved Series N" bulkhead receptacle equipped with a glass-to-metal seal. A neoprene O-ring completes the upper-chamber seal. Tubulation at the top and bottom of the chamber permits gas to flow through the conductivity cell. The center conductor terminates short of the end of the outer conductor and is supported and held coaxial with the outer conductor by an alumina plug which rests on the bottom of the chamber. This plug also serves as support for the sample, which fills the lower end of the cell and is held in position both by gravity and the downward-flowing carrier-gas stream. Single-crystal samples are measured by applying silver paint contacts and treating them as a parallel plate capacitor.

At low frequencies ($10^3 \leq f \leq 10^8$ Hz), the cell and sample combination has the characteristic of a lossy capacitor. To determine the loss (and hence the conductivity), the sample cell is placed in parallel with the tuning capacitor of a Q-meter and the resonant capacitance is adjusted to obtain a resonance condition.

The Q-meter is set up as a series RLC circuit where the "unknown," the conductivity cell with the specimen, is connected across the capacitor terminals. The Q-meter is first balanced at the desired measurement frequency, without the cell being connected, by using an appropriate plug-in coil with inductance L and adjusting the internal variable capacitor for maximum Q. The values for Q, for the inductance L, and for the frequency are noted. The conductivity cell is then connected across the capacitor terminals, the bridge rebalanced, and the new value of Q measured. This procedure is then repeated for other desired measurement frequencies.

3.2.3 Derivation of Circuit Equation

The essential circuit is indicated in Figure 4. The complex impedance may be written as

$$Z(j\omega) = j\omega L + r + \frac{1}{\frac{1}{R} + j\omega C} \qquad (1)$$

where r is the series resistance of the circuit, and R is the sample resistance placed across the Q-meter capacitance. The current is given by

$$I(t) = \frac{1}{Z(j\omega)} V_{in}(t) \qquad (2)$$

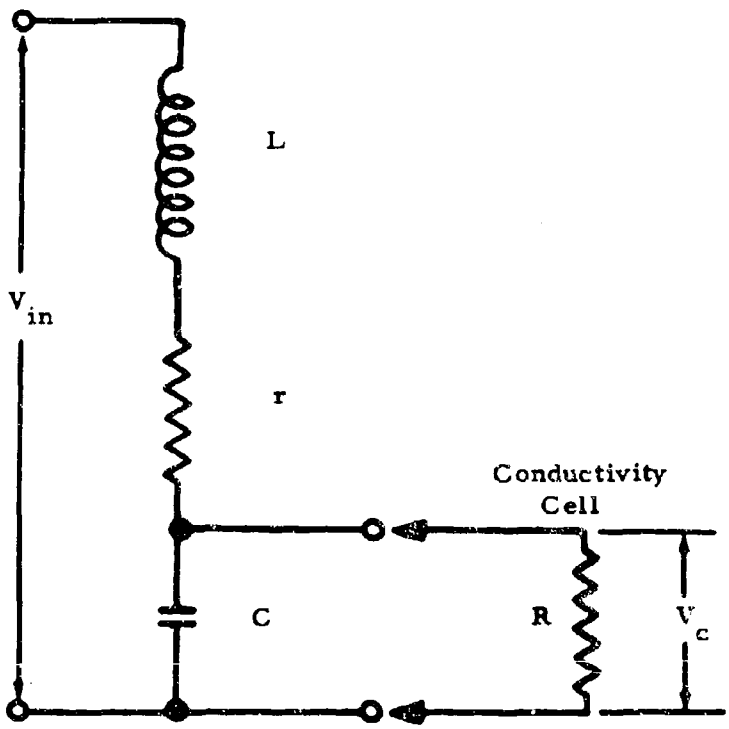

Fig. 4 - Circuit Essentials for Conductivity Measurement

and thus the voltage appearing across the capacitor is

$$V_c(t) = \frac{1}{\frac{1}{R} + j\omega C} I(t) \tag{3}$$

so that

$$\frac{V_c}{V_{in}} = \frac{1}{Z} \frac{1}{\frac{1}{R} + j\omega C} \tag{4}$$

$$= \frac{1}{\left(\frac{r}{R} + 1 - \omega^2 LC\right) + j(\omega L/R + r\omega C)} \tag{5}$$

and the "gain function" or modulus becomes

$$\frac{V_c}{V_{in}} = \frac{1}{\sqrt{\left(\frac{r}{R} + 1 - \omega^2 LC\right)^2 + (\omega L/R + r\omega C)^2}} \tag{6}$$

At resonance, with $\omega = 1/\sqrt{LC}$, it can be shown that

$$\frac{V_c}{V_{in}} = q \tag{7}$$

where q is the so-called circuit "quality."

Then at resonance,

$$q = \frac{1}{\sqrt{\left(\frac{r}{R}\right)^2 + \left(\frac{1}{R}\sqrt{\frac{L}{C}} + r\sqrt{\frac{C}{L}}\right)^2}} \tag{8}$$

For ordinary values of r, R, L, and C,

$$\left(\frac{r}{R}\right)^2 \ll \left(\frac{1}{R}\sqrt{\frac{L}{C}} + r\sqrt{\frac{C}{L}}\right)^2 \tag{9}$$

so that

$$q = \frac{1}{\frac{1}{R}\sqrt{\frac{L}{C}} + r\sqrt{\frac{C}{L}}} \tag{10}$$

With the sample in the circuit,

$$q_{in} = q \tag{11}$$

and with the sample out of the circuit so that ideally $R = \infty$,

$$q_{out} = \frac{1}{r}\sqrt{\frac{L}{C}} \tag{12}$$

Thus,

$$\frac{1}{q_{in}} - \frac{1}{q_{out}} = \frac{1}{R}\sqrt{\frac{L}{C}} \tag{13}$$

letting

$$\Delta q \equiv q_{out} - q_{in} \tag{14}$$

and rearranging, it follows that

$$R = \sqrt{\frac{L}{C}} \quad \frac{q_{in}\, q_{out}}{\Delta q} \tag{15}$$

Reduced to laboartory measurables, this becomes

$$R = \omega_o L \, \frac{q_{in}\, q_{out}}{\Delta q} \tag{16}$$

where $\omega_o = 2\pi f_{res}$ and f_{res} = frequency at resonance

L = value of external inductance

q_{in} = circuit "Q" with conductivity cell connected in parallel with capacitor

q_{out} = circuit "Q" with capacitor alone (conductivity cell removed)

$\Delta q = q_{out} - q_{in}$

At higher frequencies ($10^8 < f < 10^{10}$ Hz), the conductivity cell may be treated as a transmission line, which is open circuited at the end and terminated with the sample, which is "lossy." A General Radio oscillator type GR 1021-P2 is used as power source up to 920 MHz, a Hewlett-Packard type 616A up to 4,000 MHz, and a

klystron to get a point near 10,000 MHz. A slotted line is used to determine the voltage standing wave ratio (VSWR) in front of the cell. The shift in the VSWR and in the voltage minimum produced when sample is introduced into the cell is measured, and from these the conductivity of the sample can be determined using standard microwave techniques.

3.3 REFLECTOMETER FOR USE WITH GAS CHROMATOGRAPH

A special optical apparatus enables changes in the reflectance of samples to be measured while they are in the helium stream of the gas chromatograph, since exposure to air produced changes in, or bleaching of, the reflectance. The sample is in the form of a powder contained in a quartz cell and is viewed in one of two ways. In the first method, the powder is viewed from beneath, as it rests on a lower quartz window. In the second method, the top surface is viewed from above through an upper quartz window. The helium stream can be arranged to "fluidize" the powder for uniform irradiation by a uv lamp through the lower quartz window.

In most of the measurements reported here a single-beam system was used, in which white light is chopped and falls at normal incidence on the sample. Light diffusely reflected at 45 deg is passed through a monochromator and detected by a photodetector and tuned amplifier. The wavelength dial of the monochromator is motor driven, and an electric signal analogous to the drum position is fed into the X-axis of an X-Y recorder. The amplified output of the photomultiplier situated at the monochromator exit slit is applied to the Y-axis. Neutral density filters are positioned in the optical path of the reflected light as required to avoid fatigue of the photomultiplier. Traces are recorded several times with both increasing and decreasing wavelengths to demonstrate reproducibility.

A reference sample made of MgO can be moved into the place of the sample under investigation. In this way, reasonably good measurements can be made of diffuse reflectance as a function of wavelength. An MgO reference standard was prepared by smoking with magnesium ribbon. The system response to this standard is used in conjunction with the spectrum reported in the literature[4-6] for the calculation of our reflectance reference curve. A Kodak diffuse reflectance board is used as working comparator to check the system just prior to and after each reflectance determination.

However, this single-beam system involves rather tedious data reduction with its associated errors. Accordingly, a dual-beam system was designed and built. The optical arrangement is shown in Figure 5.

Light from a single source is allowed to follow one of two optical paths, depending upon the instantaneous position of a mechanical chopper. When the light beam traverses one path, the light is reflected from the surface of a reference specimen, and when the light traverses the other path it is reflected from the surface of the test sample. Both

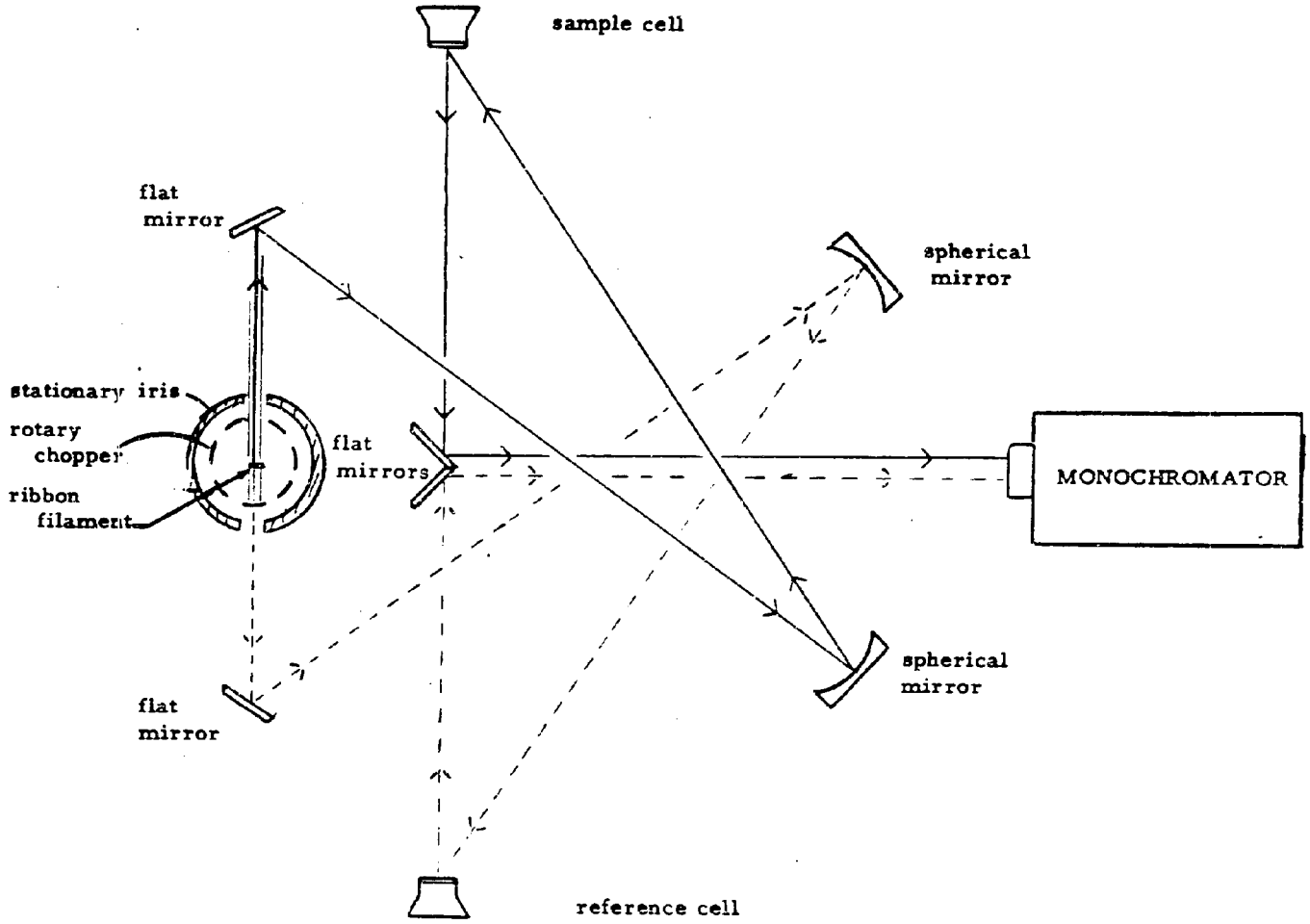

Fig. 5 - Schematic of Dual Beam Set-Up (Not to Scale)

light paths converge on the entrance slit of a scanning monochromator, traverse the monochromator, and then fall on a photomultiplier mounted at the exit slit of the monochromator. The light signal thus presented to the photomultiplier consists of a periodic time sequence with amplitudes related to the reflectance of the reference specimen and the test sample.

The waveform has the shape shown in Figure 6. V1 and V2 are proportional to reflectance of the sample and references, respectively. Transients occur while the beam is being chopped off one sample and onto the other, as shown at A and B in Figure 6. To process this signal, a gated amplifier system is used as shown in the block diagram in Figure 7. There are two channels, the signal channel and a reference channel which is used to synchronize the signal channel with the mechanical chopper. In the signal channel, the composite signal, generated by the PM tube, is first amplified by a DC amplifier. The amplified composite signal is presented to the inputs of a pair of analog gates. The gates are controlled by the reference channel, with one gate being opened for a short time while the light beam is reflected from the reference specimen and the other gate is then being opened for a short time while the light beam is reflected from the test sample. The gated signals are integrated by RC time constants and passed through identical buffer amplifiers. The output from the reference signal buffer amplifier is displayed on meter 1, which indicates the magnitude of the light reflected from the reference specimen. This output also is compared with a DC reference voltage, and any difference between the reference signal and this DC voltage is amplified by the AGC amplifier and used to control the gain of the input DC amplifier. The resulting AGC feedback loop serves to maintain a constant output from the reference signal buffer, as indicated on meter 1, and a ±100 percent change in signal from the reference specimen reaching the PM tube is reduced to a ±1 percent change in signal level at meter 1.

Meter 3 then reads the ratio of the reflectance of the sample to that of the reference specimen at the same wavelength.

The outputs from both buffers are applied to the inputs of a difference amplifier which indicates on meter 2 the difference in intensity between the reference sample and the test specimen. The AGC loop maintains a constant reference signal to the difference amplifier, so that changes in the reflectance of the test sample are read directly on meter 2. In this way, small differences can be readily measured, since this meter reads zero when both the reference specimen and sample have the same reflectivity. The signal applied to meter 3 is also applied to the Y-axis of the X-Y recorder as in the

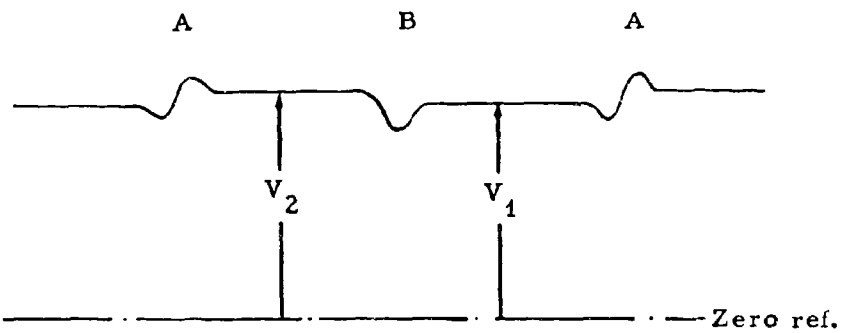

Fig. 6 - Photomultiplier Output Near Equal Reflectivity

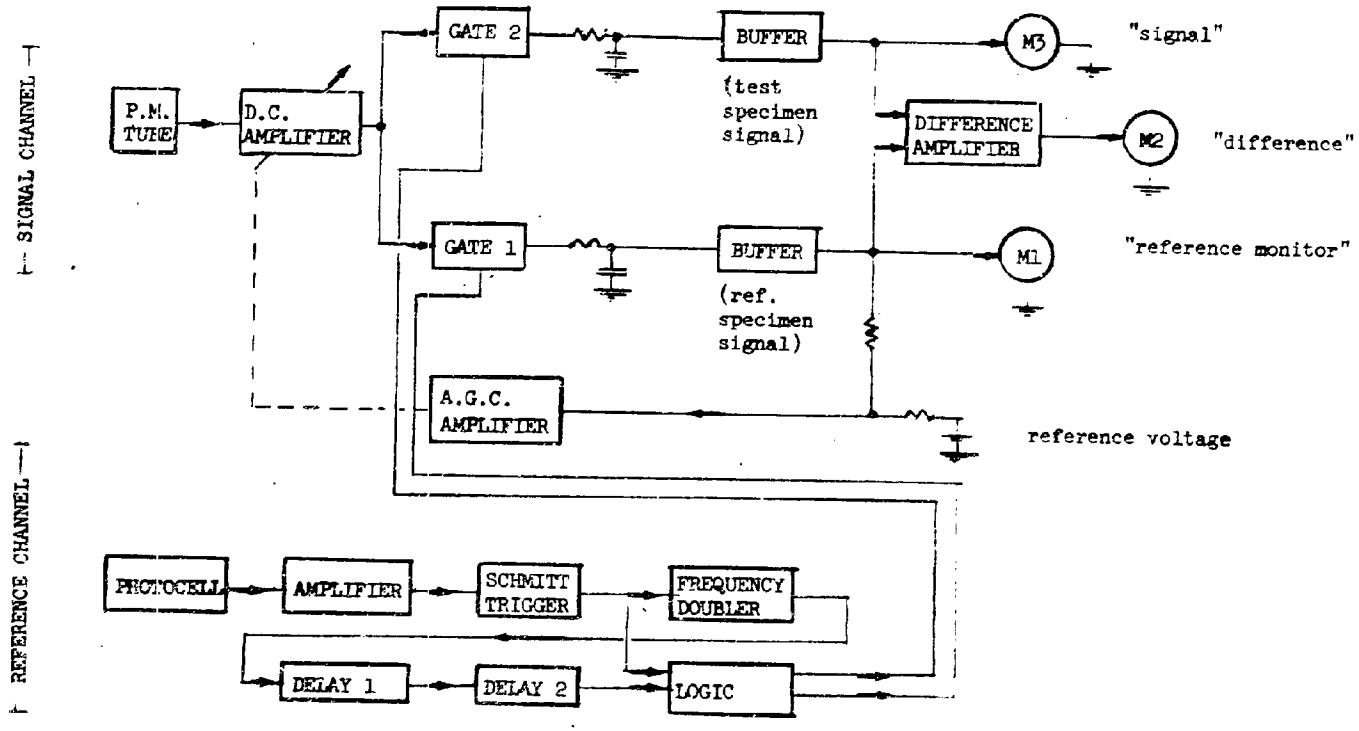

Fig. 7 - Functional and Block Diagram for Dual Beam Transient Gating Electronics

single-beam version.

Provision is made for varying the angle at which diffuse reflectance is measured, in view of the anomalous results recently found at Lockheed using the "light pipe" in-situ reflectometer, which had a fixed angle of measurement.

3.4 IN-SITU APPARATUS FOR MEASUREMENT OF REFLECTANCE CHANGES IN COATINGS AFTER EXPOSURE TO COMBINED ULTRAVIOLET AND PARTICULATE IRRADIATION

This equipment, designed and built by Convair Division of General Dynamics Corporation, enables eight samples to be mounted in a vacuum chamber, to be exposed one at a time to either uv or charged particle irradiation or both at once, and to have their reflectance measured over the range of 0.23 to 2.3 μ without removal from the vacuum system.

The apparatus consists of a horizontal 12 in. diameter vacuum chamber incorporating an integrating sphere, particulate beam tube, sample cooling thermostat, and sample wheel as shown schematically in Figure 8. Photographic views are shown in Figures 9, 10, and 11. The samples are mounted on a central axle and may be rotated 180 deg from the irradiation position into the integrating sphere for reflectance measurements. Monochromatic beams are provided by a Beckman DK-2 spectroreflectometer and are made incident to the sphere by transfer optics as shown in Figure 8. Ultraviolet radiation was provided by a General Electric BH-6 lamp, and electrons and protons were provided by the Convair Dynamitron. In the following subsections, these components are discussed in some detail.

3.4.1 Spectrophotometer

A Beckman model DK-2 spectrophotometer was employed to provide light dispersion, detection, and recording. This is a dual-beam instrument which ordinarily is used to measure percent absorption as a function of wavelength. It is readily adapted to the requirements of reflectance measurements, since it is a ratio recording device. With the present arrangement, it was necessary to "reverse" the beams, i.e., make the sample beam follow the path conventionally followed by the reference beam, and vice versa. This was accomplished by a simple modification of the instrument electronics. The instrument scans the full spectrum and provides readout on a chart.

3.4.2 Transfer Optics

The transfer optics for the sample and reference beams between the Beckman DK-2 and the integrating sphere consist of six front-surfaced aluminized mirrors and two sapphire windows. The sapphire windows are a matched pair and were tested for transmittance and thermal stability before installation in the system. Each beam employs one concave mirror and two plain mirrors and one window

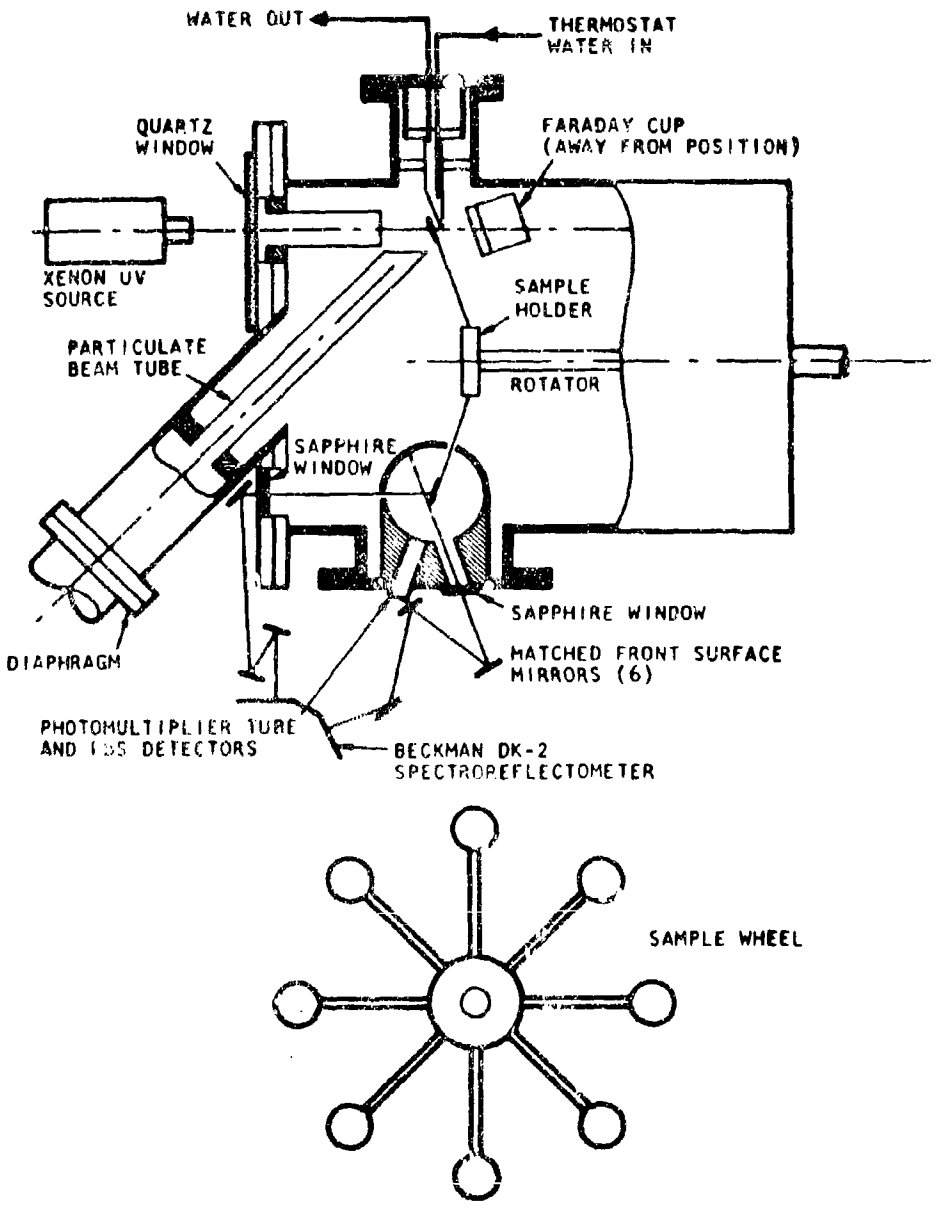

Fig. 8 - Diagram of Convair Apparatus

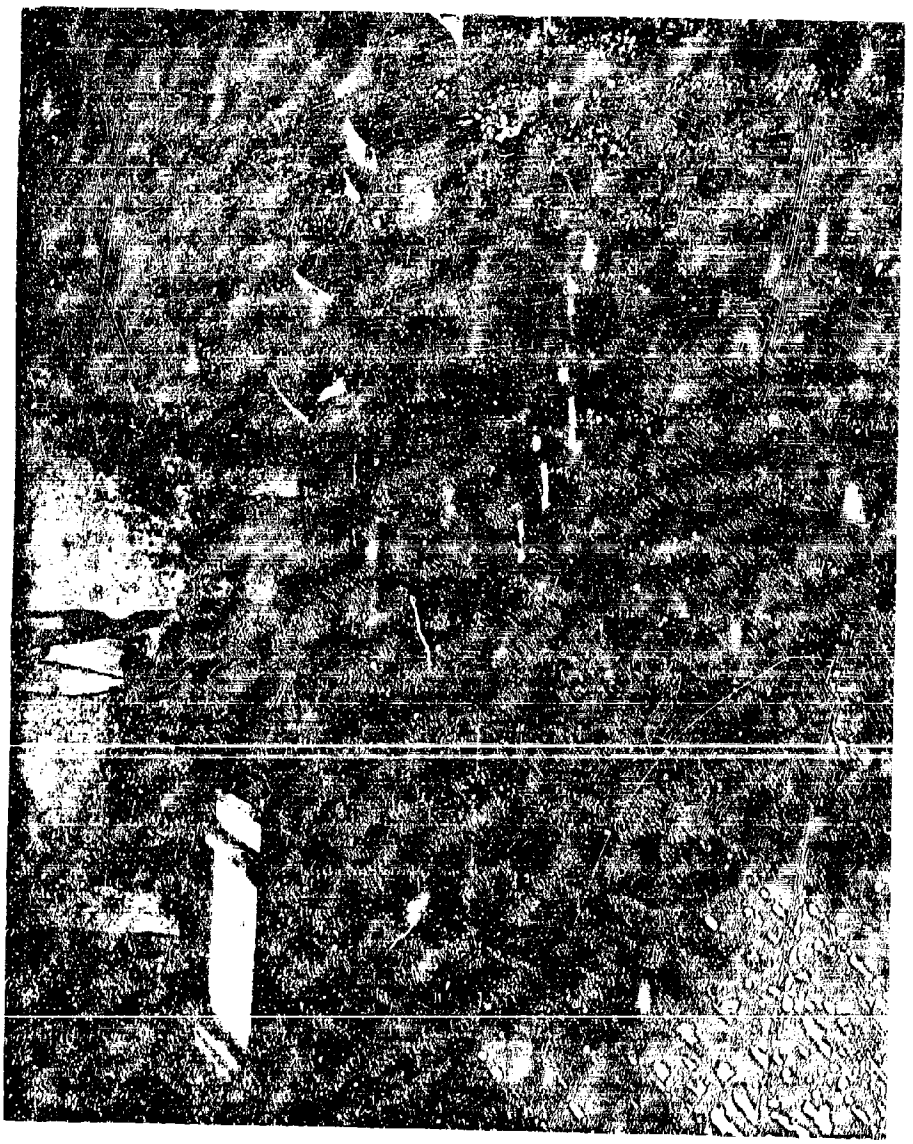

Fig. 9 - Specimen, Vacuum Chamber, Optical Parts and Recording Equipment

NOT REPRODUCIBLE

Fig. 10 - View Showing Mating of In-Situ Apparatus to Dynamitron

Fig. 11 - Accelerator Section and In-Situ Apparatus

which serves to admit the beam to the vacuum tank as shown schematically in Figure 8. By means of the movable mirror mounts the beam lengths were adjusted to be identical. The front surface mirrors were checked for thermal stability and ground, polished, and aluminized in the Convair optical section. The full set of six mirrors were aluminized at one time to ensure uniformity between the two beams.

3.4.3 Integrating Sphere

The integrating sphere employs a center-mounted sample and is of the absolute type in that it requires no reference sample. It has a 5 in. inside diameter, and the inner surface is coated with 2 mm of MgO.

The monochromatic sample and reference beams enter the sphere through openings as shown schematically in Figure 8. The sample beam strikes the sample in the center of the sphere. The reference beam strikes the sphere wall at approximately the same position as a specularly reflected beam from the sample would strike the wall. This optical arrangement helps greatly to eliminate errors due to non-uniform illumination of the sphere. The trace corresponding to 100 percent reflectance is obtained by rotating the sample out of position, so that the sample beam strikes the sphere wall at a point approximately opposite that at which the reference beam strikes the wall.

The detectors are mounted so as to view symmetrically the point at which the sample and the reference beam strike the sphere. A photomultiplier tube is used from 0.23 to 0.6 μ, and a lead sulfide cell is used from 0.6 to 2.3 μ. The face of the end-on photomultiplier tube and of the lead sulfide cell mount on the surface of the sphere.

3.4.4 Sample Wheel and Thermostatting

The samples are attached to a sample wheel which is mounted to a central axle in the chamber. Front and side views of the sample wheel are shown in Figure 8. The side view is shown as the sample is contained in the vacuum tank. The sample wheel can accomodate eight 1-in. diameter samples; one sample at a time can be irradiated. The substrate discs are made from stainless steel 0.020 in. thick. Samples are placed in the irradiation position for application of radiation flux and placed in the measurement position for the determination of reflectance characteristics. This placement is accomplished by rotating the sample wheel using a cylindrical magnet, which can be seen in Figure 9 at the far right end of the vacuum chamber. By using magnetic coupling for the rotation of the sample

wheel, the difficulties associated with vacuum seals were eliminated. A portion of the magnet housing was marked so as to provide indexing of the wheel position in terms of sample numbers.

A sample being irradiated requires cooling to dissipate the heat deposited in it. The metal bellows arrangement, shown in Figure 8, was used to provide thermostatting of the sample. After a sample is rotated into position, a 1-in. diameter metal tube, cooled by a constant flow of water, is moved inward to a point where the angled surface is in full contact with the sample backing. This provides temperature control throughout the irradiation of the samples. After an irradiation is complete, the cooling device is moved away from the sample to allow the wheel to be rotated.

3.4.5 Irradiation Geometry

In the ideal case, the particulate and uv radiations should strike the samples simultaneously and from the same direction, but the constraints imposed upon a laboratory simulation preclude this procedure since one radiation beam would have to be transmitted through the source of the other. If the uv source were of sufficient power to permit its removal to an appreciable distance from the target or if it radiated a parallel beam, both beams could be caused to impinge normally on the samples; currently available uv sources do not meet these criteria. To cause both beams to impinge on the sample as close to normal as possible, it was decided to have the beams 45 deg apart, with the sample positioned so that each beam strikes the sample with an incident angle of 22.5 deg from the normal.

The sample, when positioned for irradiation, is at an angle of 22.5 deg from the normal for the flux of ionizing radiation and also for the flux of uv light. The geometrical arrangement, shown in Figure 8, makes possible simultaneous irradiations with uv and charged particles. Both the charged particle beam and the uv beam are confined by the internal defining tubes shown in the figure so as to prevent radiation from striking samples other than the sample in the irradiation position.

3.4.6 Vacuum Chamber

The chamber is mounted on a rigid aluminum frame. An Ultek ion pump is suspended below the tank and is connected to the tank through a 6-in. gate valve. The ion pump is operated continuously. Before venting the tank to atmospheric pressure, the gate valve is closed, the pump being left on. This procedure shortens the pump-down

time needed for the next evacuation. Four Vac-sorb pumps mounted on a manifold can be used individually or together for initial pumping from atmospheric pressure. The use of four cryo-pumps gives a short pump-down time and gives a pressure low enough to avoid problems with the ion pumps. In some instances, the pump-down time required to pass from atmospheric pressure to 10^{-7} torr was less than 15 min.

Initially there was a problem with plasma discharge from the ion pump at the start up: these discharges can cause significant changes in sample properties. The problem was essentially eliminated by a change in operating procedure and a modification of the system. The procedure now used is to ensure that the pressure in the tank is reduced to a level below the Paschen region before the gate valve is opened to the ion pump. In addition, an ion deflection system consisting of alternately charged grids was installed to help control any back-streaming of ions that might occur.

Pressure measurement was made using a glass ion gage, with a CVC copper foil trap installed between the gage and system to eliminate false pressure readings from any contamination that might be emitted from the samples.

The oil-pumped accelerator vacuum system is separated from the clean ultrahigh vacuum system of the reflectance chamber by a thin window. The window, which need not support atmospheric pressure, can be of 0.00025-in. Mylar. Currently a 0.002 in. aluminum window is used, which causes an energy loss that is negligible for electrons but severe for protons. To obtain an energy of 1 MeV after passing through the window, 1.025 MeV electrons must be used, while for protons an initial energy of 2 MeV is needed. A collimating aperture is provided after the window so as to eliminate the scattered beam and provide a well-defined area. Magnetic sweeping coils are available to scan the beam over the sample, but the uniformity is satisfactory without their use.

3.4.7 Ionizing and Ultraviolet Radiation

A section of the accelerator and vacuum system can be seen in Figure 11 with the in-situ apparatus in the background to the far right. Electrons or protons generated and accelerated in the Dynamitron are directed down a beam tube to a deflection magnet where the beam is deflected 90 deg and directed into the in-situ apparatus, through the particulate beam tube shown in Figure 8, the 2-mil aluminum diaphragm, and the beam diameter limiting tube. Measurements of flux are made using a Faraday cup with an opening having the same size as the sample,

which can be moved into the sample irradiation position. The Dynamitron can provide electrons or protons in the energy range from 0.4 MeV to 2.5 MeV.

3.4.8 Low Energy Ion Source

A duoplasmatron ion source, built at Gulf General Atomic, permits irradiation of samples with hydrogen ions or electrons with energies from 100 eV to 60 keV. The ions are mass analyzed to remove the H_2^+ and H_3^+, leaving a pure proton beam. Electrons can be obtained simply by reversing the sign of the extraction and accelerating voltages. The beam of ions or electrons is not completely uniform, and magnetic scanning is used to provide uniform irradiation of a 1 in. diameter sample. The current available is 10 μA of H^+ and >1 ma of electrons. This ion source replaces the particulate beam tube on the in-situ apparatus. When using protons, the ion beam may be neutralized with electrons, a procedure that is intended to eliminate surface charge-up of the dielectric samples. Provision is also made for a more direct method of keeping the sample surface neutralized, by using a flood of electrons of thermal energy from a filament near the sample, but shielded from it to avoid deposition of tungsten.

Since the proton flux must be measured in a neutralized beam, a simple Faraday cup is not adequate; therefore, a special Faraday cup is also used. Simply turning off the power supply to the neutralizing filament is also not sufficient because (1) the beam is likely to be partially neutralized anyway, and (2) the removal of neutralization will change the beam spread slightly. The Faraday cup has two negatively biased electrodes with apertures in front of its entrance; one serves to repel electrons in the beam and the other to contain secondary electrons that would otherwise be emitted from the Faraday cup. The Faraday cup is coated with gold black to avoid complications from uv-induced photoelectron emission. Measurements can then be made without turning off the uv lamp.

The ultraviolet source used consists of two General Electric BH-6 lamps. These lamps are mounted in a water-cooled metal box. Both lamps are air cooled by air jets at the locations recommended by the manufacturer. One or both lamps may be used for irradiation.

Recently, a 3000-watt xenon arc light source has been installed. In addition, a system for periodically making measurements of the light source has been designed and is being installed.

The spectral distribution of irradiance at the sample is required, since the output from the arc tends to decrease as the arc ages. The decrease occurs in the critical uv portion of the spectrum.

To make an irradiance determination, the arc is repositioned so as to enter a small integrating sphere through a limiting aperture and (if required) an attenuator. The arc is kinematically mounted in either the sample irradiation or irradiance-calibration position and can be readily shifted from one position to the other. The Beckman spectrophotometer is then used to compare the xenon source with a National Bureau of Standards irradiance standard.

3.4.9 Data Reduction

The Beckman DK-2 produces in chart recorder form a plot of reflectance versus wavelength from 0.30 through 2.10 μ. A template marked in 39 discrete units of wavelength is imposed on the Beckman chart and the corresponding values of reflectance are noted. The reflectance value at 2.10 μ is assumed to hold for seven additional wavelengths from 2.50 to 7.00 μ. The 46 values for the total reflectance obtained in this way are then keypunched on data originating cards. An in-house CDC 6400 computer program is used to compute the solar absorptivity from the 46 data points for reflectance. The solar spectrum energy used in the computer program is taken from the well known Johnson curve. A correction is made for the approximately 6 percent of the solar energy falling outside our measurement range. In addition, a plotting program enables the 38 data points originally taken from the Beckman chart to be plotted in standard form, together with sample identifying data. An example is shown in Figure 12. A print out of the data and computer values of solar absorptance is also given as shown in Figure 13.

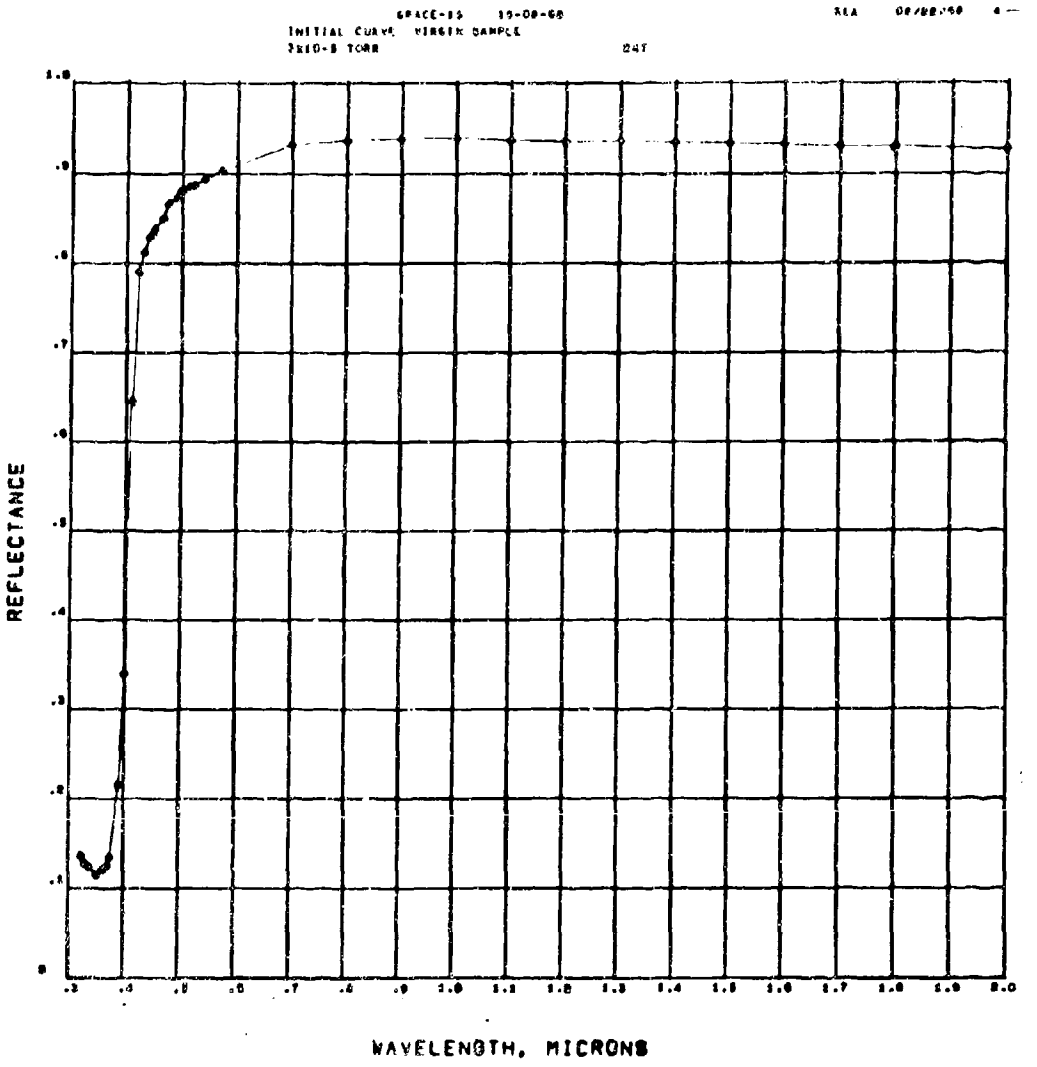

Fig. 12 - Representative Computer Plot of Diffuse Reflectance Spectrum

REFLECTIVITY DATA RADIANT ENERGY TRANSFER GROUP SPACE SCIENCE LABORATORIES GD-ASTRONAUTICS
TICX GRACE -15 13-08-68
HOH BINDER VIRGIN SAMPLE
10-6 TORR

244 B

WAVE LENGTH	REFLECT-ANCE	WAVE LENGTH	REFLECT-ANCE	WAVE LENGTH	REFLECT-ANCE	WAVE LENGTH	REFLECT-ANCE//
3.000E-01	1.300E-01	3.200E-01	1.280E-01	3.300E-01	1.230E-01	3.350E-01	1.180E-01
3.500E-01	1.090E-01	3.600E-01	1.200E-01	3.700E-01	1.230E-01	3.750E-01	1.340E-01
3.900E-01	2.000E-01	4.000E-01	3.190E-01	4.100E-01	5.500E-01	4.200E-01	7.780E-01
4.300E-01	8.090E-01	4.400E-01	8.240E-01	4.450E-01	8.330E-01	4.500E-01	8.390E-01
4.650E-01	8.500E-01	4.750E-01	8.620E-01	4.900E-01	8.730E-01	4.950E-01	8.730E-01
5.000E-01	8.780E-01	5.100E-01	8.800E-01	5.200E-01	8.850E-01	5.400E-01	8.890E-01
5.700E-01	8.960E-01	7.000E-01	9.300E-01	8.000E-01	9.350E-01	9.000E-01	9.390E-01
1.000E+00	9.390E-01	1.100E+00	9.390E-01	1.200E+00	9.380E-01	1.300E+00	9.370E-01
1.400E+00	9.370E-01	1.500E+00	9.370E-01	1.600E+00	9.300E-01	1.700E+00	9.300E-01
1.800E+00	9.290E-01	2.000E+00	9.260E-01	2.500E+00	9.260E-01	3.000E+00	9.260E-01
3.500E+00	9.260E-01	4.000E+00	9.260E-01	4.500E+00	9.260E-01	5.000E+00	9.260E-01
5.500E+00	0.	6.000E+00	9.260E-01	6.500E+00	0.	7.000E+00	9.260E-01
7.500E+00	0.	8.000E+00	0.	8.500E+00	0.	9.000E+00	0.
9.500E+00	0.	1.000E+01	0.	1.050E+01	0.	1.100E+01	0.
1.150E+01	0.	1.200E+01	0.	1.250E+01	0.	1.300E+01	0.
1.400E+01	0.	1.500E+01	0.	1.600E+01	0.	1.700E+01	0.
1.800E+01	0.	1.900E+01	0.	2.000E+01	0.	2.100E+01	0.
2.200E+01	0.	2.300E+01	0.	2.400E+01	0.	2.500E+01	0.
2.600E+01	0.	2.700E+01	0.	2.800E+01	0.	2.900E+01	0.
3.000E+01	0.	3.100E+01	0.	3.200E+01	0.	-0.	-0.

MISSIVITY REQUIRED 100 300 500 SOLAR ABSORPTIVITY X OTHER
200 400 CARBON ARC ABSORPTIVITY

SOLAR ABSORPTIVITY=1.613055E-01 SUMMATION RATIO=1.613055E-01

Fig. 13 - Representative Computer Print-Out of Reflectance and Absorptivity

SECTION 4

RESULTS

As indicated in the Introduction, the measurements reported here are of a preliminary nature and do not yet make possible a detailed understanding of the mechanisms of damage to thermal control coating pigment materials. Much of the effort has been devoted to making reliable measurements, and this forms the basis of the work to be done in the continuation of this program. The studies that have been performed thus far are described here. One set of measurements was aimed at characterizing the chemical and physical processes occurring when the pigments are damaged; this involved comparing the effects of chemical reduction of the pigments with those of uv and particulate irradiation, and comparing gas evolution and absorption with changes in optical and other properties. A second set involved detailed measurements, at General Dynamics/Convair, of changes in the reflectance of pigment layers exposed to uv and particulate irradiation, the measurements being made "in situ", i.e., without removal of samples from the vacuum. The second set of measurements was made on pigments already characterized by the first set and serves to relate the performance of the pigments to the processes found to be occurring.

4.1 CHEMICAL REDUCTION OF RUTILE POWDERS AND SINGLE CRYSTALS

A series of measurements was made on the chemical reduction of rutile. These measurements were motivated by the following considerations. Most of the vast body of literature on color centers and electron donors in rutile has concerned studies on chemically reduced rutile. It is of obvious importance to relate the uv effects on rutile, believed to involve reduction, to this body of knowledge and to compare the two processes in terms of their effects on optical properties, electrical conductivity, and EPR. Further, there are numerous discrepancies in the literature regarding reduction of rutile, some authors claiming that simple reduction of oxygen partial pressure is sufficient to promote reduction at elevated temperatures (near 950°C) and others that hydrocarbons or other reducing agents are necessary. There also appear to be differences in reduction between single crystals and powders, with crystals reducing under conditions

where powders will not. This would indicate an important role of the surface in the reduction process, and correlation of the ease of chemical reduction with the sensitivity to uv degradation might give important information on the mechanisms of the latter process.

The procedures and results of the present study are described in detail in Appendix I of this report. In brief, comparisons were made (1) of the reduction behavior of different rutile specimens (powders, single crystals) exposed to the same environment and (2) of the effects of different ambients (clean and dirty vacuum, gas flows).

Very marked effects of contaminants were noted. In particular, materials evolved from pigments on rapid outgassing can cause severe reduction. This can be diminished in part by outgassing while raising the temperature slowly, giving time for the impurities to be removed. The conclusions reached were that:

1) No reduction results when rutile powder is exposed to a flow of purified helium gas at 950°C. It appears that lowering the partial pressure of oxygen in the ambient atmosphere is not sufficient to bring about reduction of TiO_2 powders.

2) No reduction results when TiO_2 rutile single crystals are exposed to a flow of purified helium gas at 950°C.

3) No reduction results for powder at 950°C when the (air) ambient pressure is reduced by a factor of 10^{-6} as long as no contaminant is generated or permitted to enter the system. This contrasts with numerous reports of reduction at 950°C or less at pressures up to several millimeters Hg.

4) A trapping train of molecular sieve and activated charcoal cooled to liquid nitrogen temperatures is effective in blocking contamination from a mechanical forepump.

5) Desorption of impurities from "as received" powder can lead to reduction even in a "clean" vacuum system.

6) Condensed contamination in the system may not be removable by heat alone but may require chemical means.

7) Even small quantities of methyl alcohol, introduced in the vapor phase, cannot be removed from the powder by

heating and evacuation near 200°C, and lead to reduction of the rutile when the temperature is increased.

8) Single crystals are more sensitive to reduction by contamination than powders.

9) The relative susceptibility of rutile powder to reduction can be influenced by "impurities" in the powder.

10) The susceptibility of some rutile pigments to chemical reduction correlates with the extent of the reflectance degradation under irradiation.

Samples of reduced rutile powders were prepared for comparison with material exposed to uv light. The reduction was accomplished by flowing 10 percent H_2/90 percent Ar (modified forming gas) at a slow rate through the tube while the sample was at 950°C for about 2 hr. Reduction of the TiO_2 was indicated by the blue coloration. This was checked for reversibility by heating in air to ~800°C for between 1/2 and 1 hr; the oxidation bleached the color back to the original white. The reduced material was also checked for its rutile crystal structure by x-ray diffraction.

Samples of outgassed pigments were prepared by heating slowly up to 900°C in a clean vacuum, followed by reoxidation and cooling in an oxygen flow. This procedure causes some sintering.

Reduction of single-crystal material was also studied for $SrTiO_3$. Sections cut from the center of the boule could be reduced using either H_2 or CO. However, some pieces cut from the outside of the same boule could not be reduced under any conditions, suggesting an impurity effect that is being investigated. Chemical analysis has shown no difference between the regions.

Since the ease of chemical reduction of a rutile powder seems to correlate with the resistance to degradation by uv, it is possible that a simple screening or acceptance test for rutile pigments prepared or stabilized in different ways could be developed.

4.2 INVESTIGATION OF UV EFFECTS ON OPTICAL PROPERTIES USING GAS CHROMATOGRAPH APPARATUS

The effects of uv irradiation on the reflectance of powder samples of rutile and strontium titanate have been studied using the reflectometer and gas chromatograph system.

Reflectance curves for a DuPont R-910 rutile powder are shown in Figures 14 through 21. The wavelength scales are nonlinear, the short wavelength region being spread to show the changes near the uv absorption edge. No smoothing of the data was undertaken. Although scatter may account for some of the fine structure, consistency of some of its features throughout part or all of this experimental series of measurements indicates that it is associated with the sample and not with the apparatus.

Trace 1 of Figure 14 was taken with the powder in the "as-received" condition. For this specimen, the same response was obtained when measurements were made in a helium gas atmosphere and under a liquid nitrogen trapped forepump vacuum with a pressure of <5 μ Hg. The specimen was then exposed to uv irradiation from the AH-6 source at a distance of 6.5 cm for 30 min. Gases evolved during this irradiation were accumulated and then analyzed with the gas chromatograph. The in-situ reflectance spectrum after irradiation is shown by the lower curve in Figure 14. The principal degradation is near the uv, but this depends on the "state" of the specimen. For this material, which was not pretreated, one can observe a continual change in the spectrum as the experiment proceeds with a series of uv irradiations, exposure to vacuum, and exposure to certain specific ambient gases. The effects of a similar 30-min uv irradiation near the end of this experimental series is shown by the curves in Figure 15. The decrease in reflectance produced by the irradiation is now rather uniform across the spectrum, but the state of the specimen was different from the initial condition corresponding to Figure 14.

It was observed that if the specimen was irradiated with uv and then kept for 16 to 18 hours under vacuum, the reflectance falls below that immediately after the irradiation. In Figure 16, the upper curve was taken just after a 30-min uv irradiation and the lower curve 16 hours later. The same trend was noted in the results shown in Figure 17 except that in this case the specimen was also illuminated during the 18-hr period by a standard tungsten lamp. When the powder is first reirradiated after exposure to vacuum for 16 to 18 hours, the reflectance is increased as seen in Figures 18 and 19. After an accumulated uv exposure of 180 min, the specimen was exposed to an

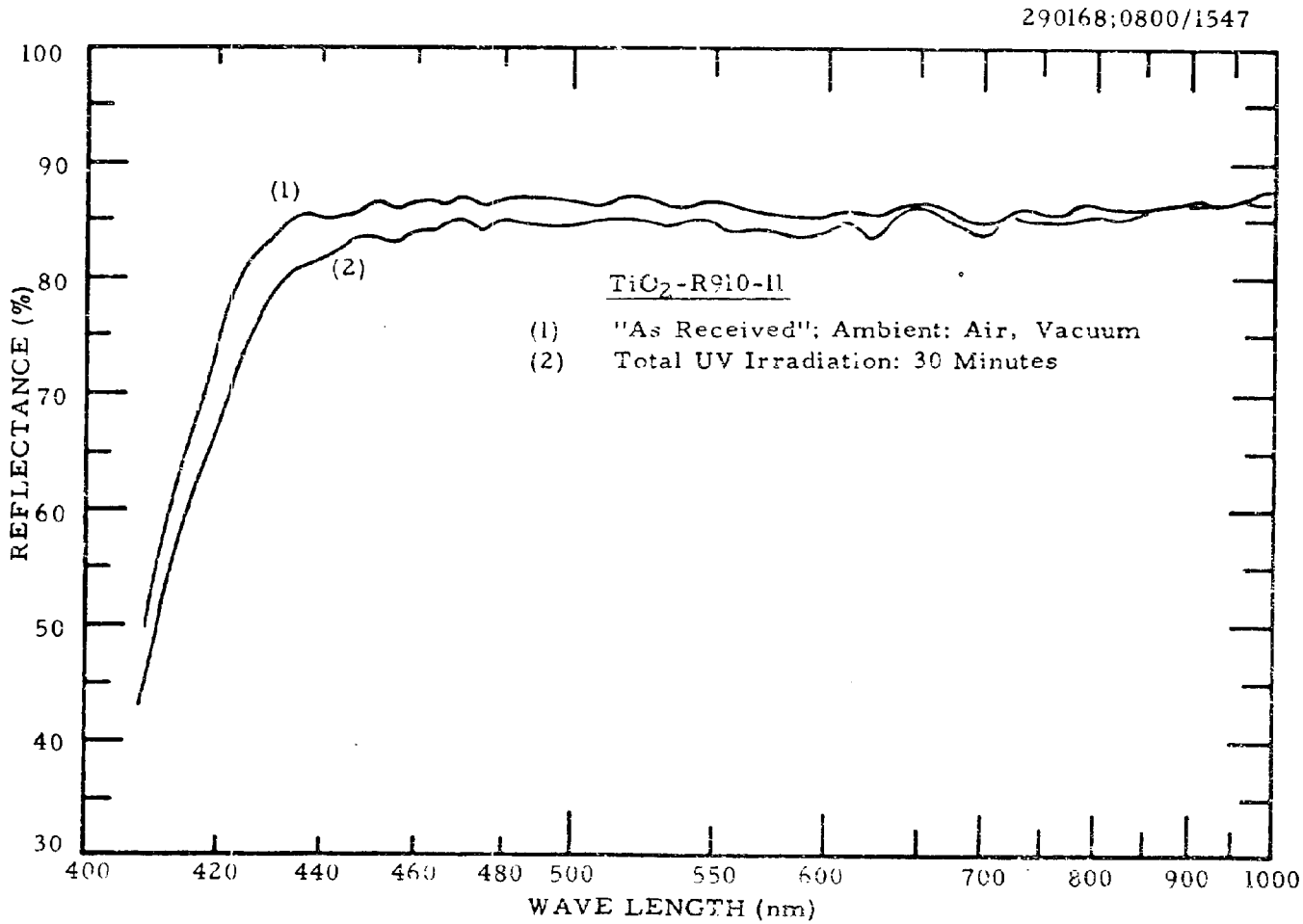

Fig. 14 - Reflectance Spectra for Conditions as Indicated

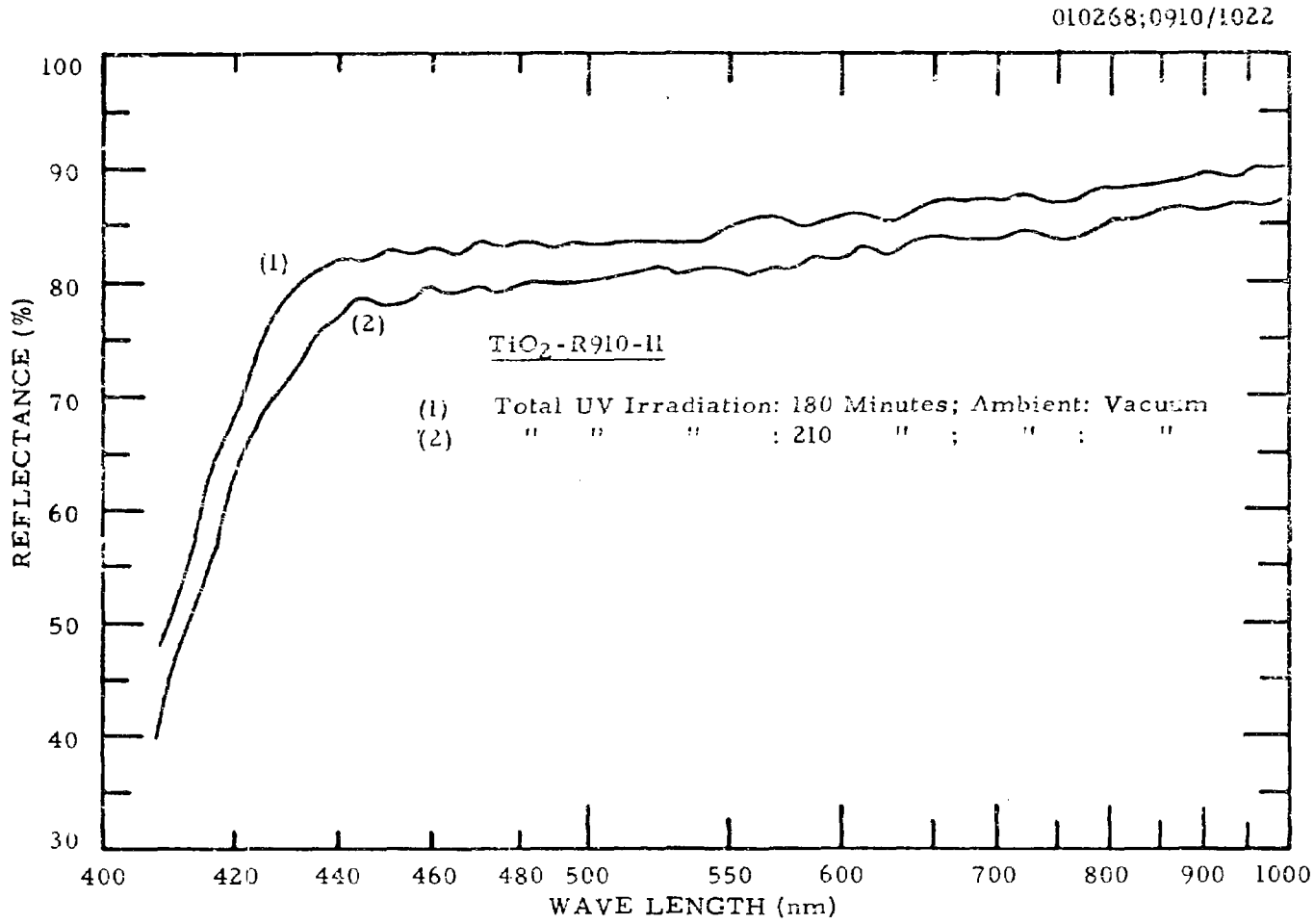

Fig. 15 - Reflectance Spectra for Conditions as Indicated

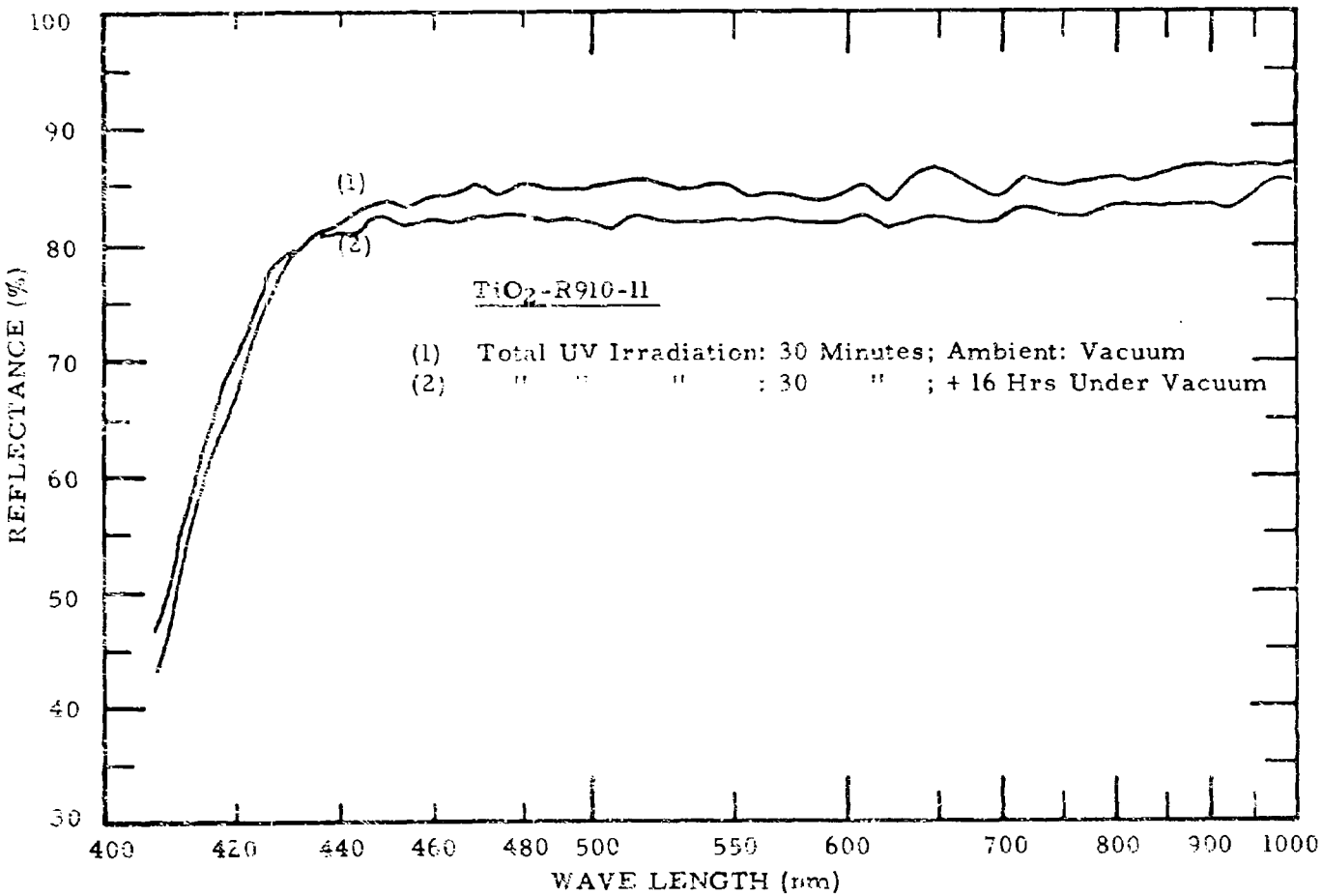

Fig. 16 - Reflectance Spectra for Conditions as Indicated

300168;1103/310168;0745

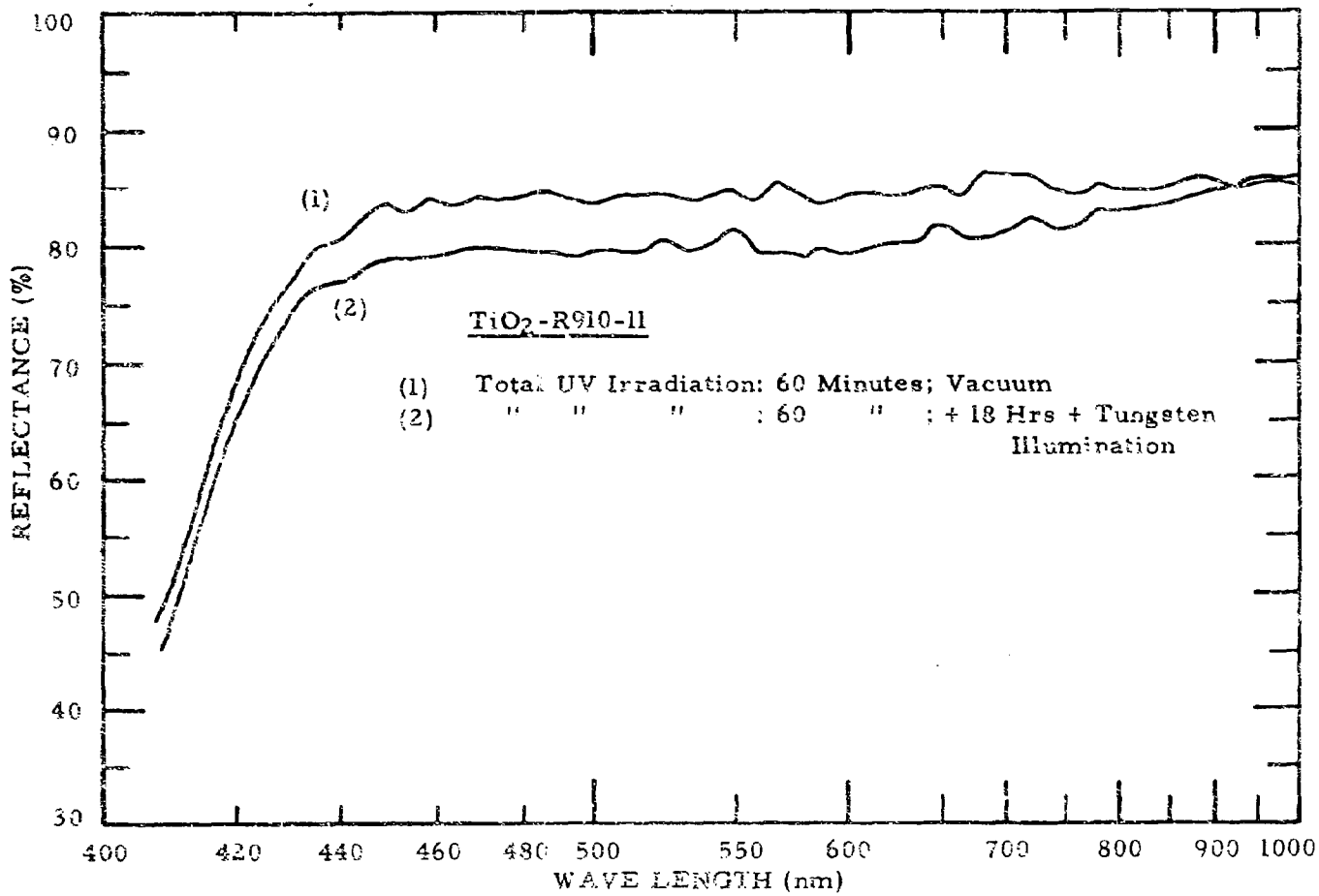

Fig. 17 - Reflectance Spectra for Conditions as Indicated

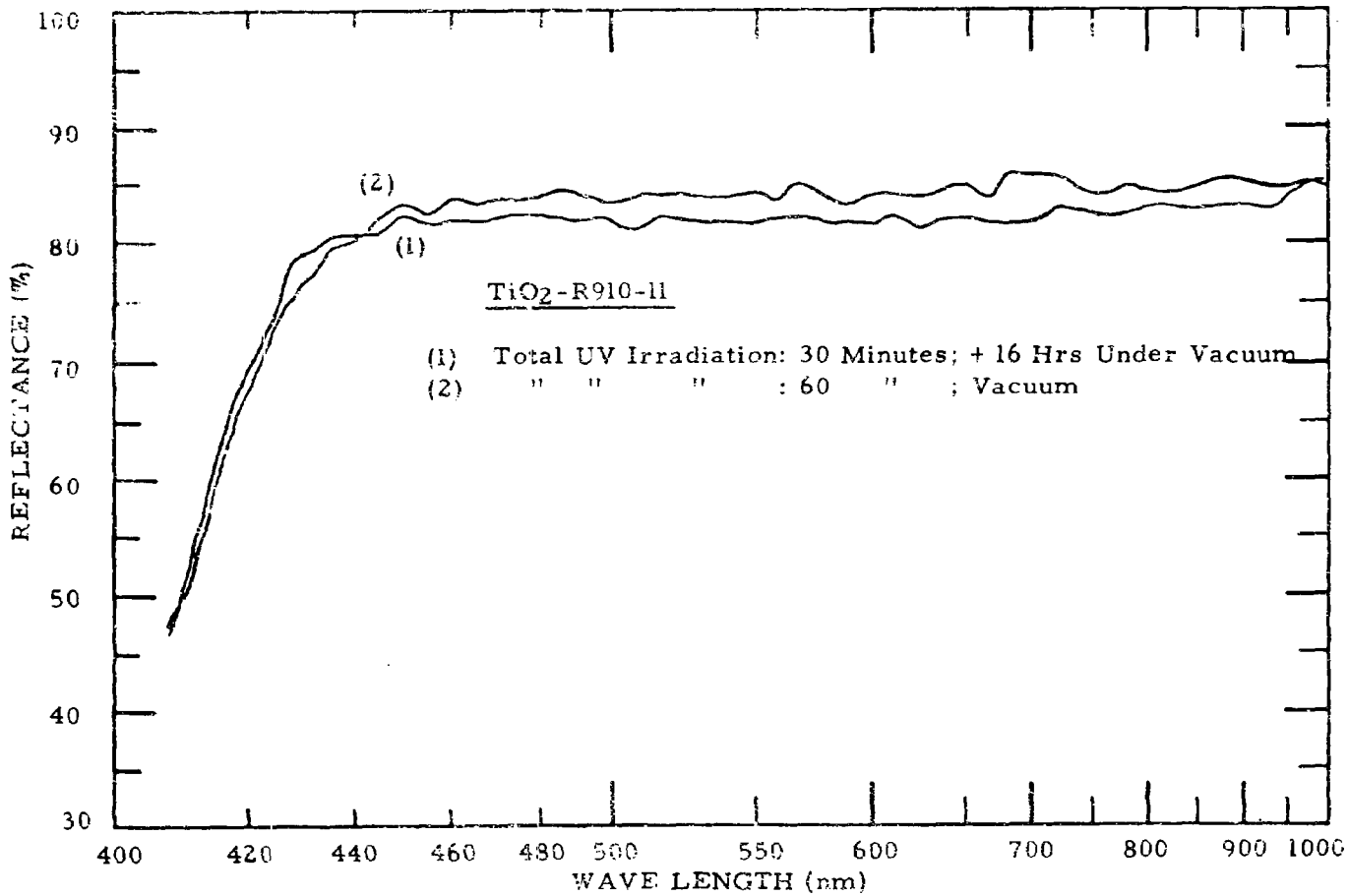

Fig. 18 - Reflectance Spectra for Conditions as Indicated

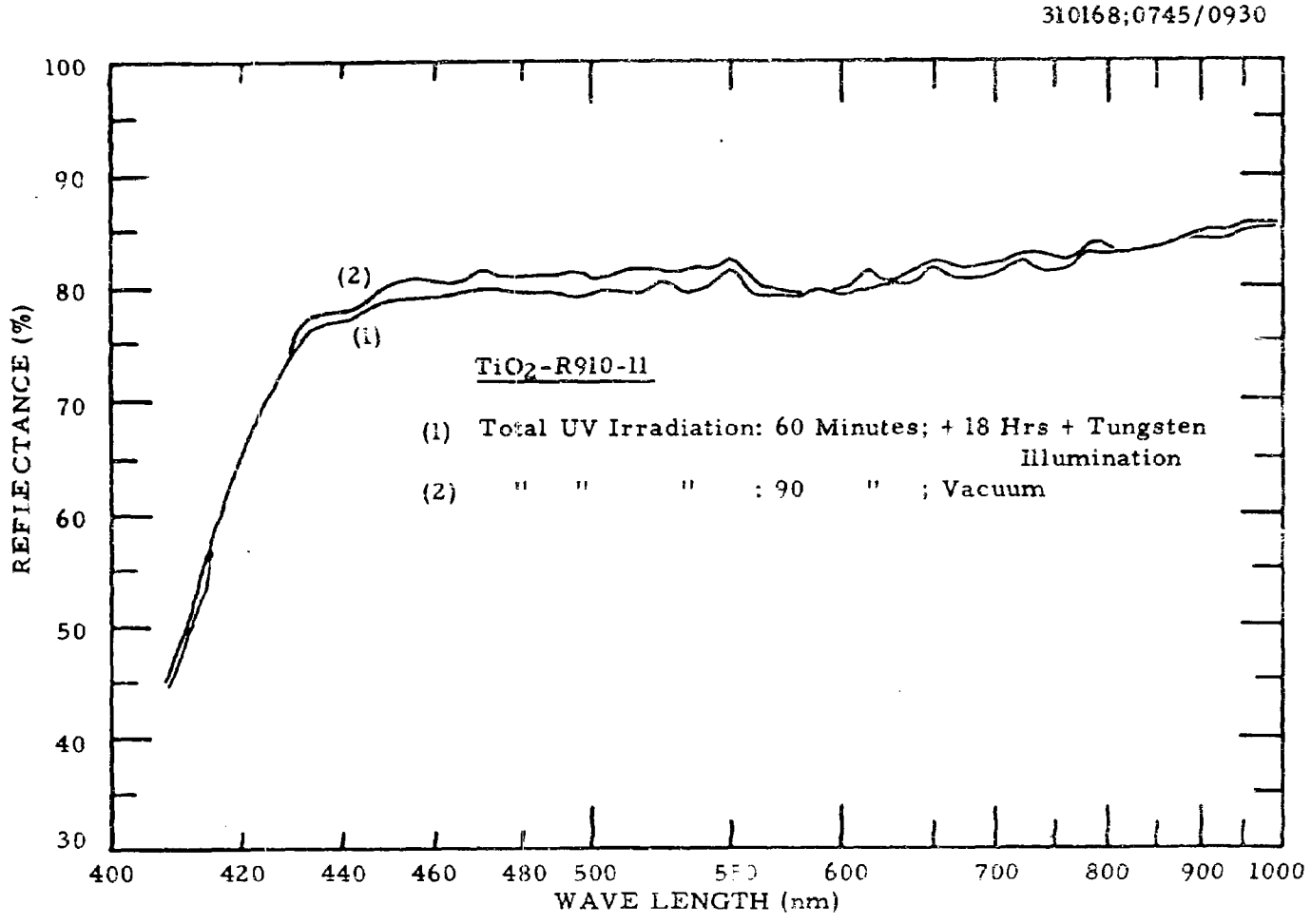

Fig. 19 - Reflectance Spectra for Conditions as Indicated

ambient atmosphere of 10 percent O_2/90 percent He. The reflectance spectrum at this stage is given by trace 1 of Figure 20. The oxygen was then removed and room air was admitted, which resulted in trace 2, taken immediately after the exchange. The air was then evacuated and the reflectance remeasured, which showed a large further recovery as indicated by trace 3 of Figure 20. The explanation for this is not clear. Initial measurements made on this specimen under vacuum and in air have shown no change. However, the specimen surface may well have been put into a nonstable condition as a result of the irradiations. The larger recovery under reduced pressure may be due to enhanced effectiveness of a surface-reactive constituent in the air on exchanging with the oxygenated surface. The reaction rate may be slower (less efficient) when the air is at atmospheric pressure than after removal where the residual reactive constituent is still abundant, while the increased mean-free-path may permit more effective exchange reactions to take place. However, the role that time plays is still not clear. In subsequent experiments, the reflectance change with uv irradiation showed no abnormalities (see Figure 5).

The different recovery resulting from exposure to oxygen and air may be seen in Figure 21. Trace 1 is the spectrum obtained after a total of 60 min of uv irradiation. This spectrum was then degraded by three irradiations of 30 min each, resulting in trace 2. Trace 3 gives the reflectance after exposure to an atmosphere of 10 percent O_2/90 percent He for 16 hr, and shows primarily a recovery in the near IR. When the oxygen is replaced by air and the reflectance is remeasured, the overall spectrum (trace 4) shows recovery.

010268;0710/0810/0910

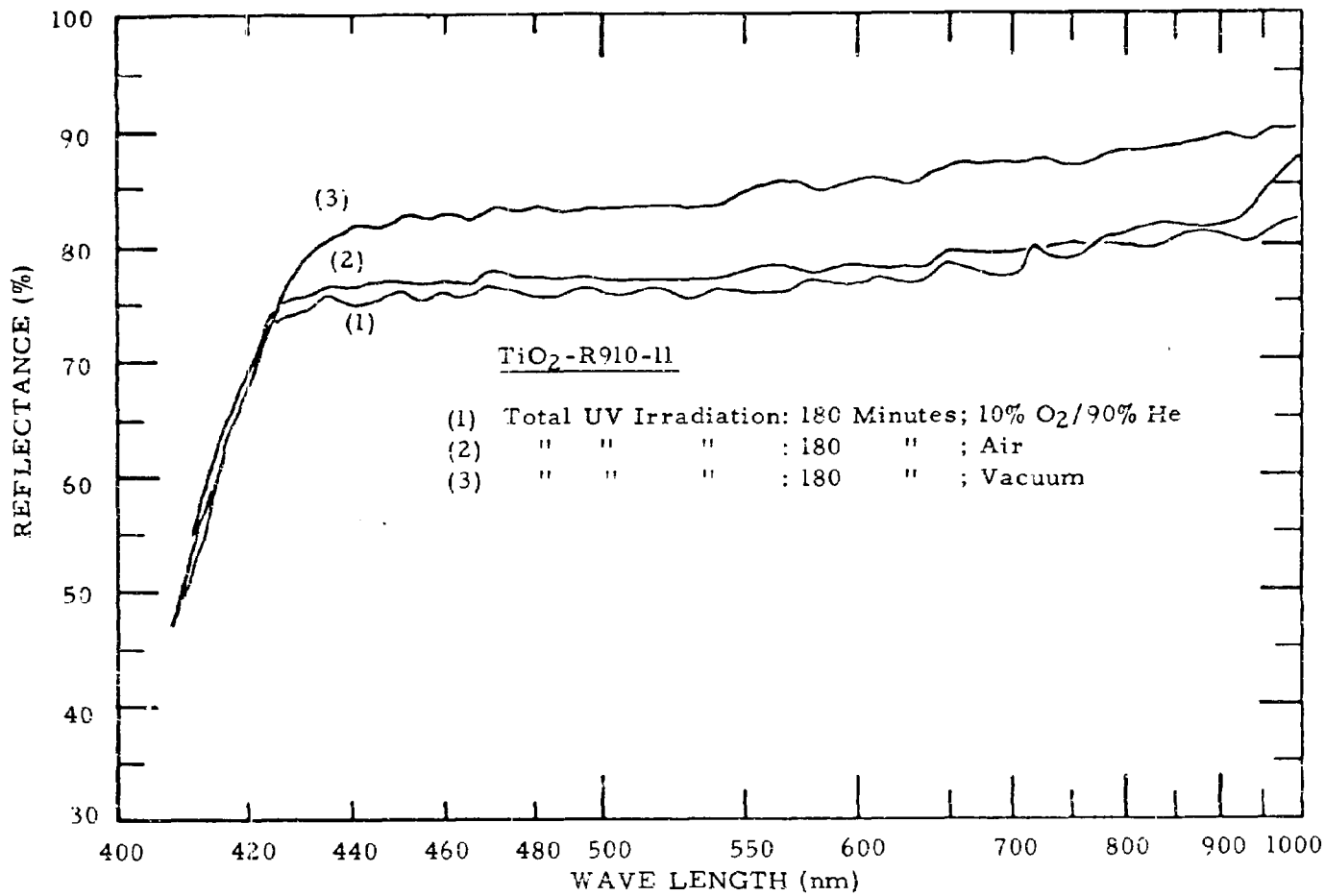

Fig. 20 - Reflectance Spectra for Conditions as Indicated

310168;0930/1515;010268;0710/0810

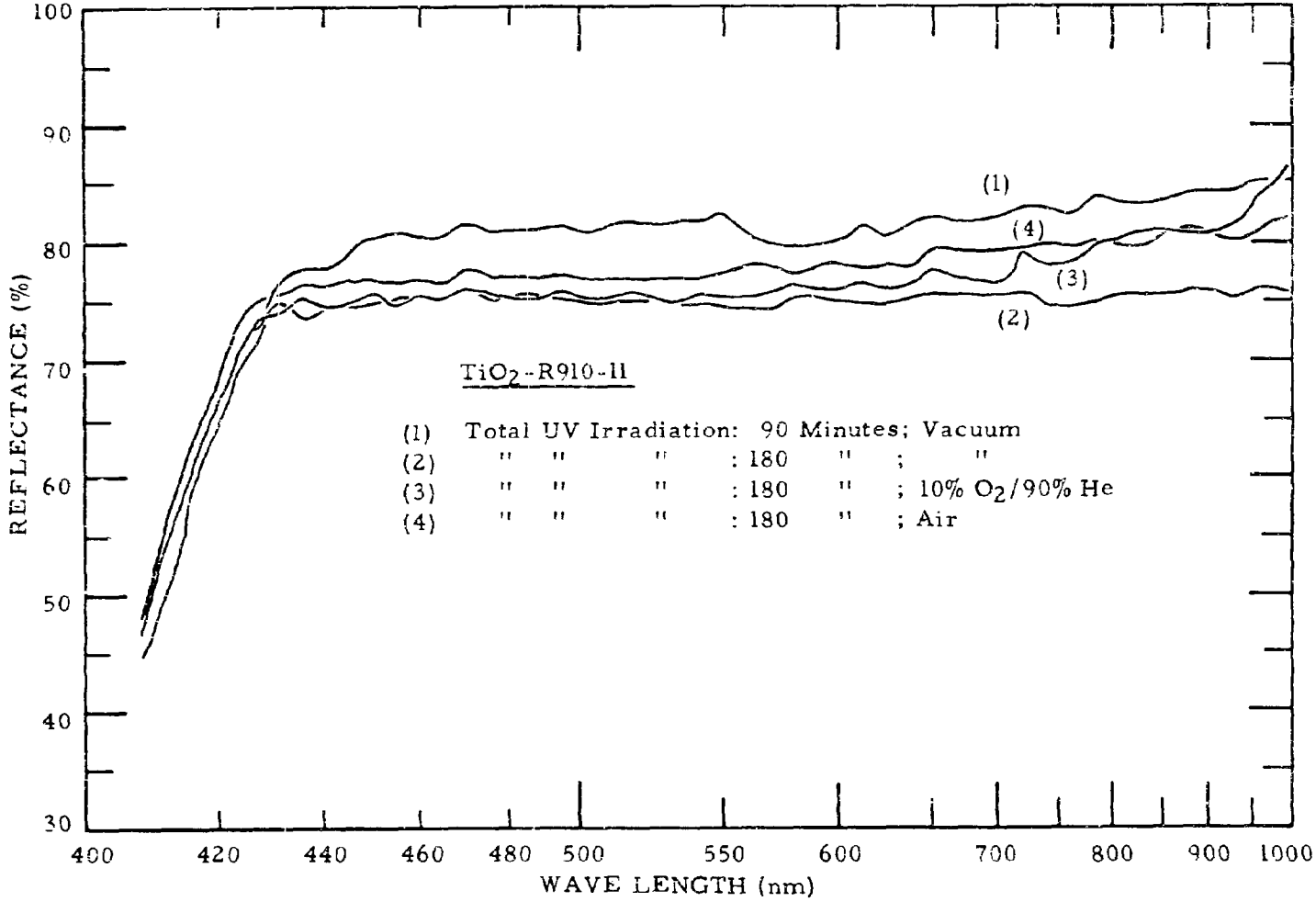

Fig. 21 - Reflectance Spectra for Conditions as Indicated

4.3 GAS EVOLUTION

Evolution of gas is associated with degradation of reflectance, and in all cases the only gas evolved has been positively identified as CO_2. No evolution of O_2 has been found (<0.1 of the CO_2). The amount evolved correlates with the degradation in reflectance, and both show a reduction in amount on successive exposures, leading to an eventual saturation in reflectance degradation and no evolution of gas. Exposure to air or oxygen causes recovery of reflectance, and subsequent reexposure to uv leads to further evolution of CO_2; and again no oxygen is detected. The amount of CO_2 is about as large as for the original exposure, and decreases to zero again after a number of exposures. The absolute amount of CO_2 corresponds to about 0.5 μgm/gm for TiO_2 samples. Since the samples contain in excess of 100 ppm of carbon, continued evolution of CO_2 is not surprising. The CO_2 is not an artifact of the measurement system. This became clear during some measurements made in a parallel program, funded by Gulf General Atomic, on coloration by uv light of alkali halide powders. It was found that coloration of powdered materials can be achieved although large single crystals of the same material are not colored. Of importance from the point of view of the present program is the fact that although evolution of CO_2 was seen during the first irradiation, this was simple degassing of adsorbed CO_2 and continued evolution was not found. The CO_2 evolution found from oxides is thus not an artifact of the gas chromatograph apparatus.

In Figure 22 a correlation is shown between CO_2 evolution and reflectance change produced by uv irradiation of R-910 rutile powder. The upper portion of the figure shows the amount of CO_2, expressed as moles of gas, which had been evolved for a given total uv irradiation time. Following 3 hr of irradiation, the sample was kept in an atmosphere of 10 percent O_2/90 percent He for about 16 hr. This was then replaced by air for about 1/2 hr before the uv irradiations were continued, in 30-min increments. The CO_2 evolution data seem to show a trend toward exhaustion, which was estimated by the extrapolations and asymptotic end values as indicated. The data were therefore replotted as shown in the central portion of Figure 22, with a logarithmic scale representing the amount of CO_2 expected to be evolved. It appears that there may be some validity for the underlying exhaustion hypothesis. The bottom portion of Figure 22 shows the reflectance at λ = 450 nm at the corresponding times. The gas evolution and reflectance changes obviously correlate, but a more detailed analysis from these experiments is unwarranted in view of the number of varied experimental conditions which were imposed on the specimen. However, it is clear that

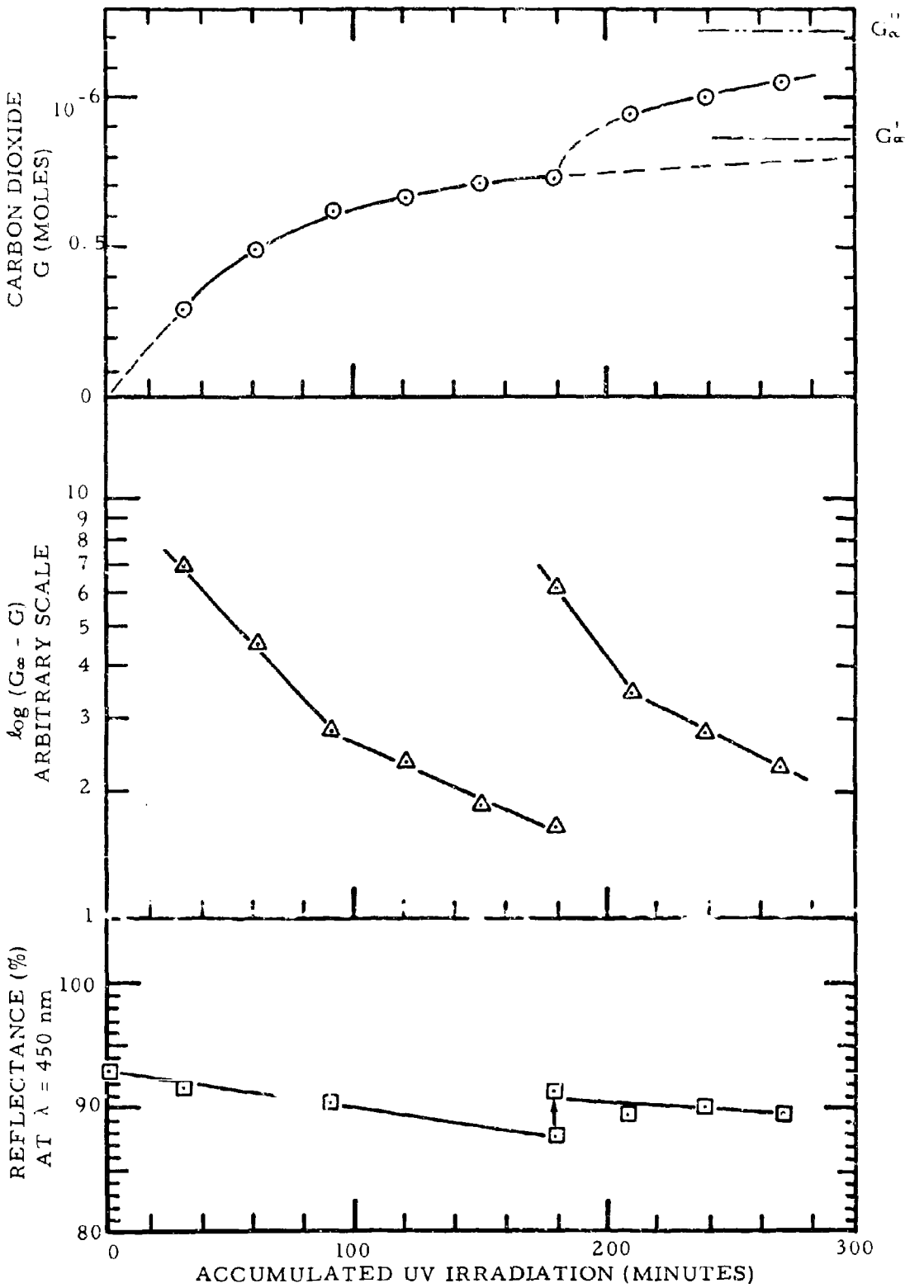

Fig. 22 - CO_2 Evolution and Reflectance as Function of Accumulated uv Irradiation Time

1) CO_2 is the only gas evolved.

2) There is a correlation between the extent of CO_2 evolution and of reflectance reduction.

CO_2 is also evolved in small amounts from rutile pigments when they are heated. This evolution begins at temperatures as low as 125°C, and presumably part is associated with adsorbed CO_2 and decomposition of carbonates. However, most of the evolution is associated with reduction of the rutile.

4.4 COMPARISON OF TiO_2 TREATED IN VARIOUS WAYS

A series of measurements has been initiated for the purpose of comparing the properties of TiO_2 that has been irradiated with charged particles with those of TiO_2 irradiated with uv light and also with those of TiO_2 that has been chemically reduced. Thus far, measurements have been made of the frequency-dependent conductivity of single-crystal TiO_2, electron irradiated and unirradiated, and uv chemically reduced TiO_2 powder. EPR measurements have also been made on the latter, giving a single line spectrum 13 gauss wide centered at g = 2.0068. No useful comments can be made at the present time, since the data are not complete. Some examples of frequency-dependent conductivity data are given in Figure 23 for rutile powder, one specimen of which had been electron beam irradiated. The behavior of the single crystal, see Figure 24, appears to be similar to that noted by Pollak and Geballe[7] for hopping conduction in silicon and attributed to electrons hopping between states localized around acceptor or donor impurities.

4.5 SURFACE TEMPERATURE OF RUTILE POWDER SAMPLES

It is planned to measure the variation with temperature of the damage rate to pigment materials by uv radiation, as this will give information on the activation energies of the processes involved. To obtain reliable results, it is necessary to know the temperature of the pigment itself during intense irradiation from mercury lamps, which may be expected to have a large heating effect, particularly when the samples are in vacuum. To study this, the change in the short-wavelength cutoff of reflectance is used as a monitor of temperature. A sample is mounted on a holder; the sample temperature is controlled by circulating fluid in the range 10° to 170°C. The holder is enclosed in a vacuum chamber, equipped with three windows. A central quartz window enables the sample to be irradiated by an AH 6 mercury lamp, whose distance can be adjusted to give up to 7 suns at the sample position. To avoid extended irradiation and possible

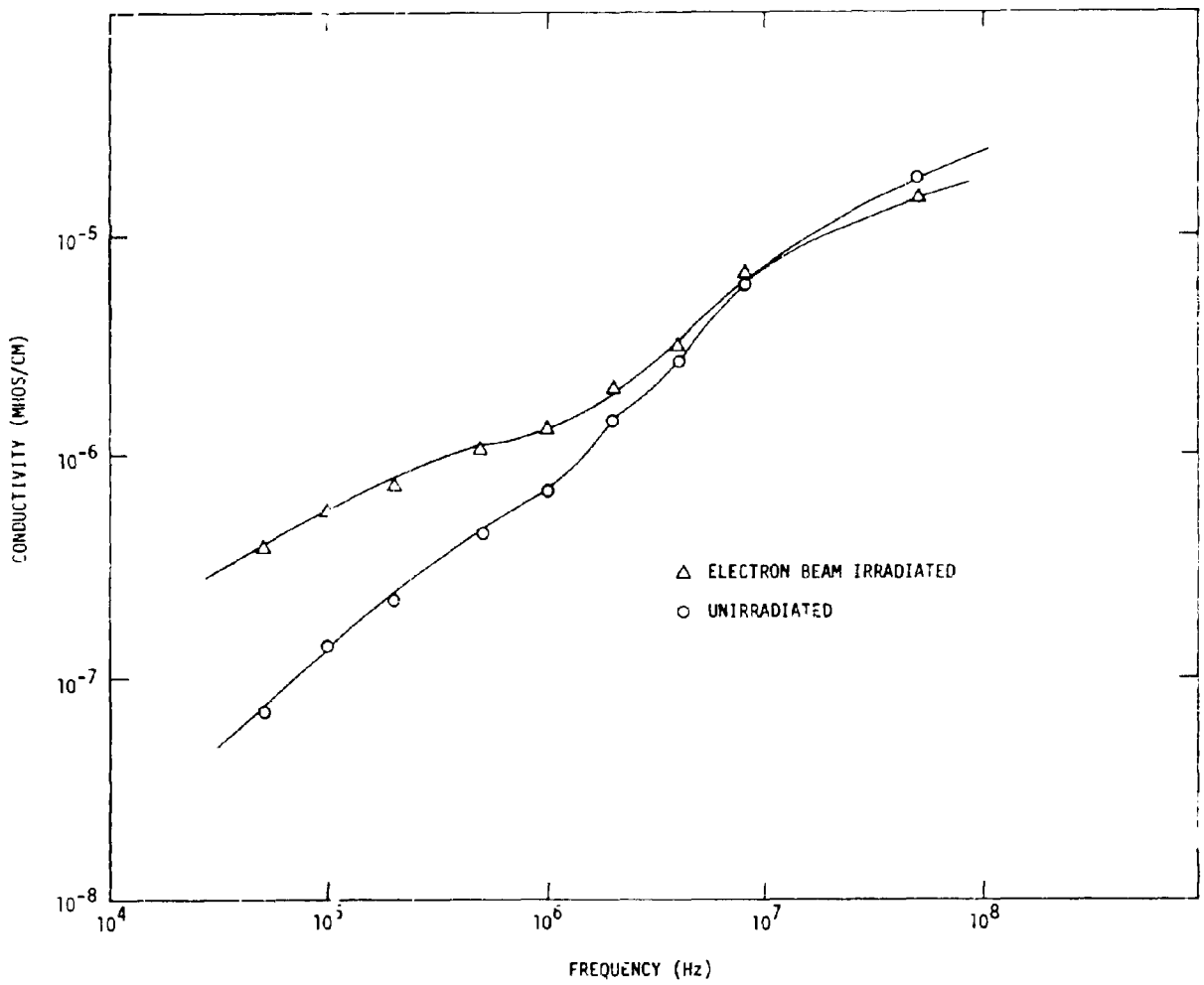

Fig. 23 - Conductivity of TiO_2 (Rutile) vs Frequency of the Applied Field.

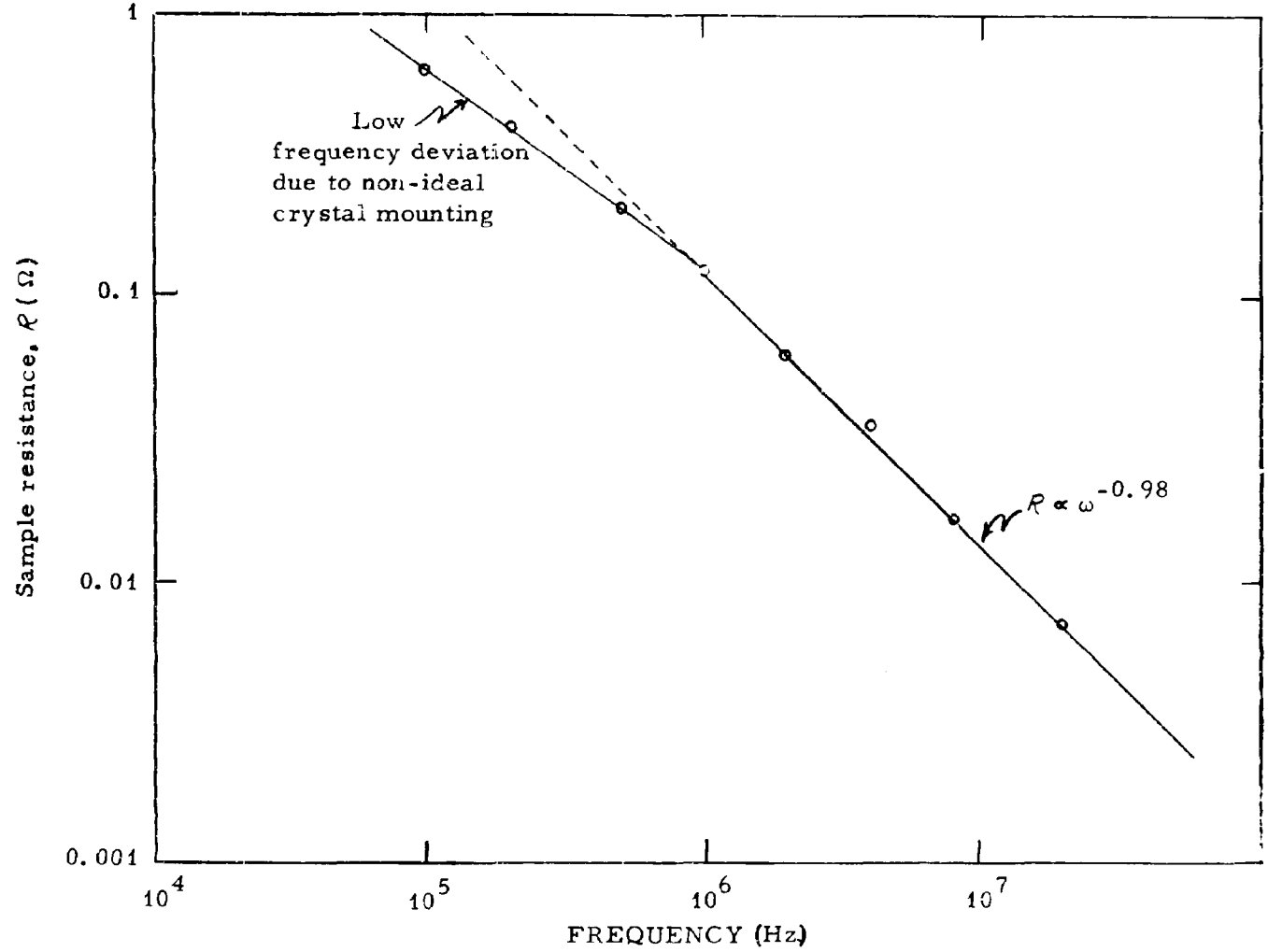

Fig. 24 - Resistance of TiO_2 (Rutile) vs. Field Frequency, f

consequent damage to the sample, a removable shutter is placed in front of the lamp. Windows are also provided for the entrance and exit of a beam of light used to measure the reflectance. This light is derived from a tungsten lamp and is chopped by a wheel at 510 Hz. The light diffusely reflected from the sample leaves through the exit window and some of it enters a Jarrell-Ash 0.75-meter grating monochromator, set to give a band width of 2 Å. The light emerging from the monochromator is detected by an RCA 6199 photomultiplier tube, whose output is fed to an AC amplifier and phase-sensitive detector, tuned to 510 Hz. With a sample in place, the monochromator is then scanned to give the reflectance near the short-wavelength cutoff for rutile.

The wavelength at a reflectance halfway between maximum and minimum was taken to be the cutoff wavelength, λ_c. The variation of λ_c with the temperature of the sample holder was then measured, and the sample temperature was assumed to be that of the holder. The cutoff wavelength λ_c was near 4300 Å at 20°C, and shifted to the red by ~ 1 Å/°C at 20°C, increasing to ~ 1 Å/°C at 150°C. The value of λ_c could be red to ~ 4 Å; i.e., the temperature could be determined to 4°C. The AH 6 lamp was then turned on, which greatly increased the noise on the output of the phase-sensitive detector. It was still possible, however, to make measurements of λ_c, although only within an accuracy of 10 Å. The temperature rise was determined for three samples: 1) loose powder in the tray, 2) a pressure-compacted, somewhat friable disc 0.1 in. thick, and 3) a water-sprayed layer ~0.003 in. thick on aluminum. The temperature rose to a maximum value in ~ 30 sec after removal of the shutter from in front of the AH 6 lamp. At 7 suns intensity, the loose sample temperature was estimated to by 200°C when the holder was at 20°C; the compacted sample indicated 50° to 60°C and the water-sprayed sample indicated 25° to 35°C.

It is concluded that care is needed in making measurements at high equivalent sun levels, and that measurements of intensity-dependence of damage rates may include a component from the increased temperature at higher sun levels. However, water-sprayed samples appear to have enough thermal conductivity to present no major problems.

4.6 MEASUREMENTS OF REFLECTANCE CHANGES PRODUCED BY IRRADIATION USING CONVAIR IN-SITU REFLECTOMETER

4.6.1 Comparison of Reflectometers

A comparison was made by transferring the samples from the vacuum reflectometer to a Convair Cary 14 spectroreflectometer equipped with a specially designed integrating sphere and transfer optics. Typical results are shown in Figure 25 for a coating of R-910 rutile with PS-7 binder. Both measurements were made in air. As can be seen, there are noticeable differences, and the reasons for these are being investigated. One possible source of difference is the mode of illumination of the spheres, which can be accomplished in two ways. In Type A, the system used in Convair's modification of the Cary 14, the sphere is illuminated with a broad spectrum of light and the reflected light is measured as a function of wavelength. In Type B, the Edwards system used in the vacuum reflectometer, the sphere is illuminated with monochromatic radiation and the reflected light is detected with a broad spectrum detector.

The selection of the type of illumination requires careful consideration of the problems involved. One problem, which has only recently been recognized is that of sample fluorescence. Paints containing the pigments used for spacecraft thermal coatings often fluoresce when irradiated with uv light. The fluorescent radiation from the sample usually falls in the green, yellow, and red portions of the spectrum. This can produce an error in the measurement of reflectance for either type of illumination.

Consider Type B illumination. When the monochromatic light is from the uv region, a fluorescent sample would give radiation in the green to red portion of the spectrum, and this radiation would be recorded by the broad spectrum detector to give an erroneously high reading for the uv reflectance. When the monochromatic light is from the visible portions of the spectrum, no difficulty would be encountered unless the paint fluoresces under excitation by visible light; this does not seem to occur for materials used for paints of importance. Now consider Type A illumination. In the uv portion of the spectrum the instrument should give the correct reflectance value; even though fluorescence in the green to red region is occurring, the monochromator does not record it. However, when the visible portion of the spectrum is scanned on the spectrophotometer, a high value for the reflectance will be obtained in the green, yellow, and red portions of the spectrum due to absorption by the sample of light in the uv part of the spectrum, and reradiation in the green, yellow, and red end of the spectrum. Thus,

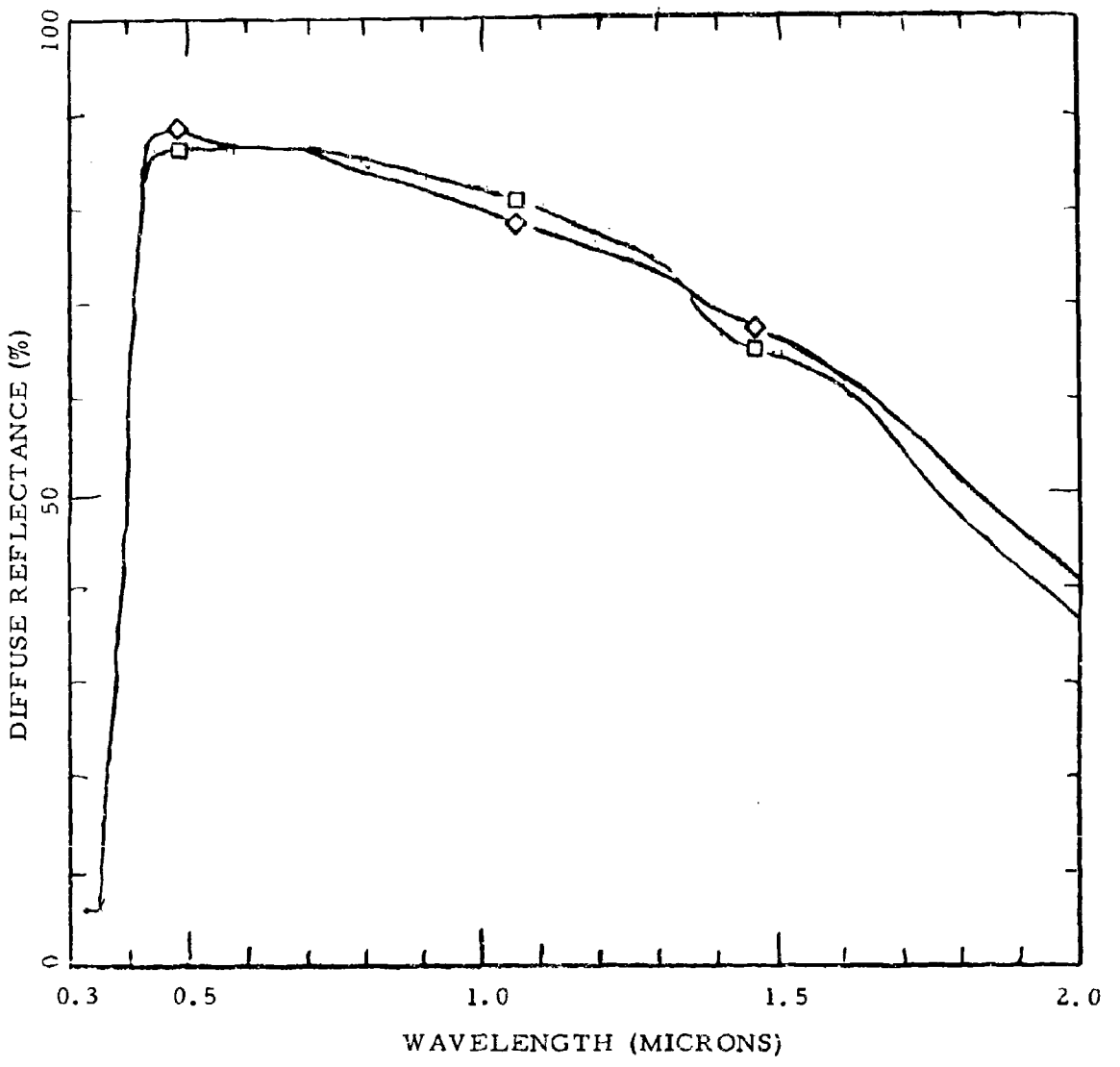

Fig. 25 - Comparison of Beckman DK2A (◇) and Cary 14 (□)

for both types of illumination a fluorescence error can occur, but in different regions of the spectrum.

In the present procedure the Cary 14 instrument measures the reflectance of all samples before insertion into and after removal from the vacuum reflectometer.

Results were obtained with the vacuum reflectometer at Convair and the reflectometer at Gulf General Atomic using the same sample, and good agreement was found.

4.7 REFLECTANCE DEGRADATION MEASUREMENTS

In this section, the results obtained using the Convair in-situ reflectometer to perform measurements of rutile degradation are presented. In all cases the absolute diffuse reflectance is plotted as a function of wavelength. The data are presented in groups of curves plotted using uv irradiation, electron irradiation, ambient condition (air, vacuum, or oxygen mixture), time, or other variables as a parameter.

The first specimen coupon (TiOx-R-910/PS7-11) was prepared from DuPont R-910 stabilized rutile titanium-dioxide powder by spraying with Sylvania PS7 potassium silicate binder as described above. The response of this sample to uv exposure in vacuum is shown in Figure 26 for various accumulated irradiation times. Also shown is the reflectance spectrum taken in air when the sample was first installed, about a week before the irradiation run was started. The curve for the initial reflectance in vacuum is incomplete at the lower wavelength due to temporary failure of the photomultiplier detector. Evacuation appears to increase the reflectance over the entire spectral range. The irradiation by uv is seen to result in degradation, which is more rapid initially, with the IR region becoming increasingly more resistant to further degradation.

After a total exposure of 100 esh had been reached, the sample was exposed to oxygen so that recovery effects could be studied. As seen in Figure 27, the resulting reflectance increase is relatively small. The average reflectance change was ≤1 percent, and the uv exposure sequence was therefore continued. The reflectance after an additional uv irradiation of 80 esh (to a total of 180 esh) after the oxygen had been removed from the vacuum chamber is compared in Figure 28 with the reflectance measured in oxygen. The degradation continued to be more pronounced at the shorter wavelengths.

The sample was then exposed to air, rather than just oxygen, to check for recovery characteristics. As shown in Figure 29, the reflectance recovery is minimal, the most pronounced effect occurring in the IR. The uv irradiation schedule was therefore resumed. The reflectance after exposure to a total of 445 esh is plotted in Figure 30. Although the decrease is definite, it should be noted that the exposure increment is greater than the entire exposure to this point, which lends emphasis to the observation that the damage occurs almost entirely during the first portion of the irradiation.

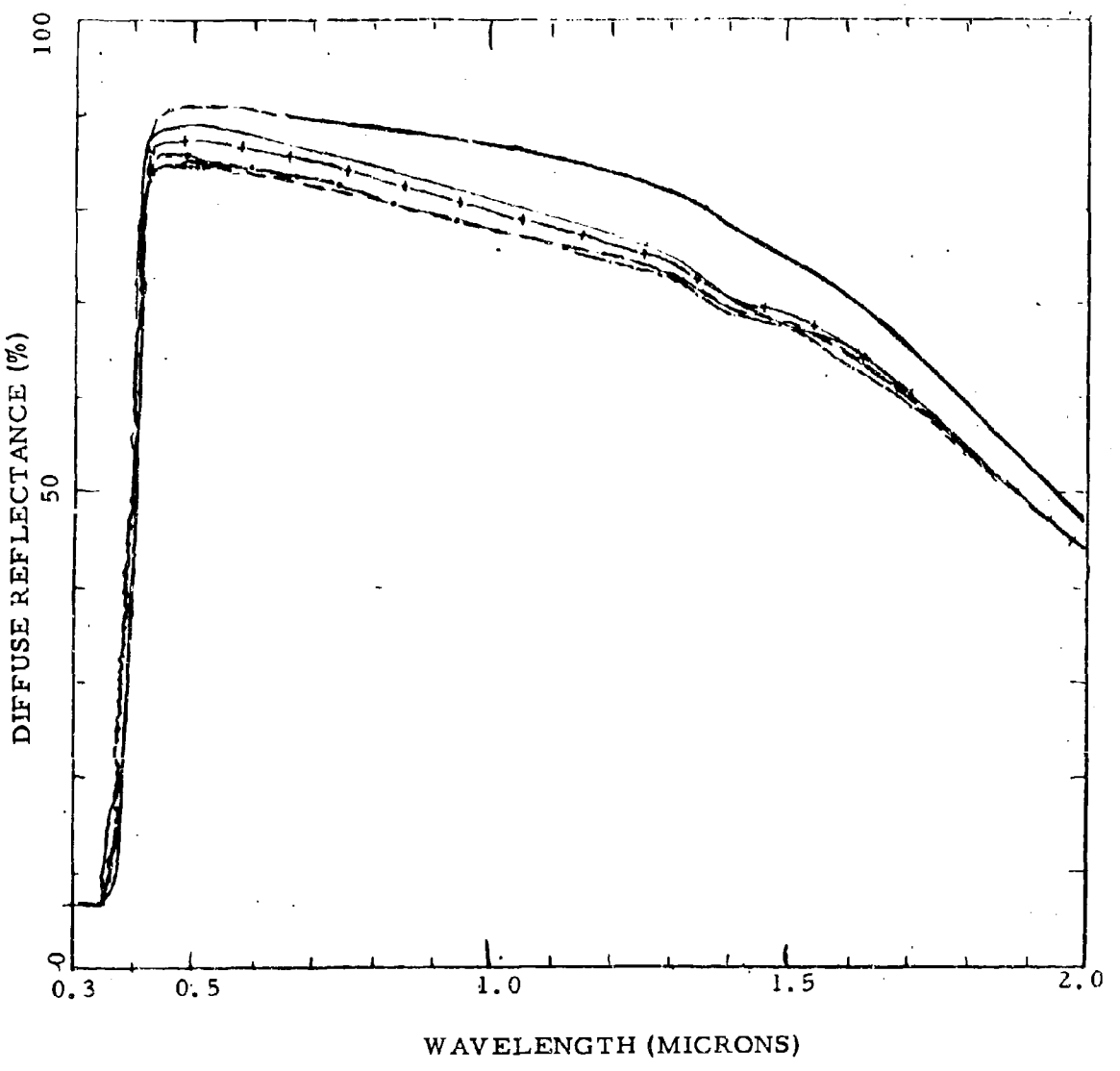

Fig. 26 - Effect of Exposure to 100 esh of uv

(— — ——initially in vacuum; ——— initially in air; —+— 5 esh; —·—10 esh; — —80 esh; ···· 100 esh)

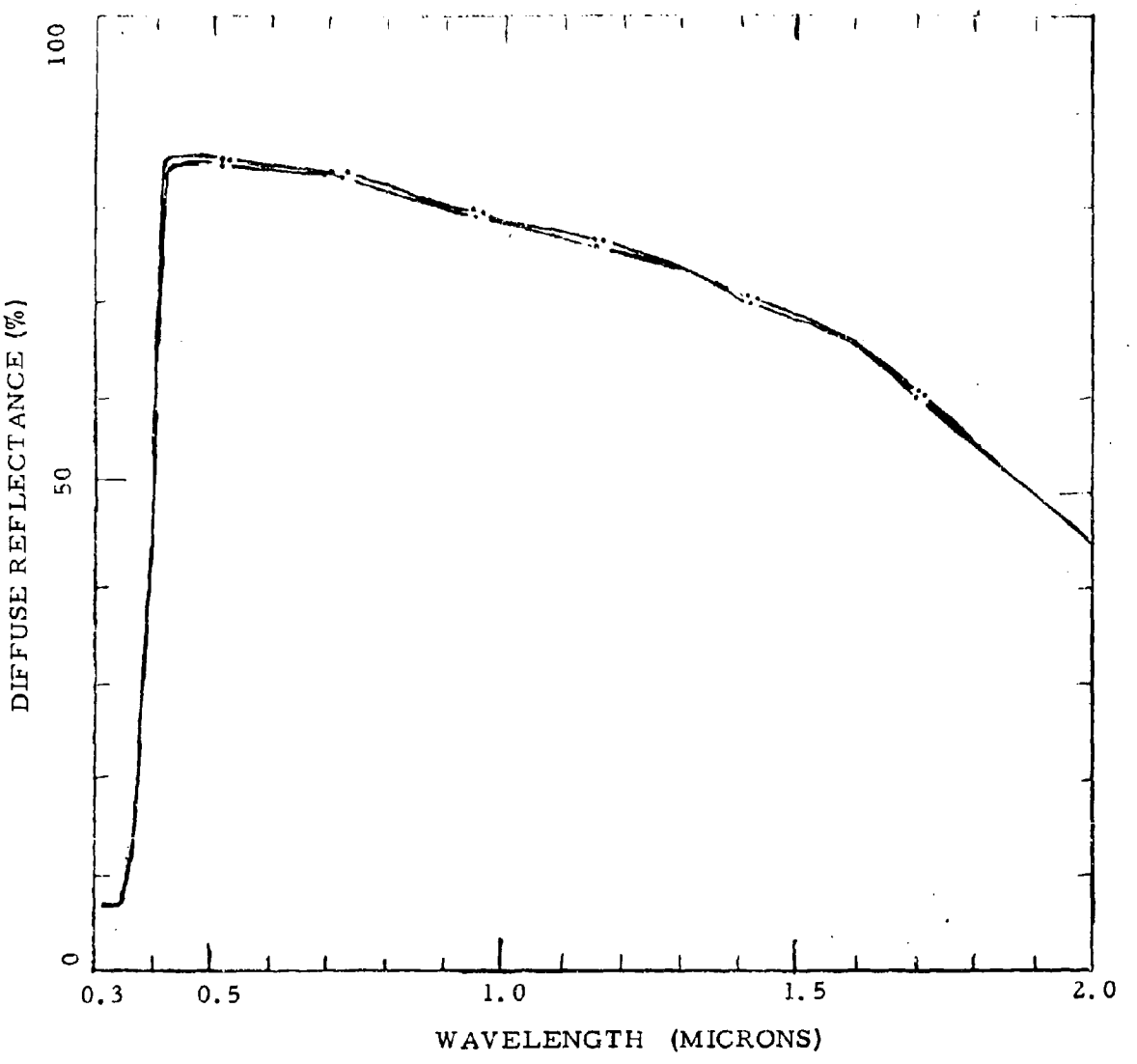

Fig. 27 - Effect of Recovery Due to Oxygen

(– · – at 100 esh; — · · — after O_2 admitted)

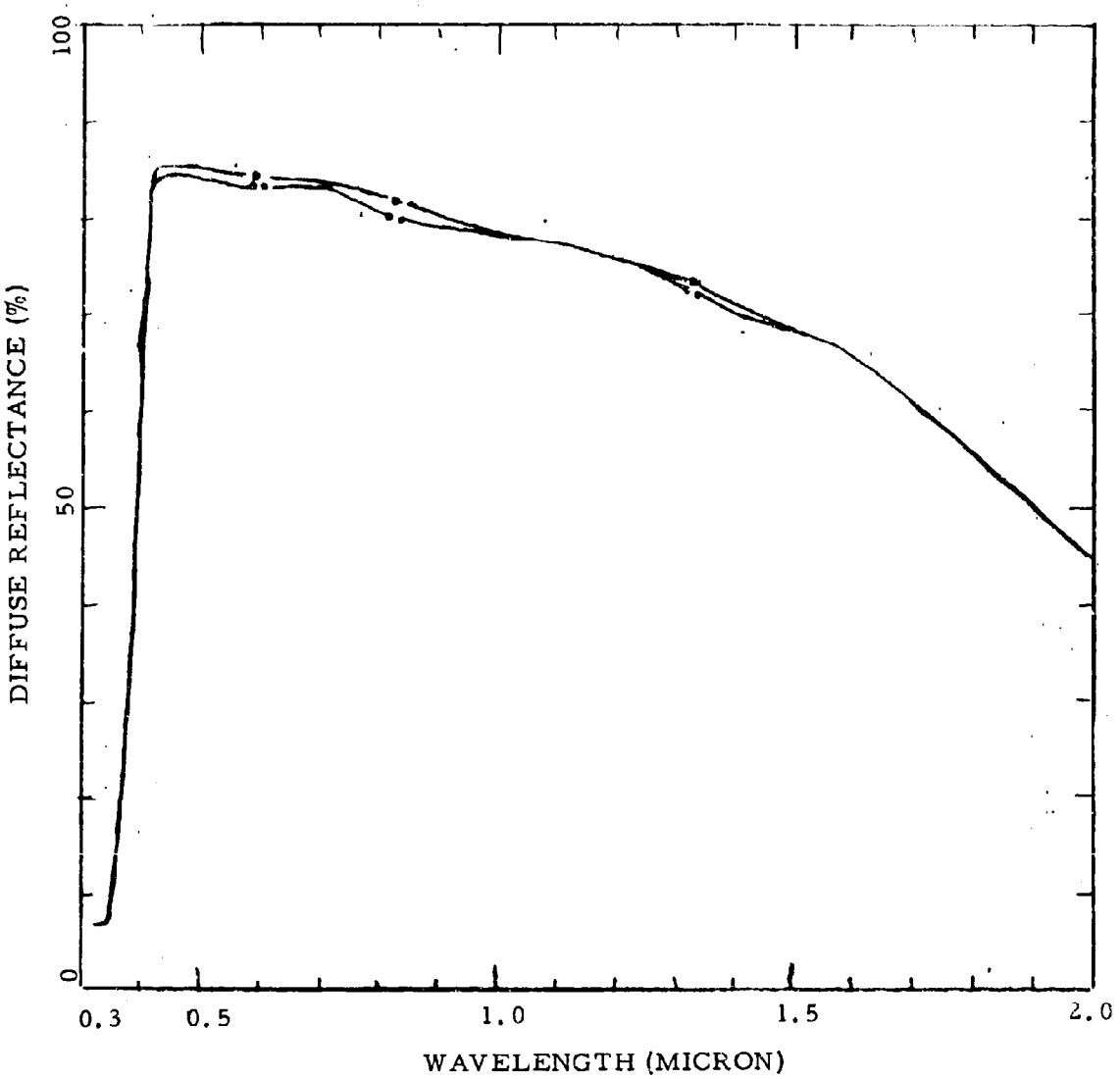

Fig. 28 - Effect of Continued uv After Oxygen Exposure

(—·— in O_2 after 100 esh;——··——after 180 esh, in vacuum)

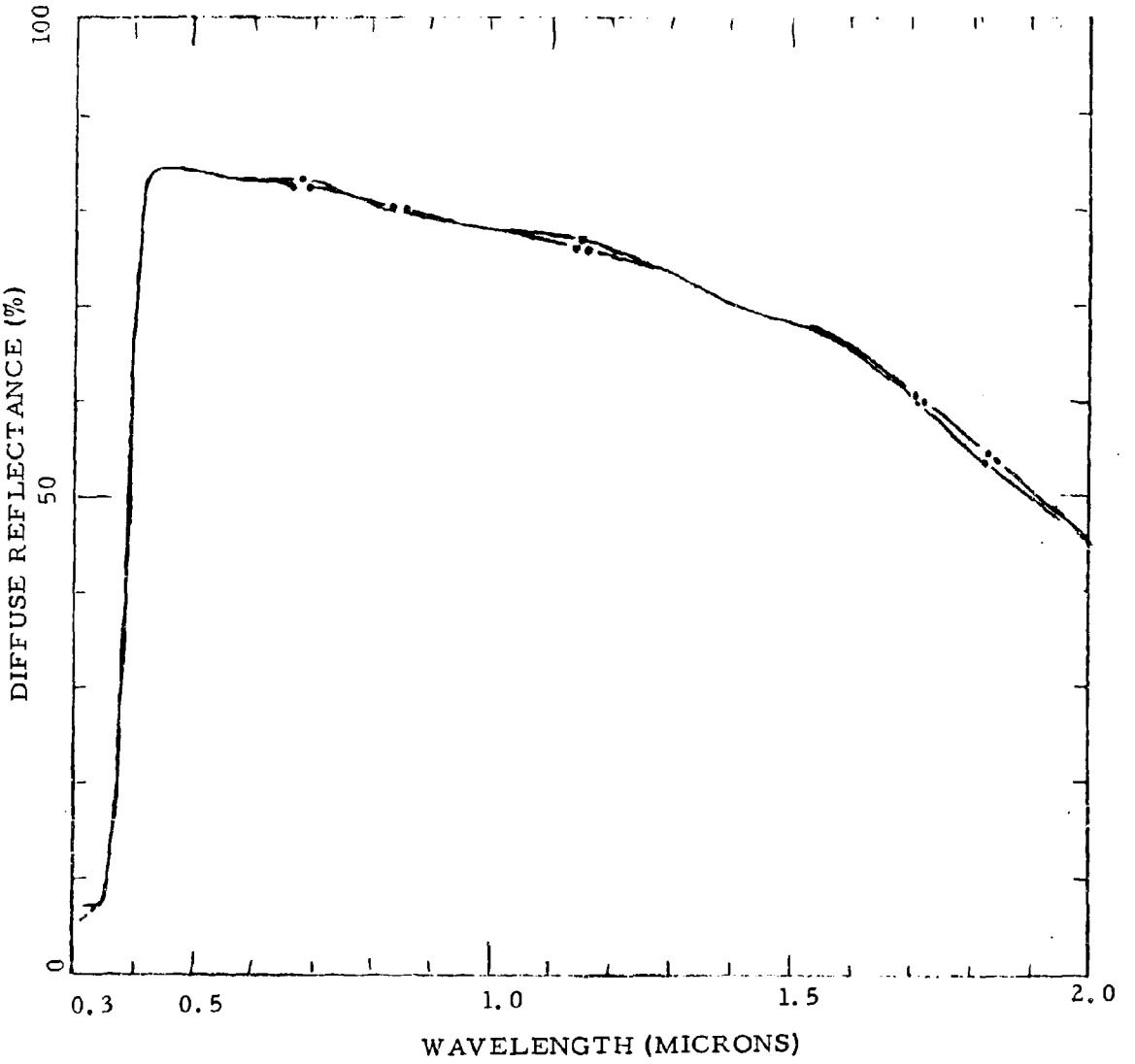

Fig. 29 - Effect of Exposure to Air after Total 180 esh uv

(— · — in vacuum at 180 esh; — · · — in air)

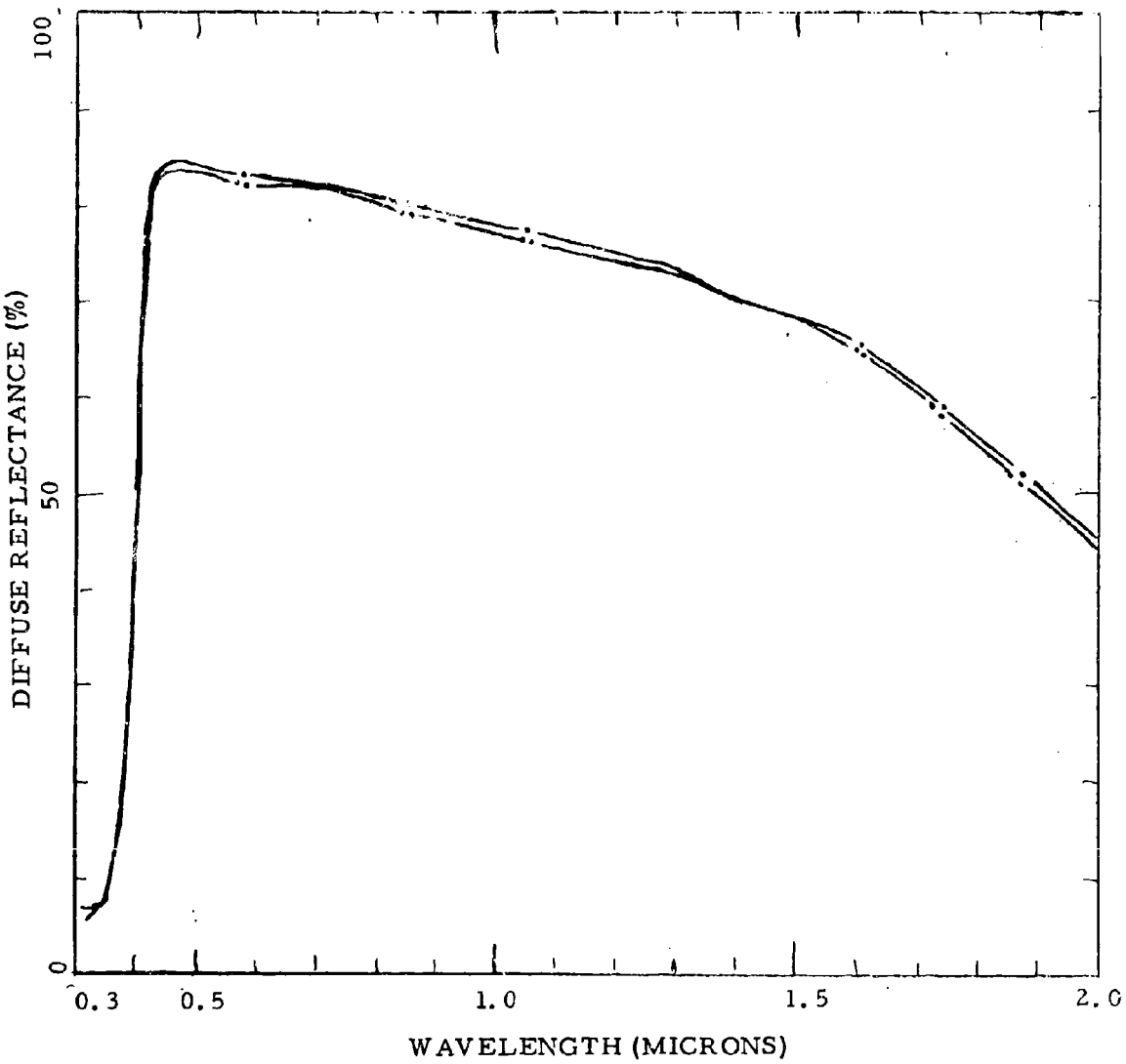

Fig. 30 - Effect of Continued uv Exposure to Total of 445 esh

(— · — at 180 esh; — · · — at 445 esh)

The next irradiation of the specimen was of a particulate nature, namely by 2-MeV electrons. The bombardment was conducted without breaking the vacuum or removing the specimen from the apparatus. The reflectance after the sample was exposed to an electron flux of $10^{12}/cm^2$ is compared in Figure 31 with the reflectance spectrum at the end of the 445-esh uv irradiation. The reflectance decrease is small and is uniform over the entire spectrum except for the low wavelength region, which seems unaffected. The specimen was then left in vacuum and reexamined after 7 days, with the results shown in Figure 32. The sample was remeasured again after 65 days had elapsed from the time of the bombardment; during this time the specimen was exposed to the same gaseous ambients used for the experiments on the succeeding sample (TiOx-R-910/PS7-12), although it was shielded from uv and electron irradiation. Examination of the curves of Figure 32 shows that for wavelengths of $<1\ \mu$, the effect of the 7-days period of standing was to remove the reflectance damage produced by the electron bombardment. After the 65-day period, much of the combined damage history had disappeared, and the sample had a final reflectance spectrum similar to its spectrum after 10-esh uv irradiation (shown in Figure 26).

The effect of cumulative uv irradiation has been summarized in Figure 33. The small recoveries due to admission of oxygen and air, described above, have been graphically adjusted in the construction of the curves. The initial vacuum response curve has been extrapolated for $< 0.65\ \mu$ and is indicated by a dotted line. This composite graph shows that this specimen was very sensitive to the initial uv irradiation. However, it must be recalled that the reflectance of the sample had apparently been markedly "improved" by its initial exposure to the vacuum ambient (Figure 26). There appears to be more degradation at the lower wavelengths but the effects reach into the IR to $\sim 1.5\ \mu$. The general fall-off with increasing wavelength of the diffuse reflectance spectrum, starting in the visible, appears to be due to the effect of the binder, since the spectra of the pure pigment generally appear flat before irradiation.

A second sample, made at the same time and having the same composition as the first was also measured*. This specimen (designated TiOx-R-910/PS7-12) was mounted simultaneously with the first sample

* The intention was to study the effects of electron irradiation made before uv irradiation. A third sample was to have had simultaneous irradiation with uv and electrons, but this experiment has not been performed.

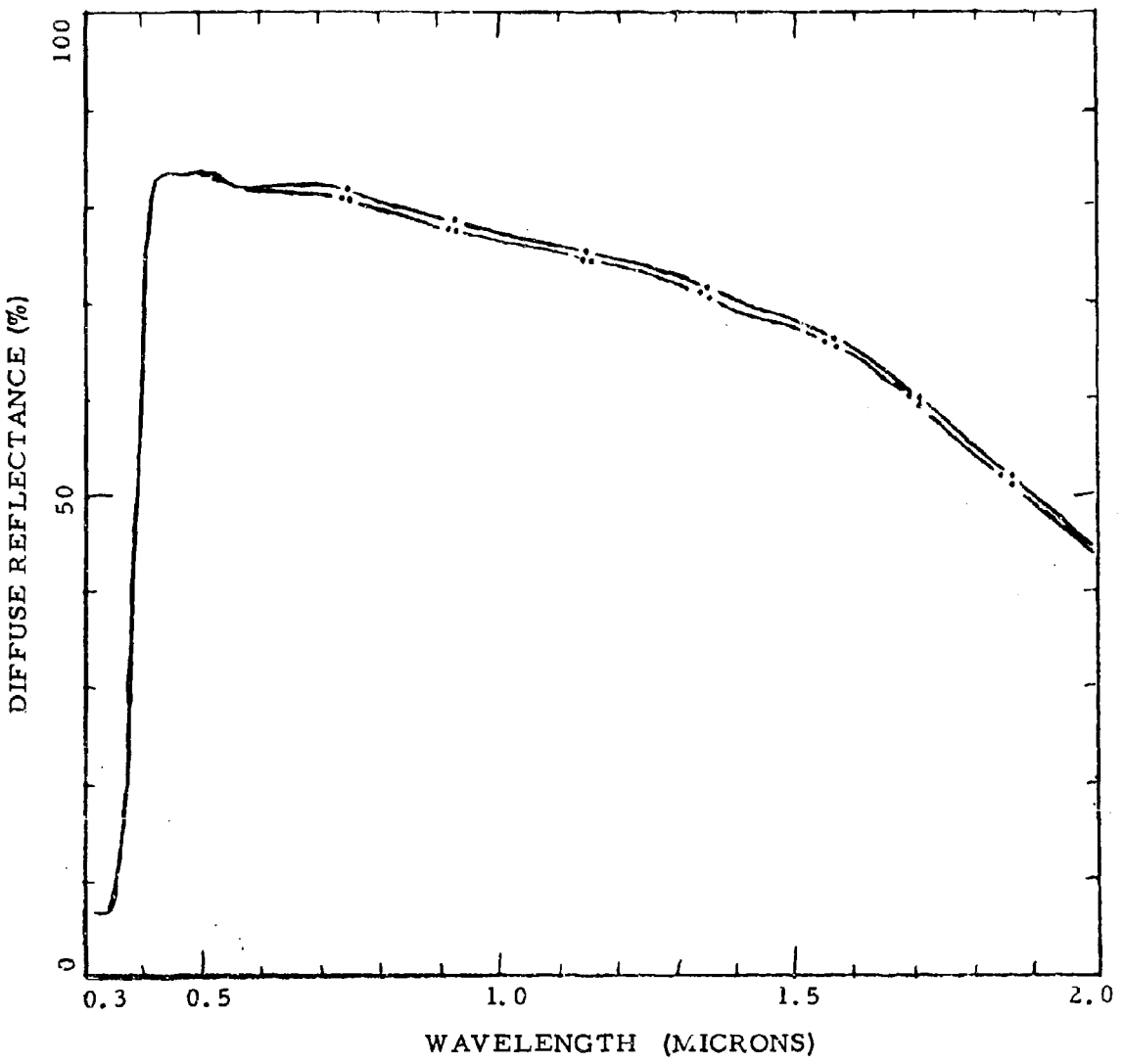

Fig. 31 - Effect of Electron Irradiation After Total 445 esh uv

(— · —at 445 esh; – – – – after 10^{12} e/cm^2 (2MeV))

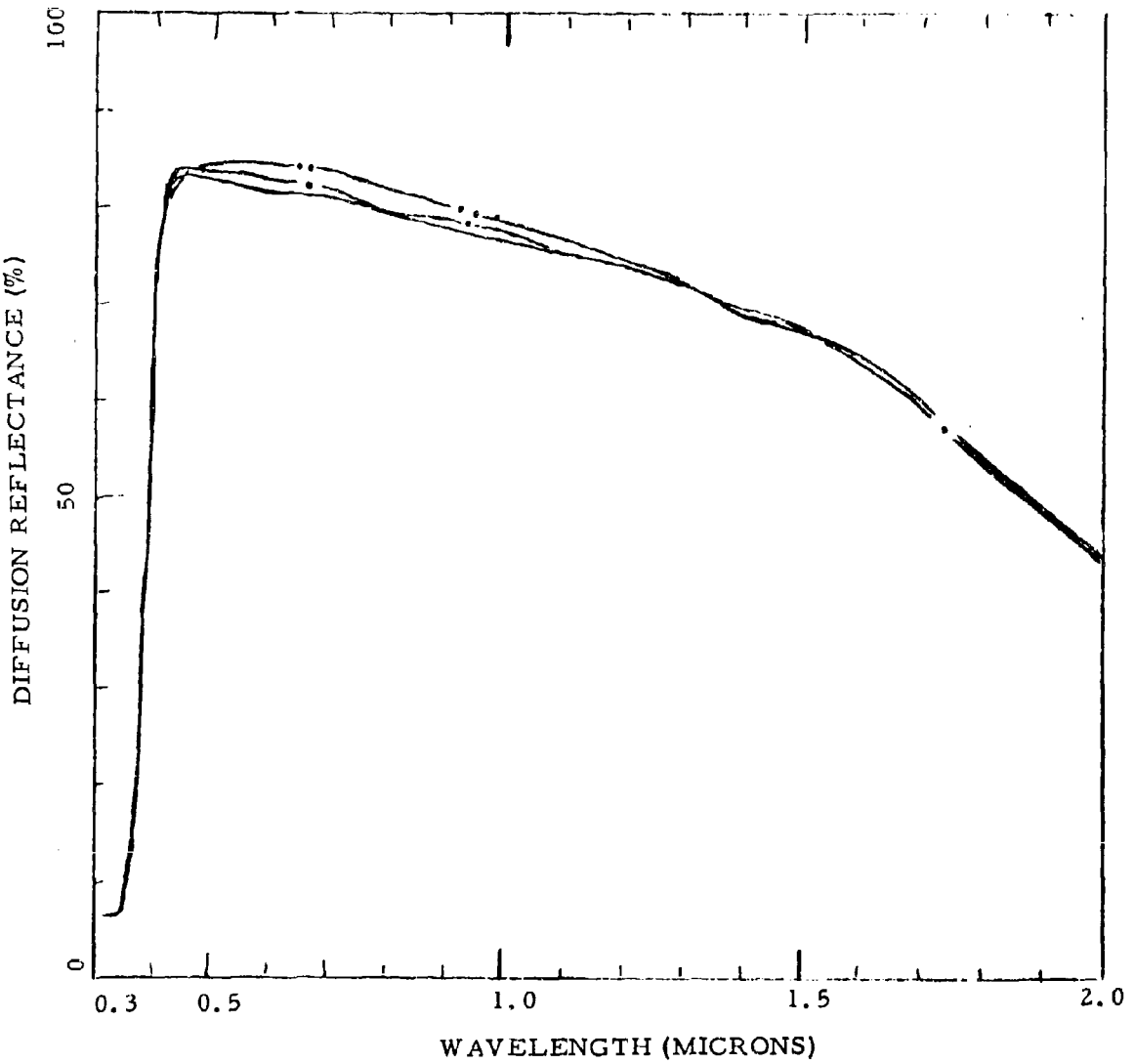

Fig. 32 - Time Effect After Electron Irradiation

(—— at 10^{12} e/cm^2; — · — rerun after 7 days; — — — after 65 days, see text)

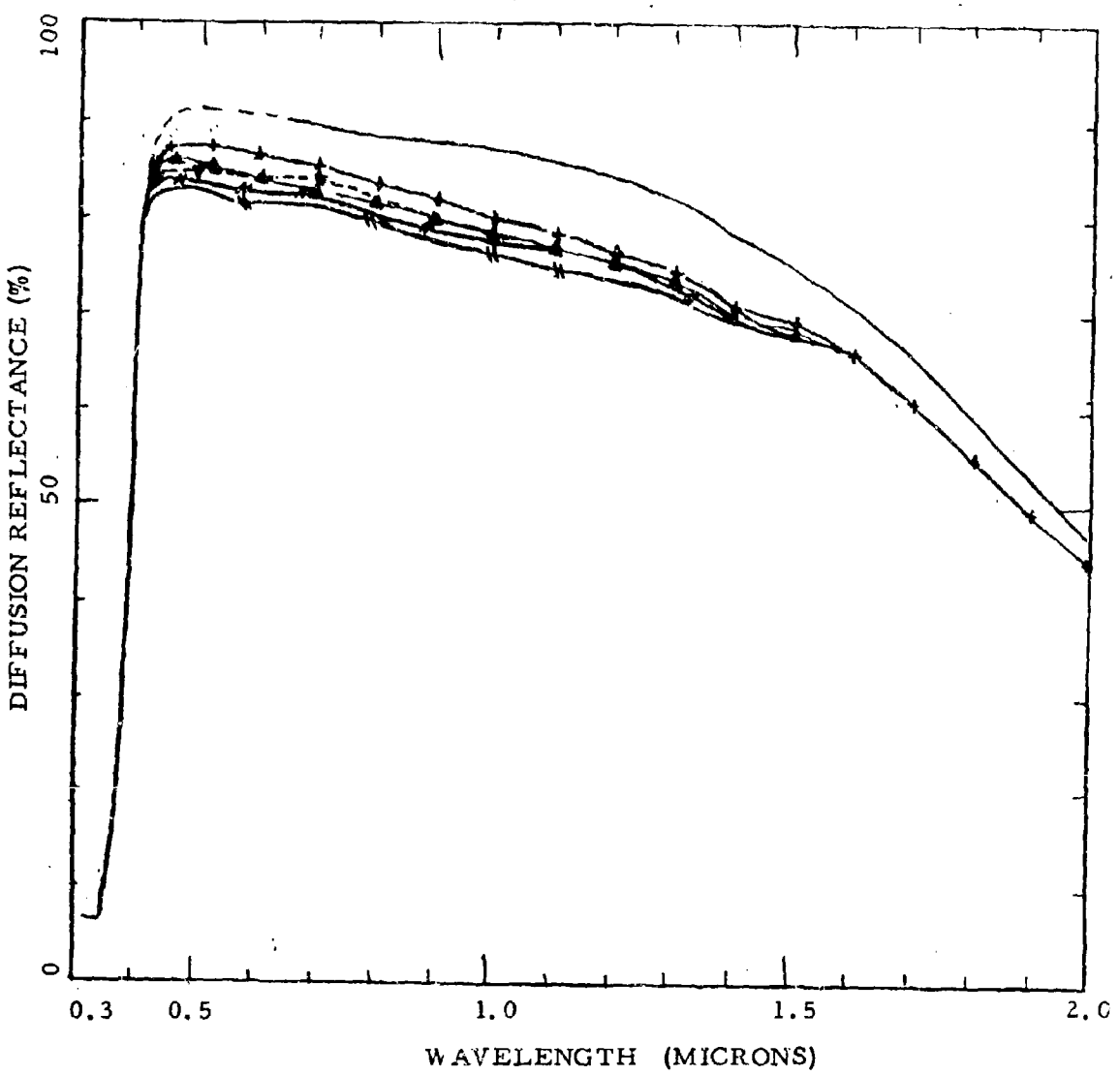

Fig. 33 - Cumulative Effect of Exposure to uv

(—— initial in vacuum;—+—5 esh;—△—10 esh;—▽—100 esh; —//— 180 esh; —\—445 esh)

in the in-situ apparatus[†] and thus both samples were exposed to the same sequences of ambient gas and vacuum. The initial reflectance spectrum in air of the second sample compares favorably with that of the first sample, as can be seen in Figure 34. A remeasurement of the second sample after 26 days, during which the experiments on the first sample were conducted, gave the reflectance plotted in Figure 35, and a subsequent reflectance spectrum taken after the second sample stood for an additional 7 days in vacuum showed no deviation from the previous curve.

A series of electron bombardments (1.75 MeV) was then performed, with the reflectance spectrum being determined in-situ after each irradiation. The irradiation sequence was: 10^{10}, 3×10^{10}, 10^{11}, 3×10^{11}, 10^{12}, and 3×10^{12} e/cm^2. The resulting changes were small and not monotonic. The smaller doses appear to produce a definite increase in reflectance at the low wavelengths and in the visible region which rounds out the shoulder but also sharpens up the absorption edge. However, the two higher doses, 10^{12} and 3×10^{12} e/cm^2, caused some degradation of reflectance at the lower wavelengths. The results are shown in Figure 36. The total accumulated dose for this specimen was about 4.4×10^{12} e/cm^2. The degradation is primarily at the short wavelengths and becomes noticeable at doses above 10^{12} e/cm^2.

After the electron irradiation, the specimen was kept for 7 days under vacuum and then remeasured. The spectrum had remained stable. Ultraviolet irradiation was then started with an initial dose of ~5 esh. This brought about the slight recovery of reflectance in the visible region and in the IR between 1.4 and 2 μ. Subsequent uv exposure resulted in degradation over most of the spectrum, with the first irradiation again apparently being considerably the most effective, as can be seen in Figure 37.

[†] A potential problem with this apparatus is that if scattered uv irradiation reaching samples not intended to be exposed. The purpose of the shield tube is to prevent such exposure.

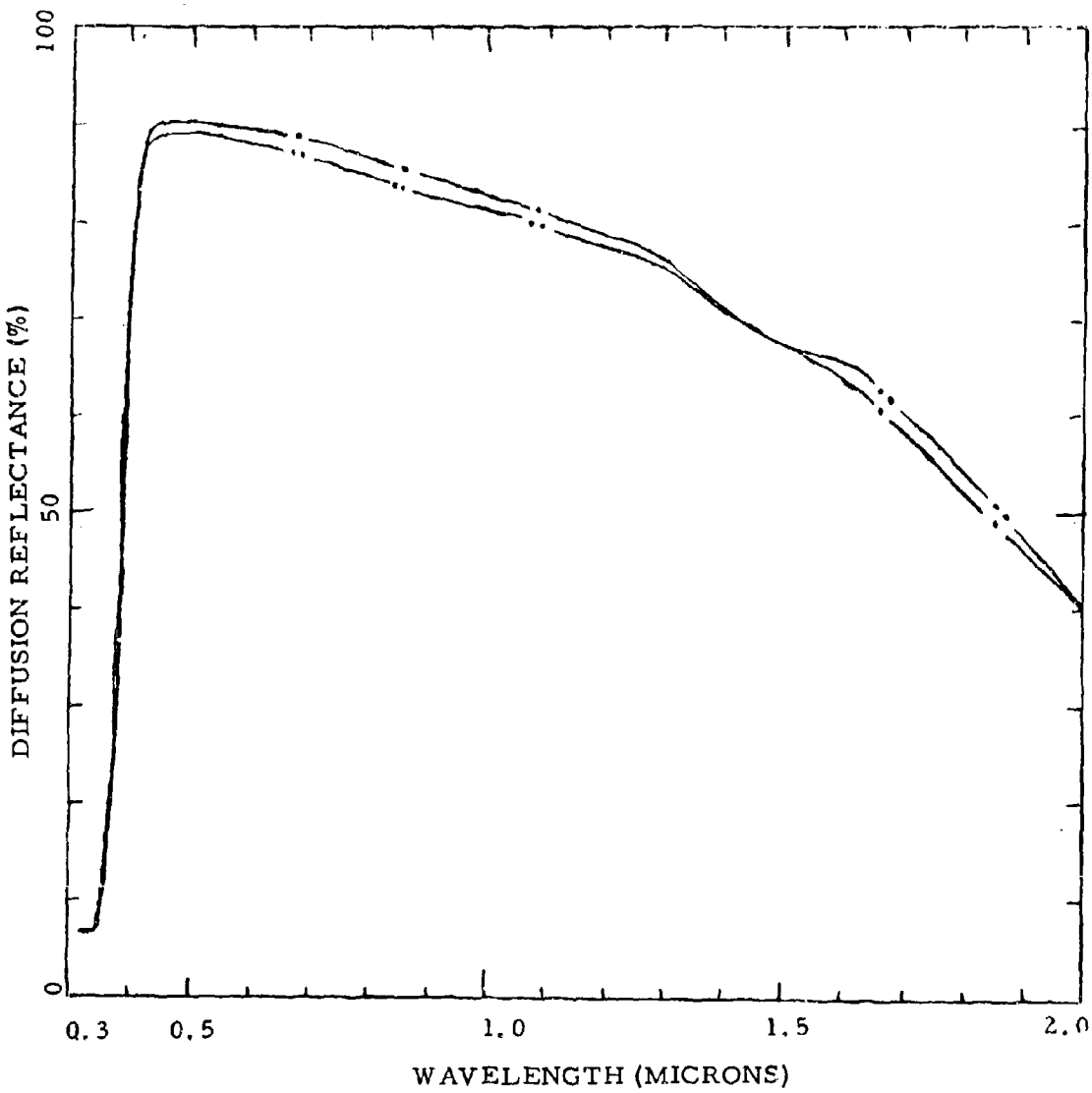

Fig. 34 - Comparison of Initial Reflectance Spectra of Rutile Specimens

(—·—TiOx-R-910/PS7-12;— · · —No. 11)

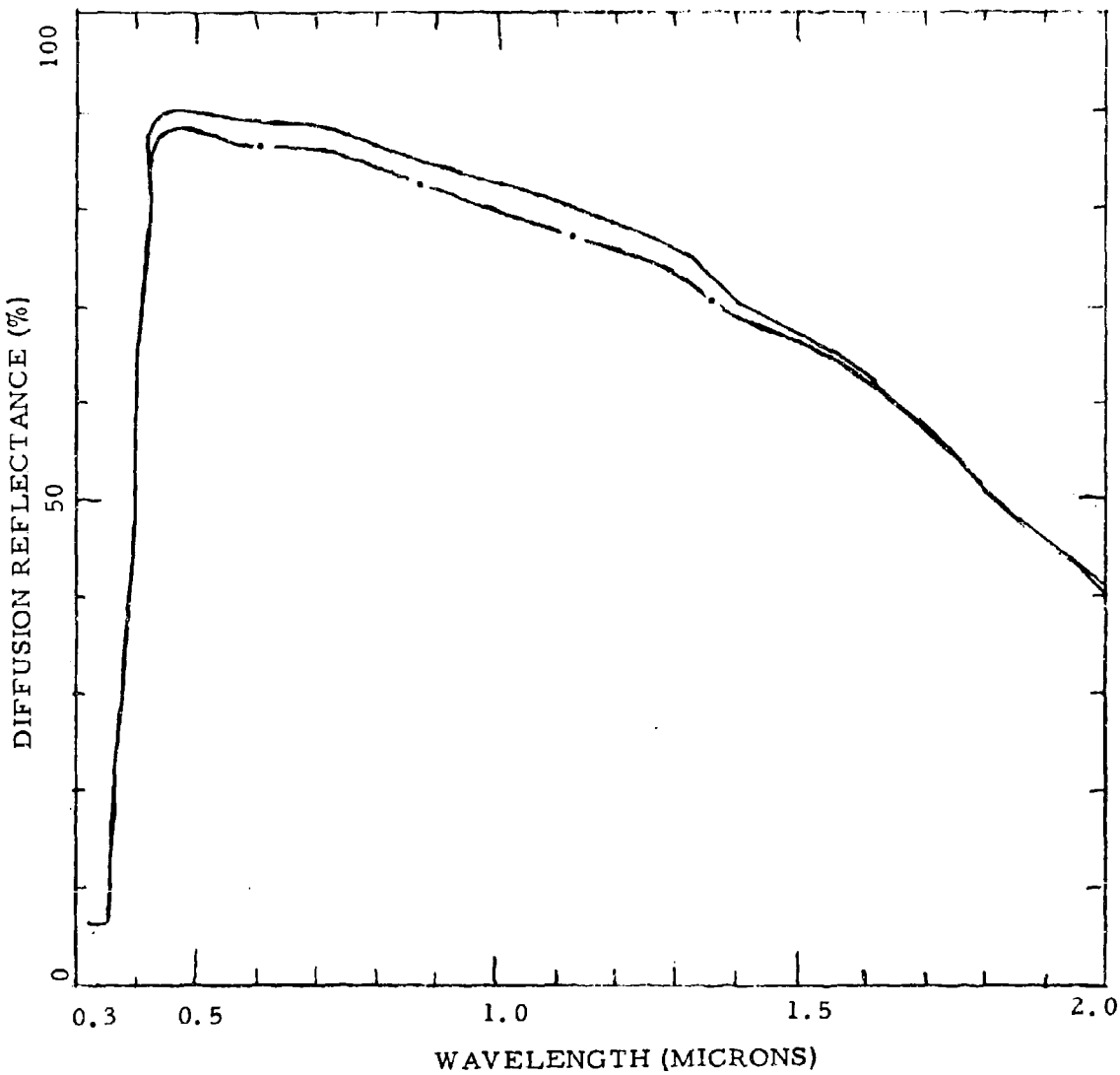

Fig. 35 - Degradation of TiOx-R-910/PS7-12 while No. 11 was Measured (see text)

(——— initial; ——·—— after 26 days)

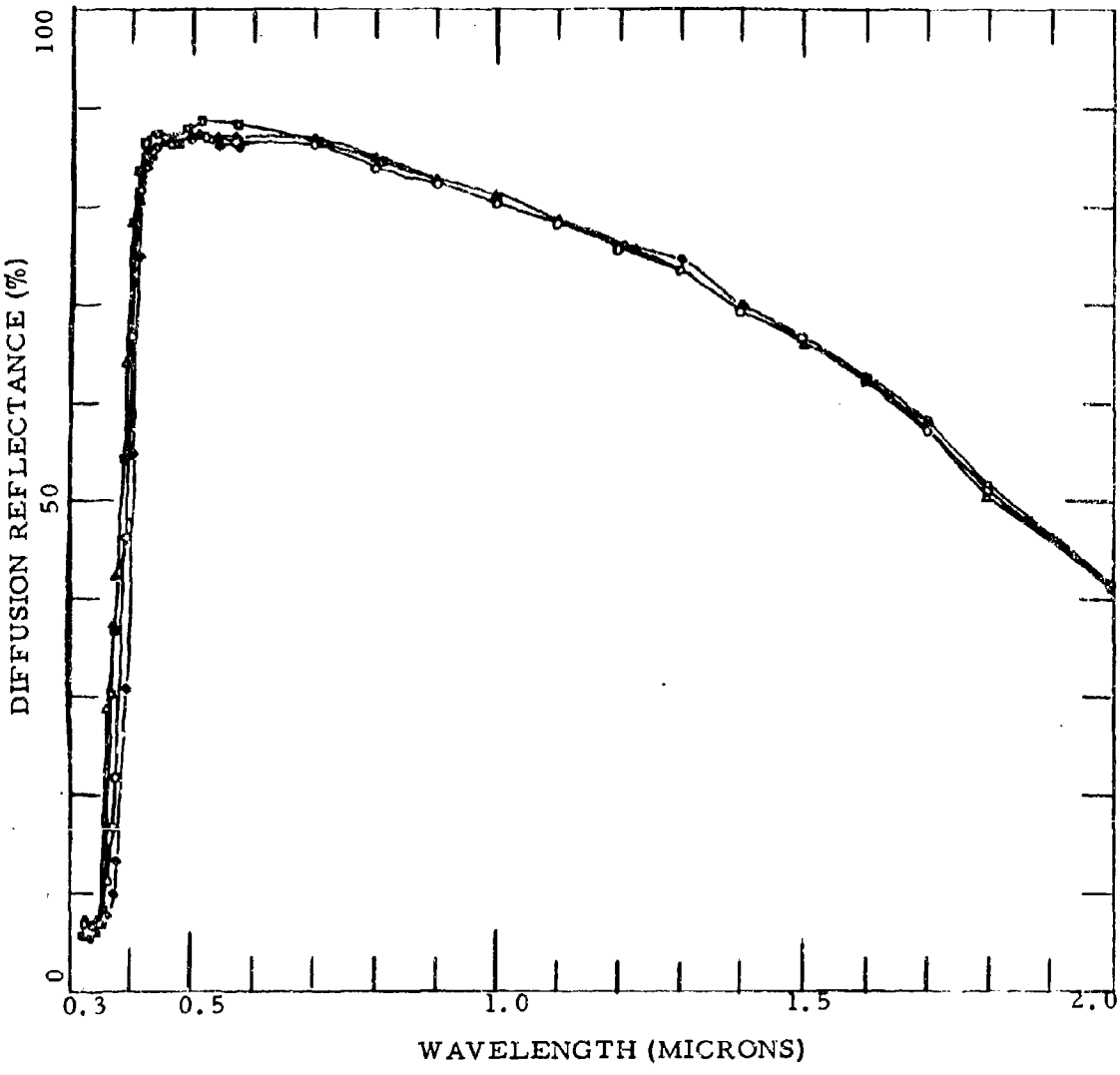

Fig. 36 - Effect of Cumulative Electron Irradiation

(—o— initial;—Δ—3 x 10^{10} e/cm^2;—□—10^{11};—◆—3 x 10^{12} all at 1.75 MeV)

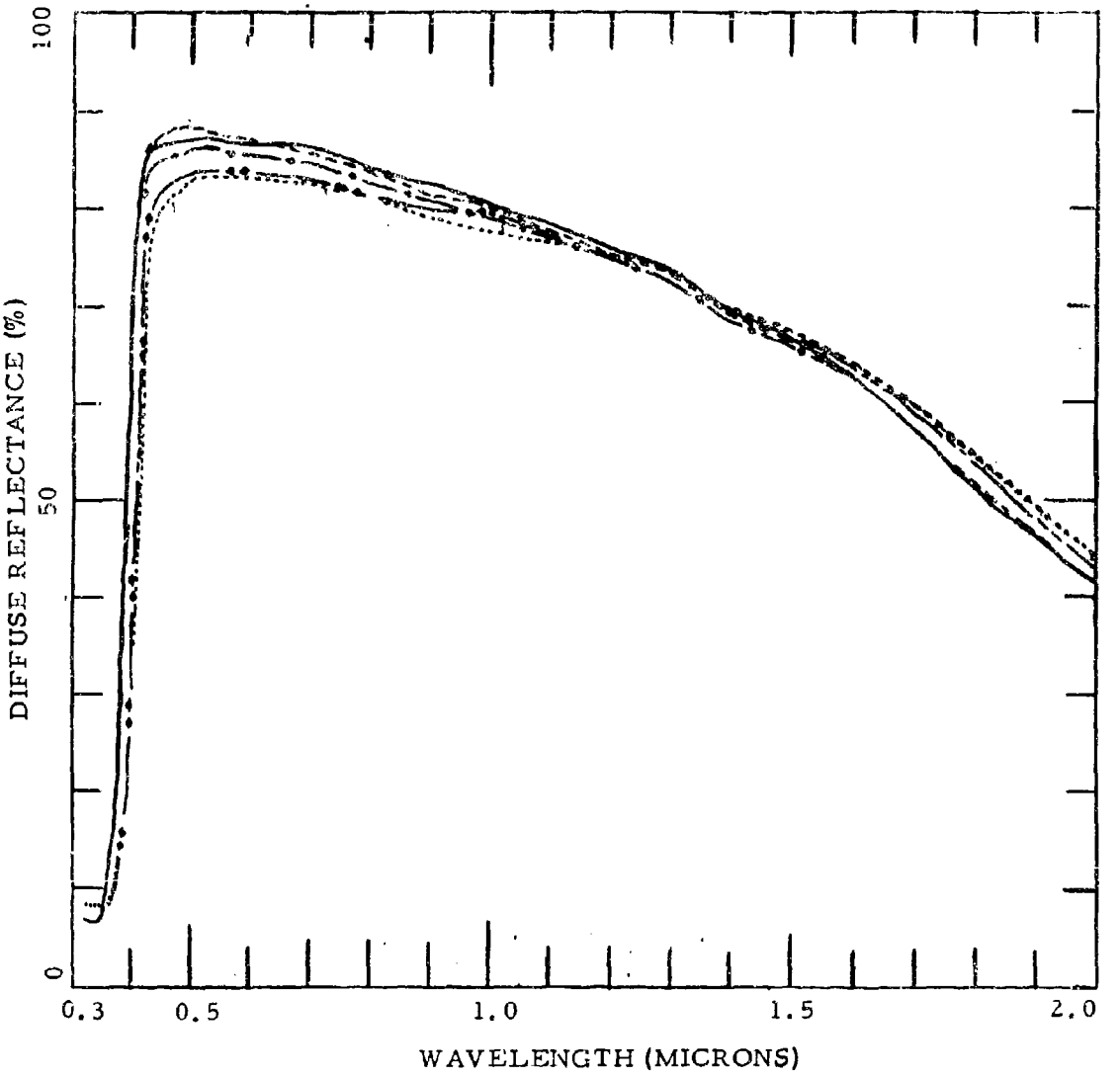

Fig. 37 - Effect of Cumulative uv Irradiation After 4.4×10^{12} e/cm^2

(—— initial; --- 4.5 esh; -·-30 esh; -··-335 esh; ···· 430 esh)

Interspersed with the uv irradiation sequence was an exposure to oxygen gas at the 5-esh point, which had a negligible, if any, effect on the reflectance. This was followed by reevacuation and bringing the system up to air. This produced a slight degradation at the short wavelengths. After reevacuation the uv exposure sequence was continued, with an interruption at the 215-esh point, when the specimen was kept for 19 days under vacuum. This standing in vacuum resulted in a reflectance recovery as indicated in Figure 38. Since it was not clear how this recovery would affect the subsequent sensitivity to uv exposure, the recovery was not taken into consideration in the summary plot given in Figure 37. After the uv irradiation was carried to 430 esh, the experiment on the second sample was terminated.

A sample was prepared of high-purity rutile material; (5037-30A, described in Section II). A coupon was obtained without the use of a binder by using the hot-dip method. (also described in Section II). The specimen was mechanically sound and showed a stable reflectance when exposed to the vacuum environment, and uv irradiations were begun, starting with short exposures. As can be seen from Figure 39, degradation of reflectance in the short wavelength and visible regions is produced by even very low exposures of uv, while an increase in reflectance appears in the IR. The rather round shoulder of the reflectance spectrum before irradiation is responsible for the off-white tinge of this material, and the absorption edge seems to be less sharp than the stabilized DuPont rutile. The experiment was terminated by mechanical failure of the specimen during manipulation in the apparatus.

Another specimen was prepared similarly with high-purity rutile, and the coated paddle was permitted to dry in air.

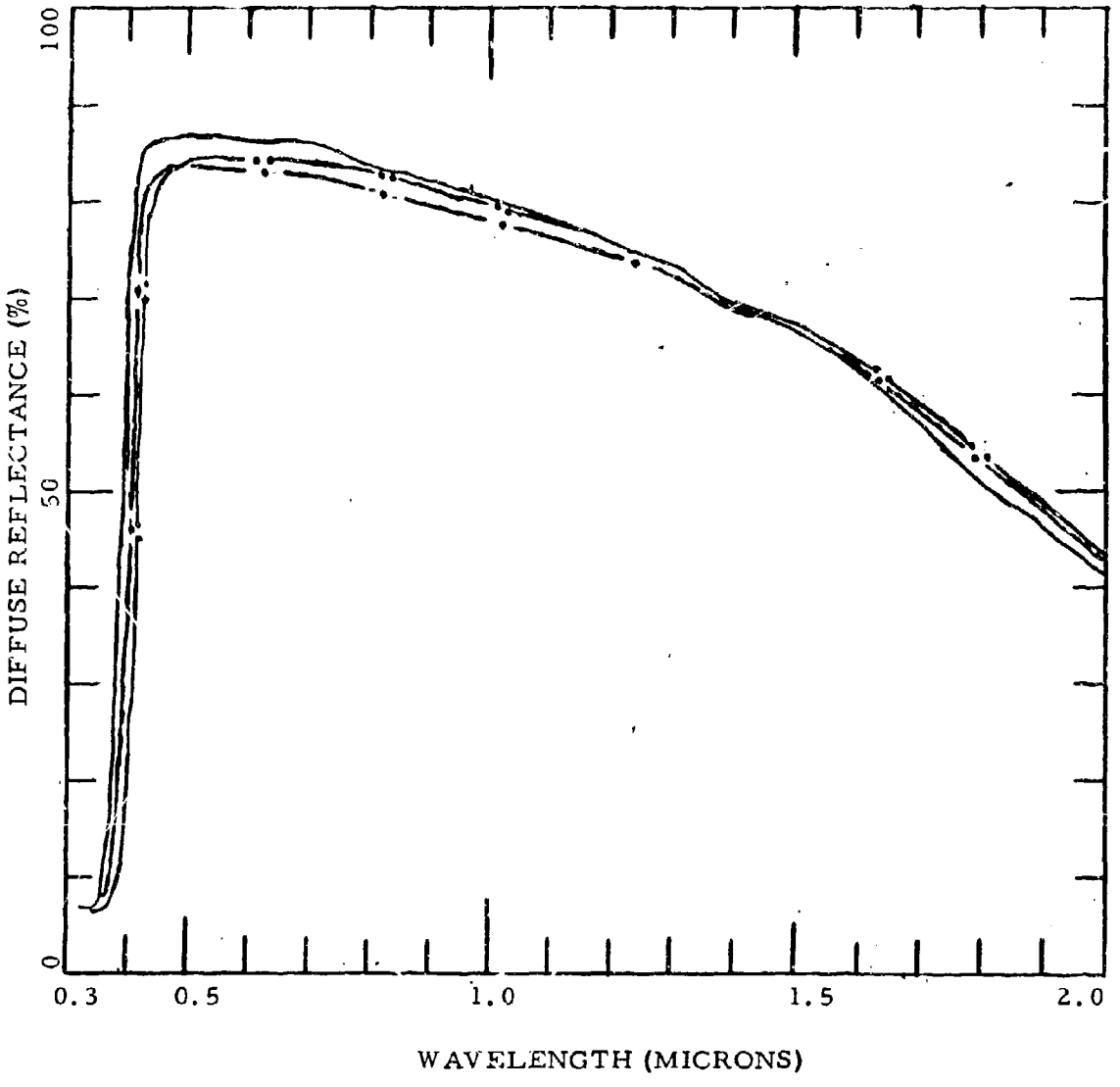

Fig. 38 - Time Effect After uv Irradiation

(—— initial; —·—215 esh; —··— after 19 days in vacuum)

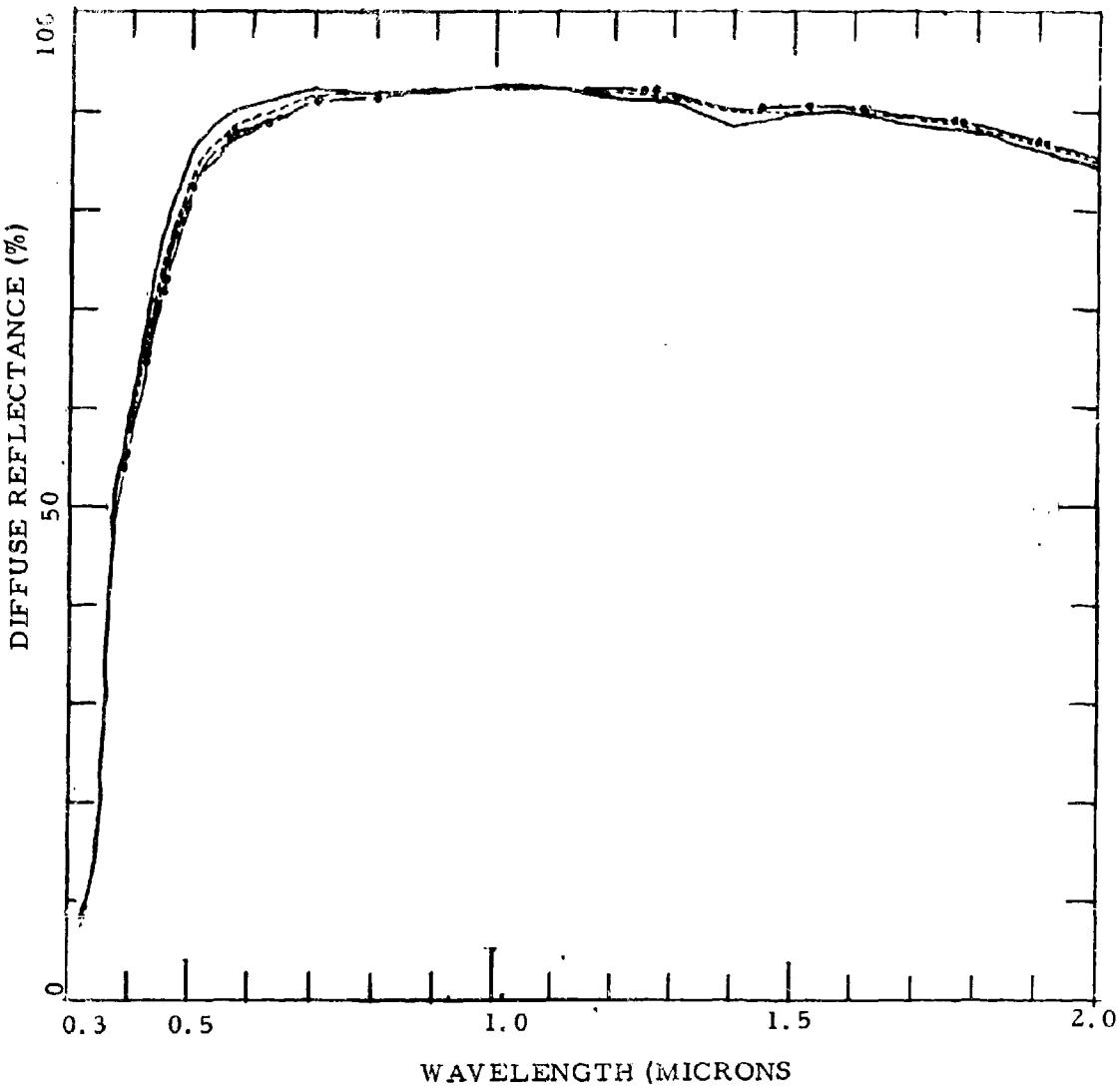

Fig. 39 - Irradiation of Pure, Binderless Rutile

(——initial; - - - 0.75 esh; —·—1.5 esh; ——··—2.25 esh)

Measurements of reflectance spectra were made in vacuum between exposures to uv irradiation. This sample showed no change in reflectance on standing in a vacuum of $\sim 10^{-5}$ torr for 2 days before the irradiations were started. The initial 0.75 esh of irradiation produced an increase in reflectance near the low wavelength shoulder, as shown in Figure 40. An additional 0.75-esh uv exposure resulted in a general increase in the reflectance for wavelengths longer than 0.5 μ, while the region near the shoulder remained unaffected. A further exposure of 0.75 esh produced only the slight effect shown in Figure 41, with possibly a small increase in the reflectance in the IR region and a small degradation in reflectance near the shoulder.

The specimen next was held under vacuum for 14 days, after which the reflectance spectrum was remeasured, with the result shown in Figure 42. The increase in reflectance produced by the previous uv irradiation has been removed, and furthermore the reflectance is at all wavelengths below that measured before irradiation. A subsequent exposure to 1.5 esh again resulted in an increase in reflectance, most markedly at wavelengths longer than 0.5 μ, as shown in Figure 43. A further exposure to 1.5-esh hardened the shoulder while the reflectance of longer wavelengths remained relatively stable, as shown in Figure 44.

The specimen was then exposed to 1 atm of N_2. This produced no change in the reflectance spectrum. After reevacuation the uv irradiation was continued up to a total of 21-esh. The reflectance again showed an increase after uv irradiation over that previously measured in vacuum. Another specimen prepared from the same slurry but which had been kept as a control in a dessicator was mounted in the apparatus and irradiated to a total of 13.5 esh. This specimen displayed the same phenomena. It should be mentioned that these specimens made from a slurry, have a rather long outgassing period, which may account for some inconsistent changes of reflectance with time in a vacuum environment. Water-sprayed samples may be outgassing less, since they are prepared in thinner layers at a higher temperature.

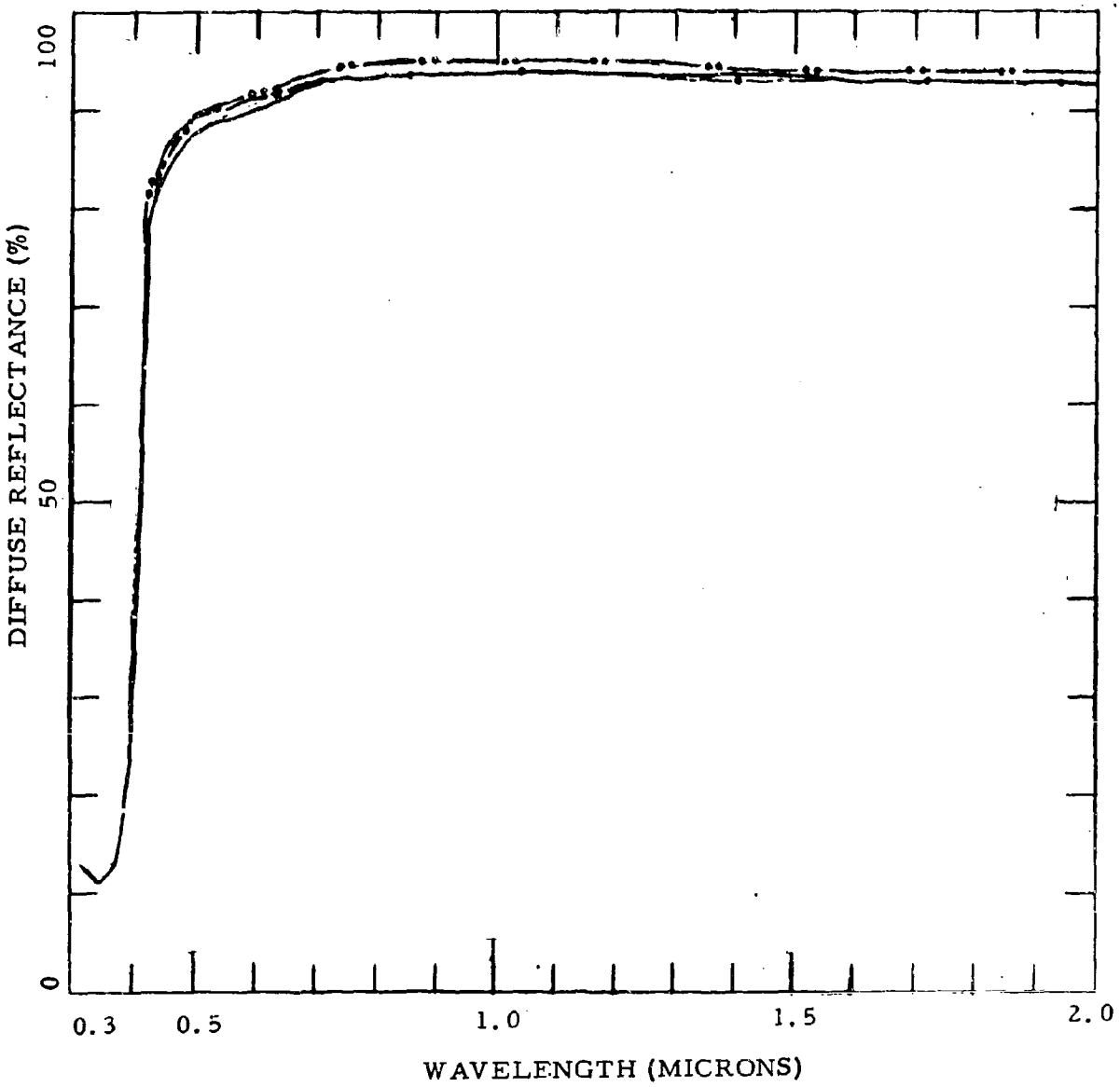

Fig. 40 - Effect of uv Irradiation on Binderless Rutile

(——— initial;——·——0.75 esh;——··——1.5 esh)

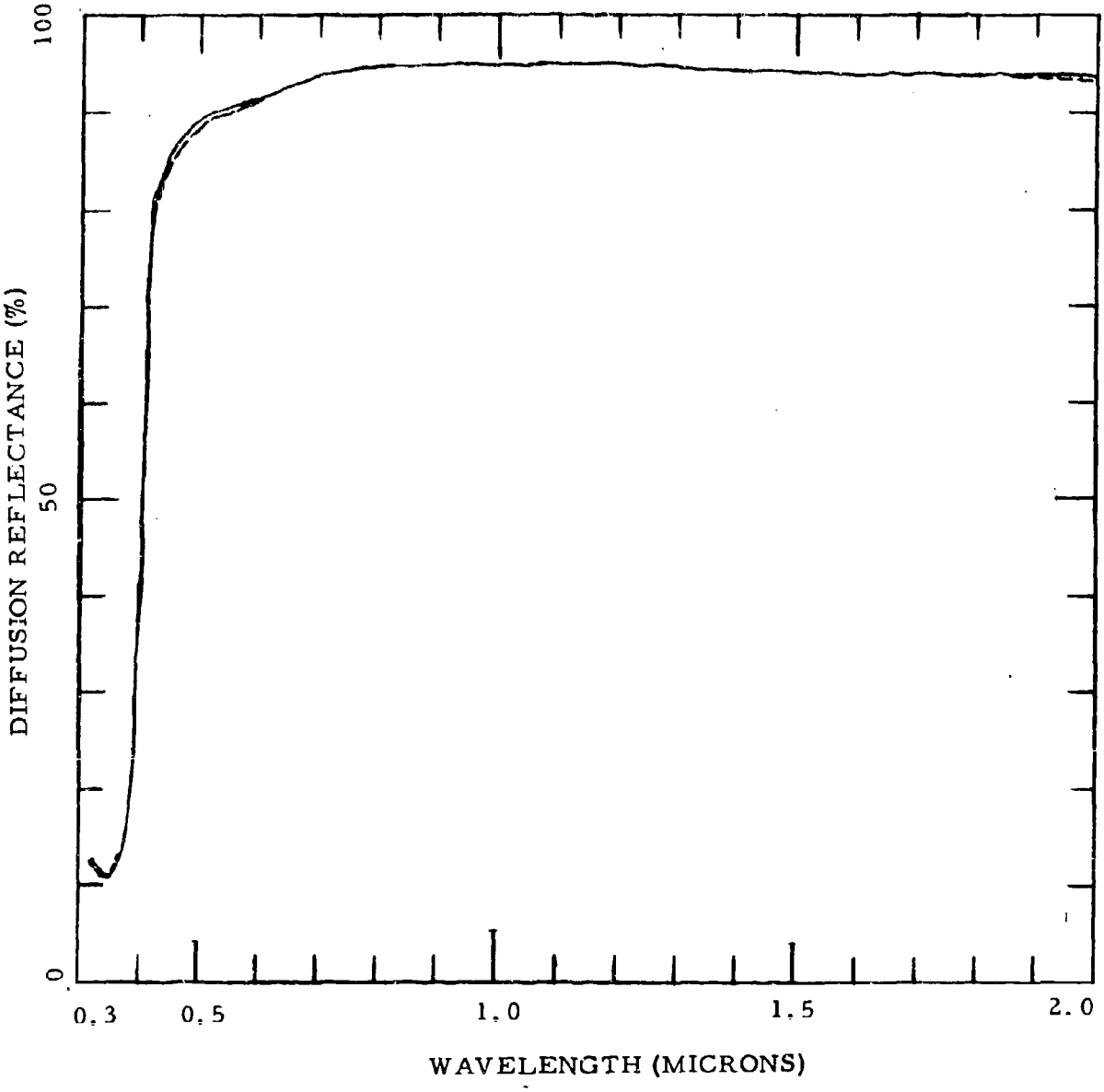

Fig. 41 - Saturation of Induced Effect

(——— 1.5 esh; – – – 2.25 esh)

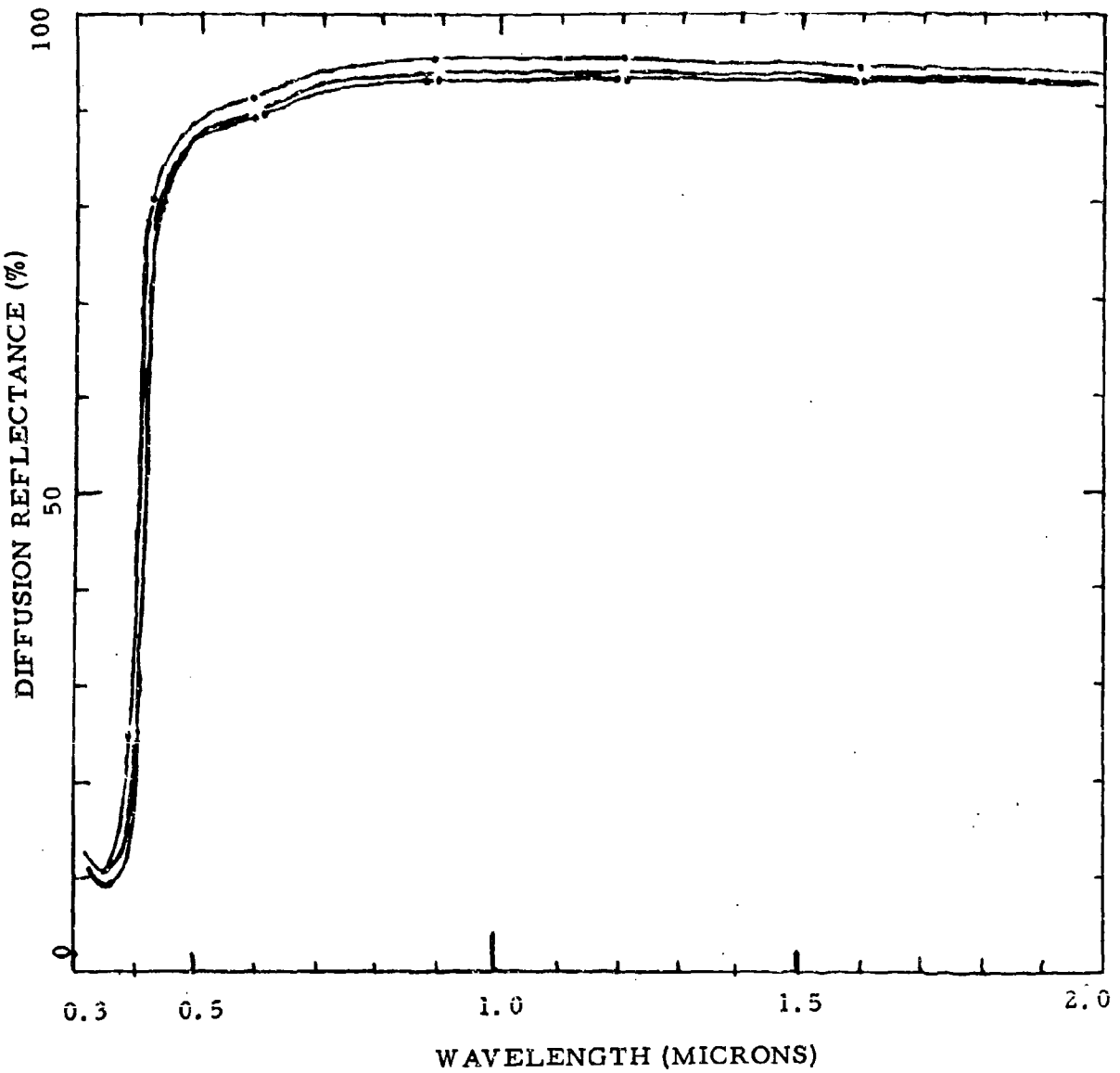

Fig. 42 - UV Enhanced Reflectance and Subsequent Degradation in Vacuum

(——initial; — · —2.25 esh; — ·· —add. 14 days)

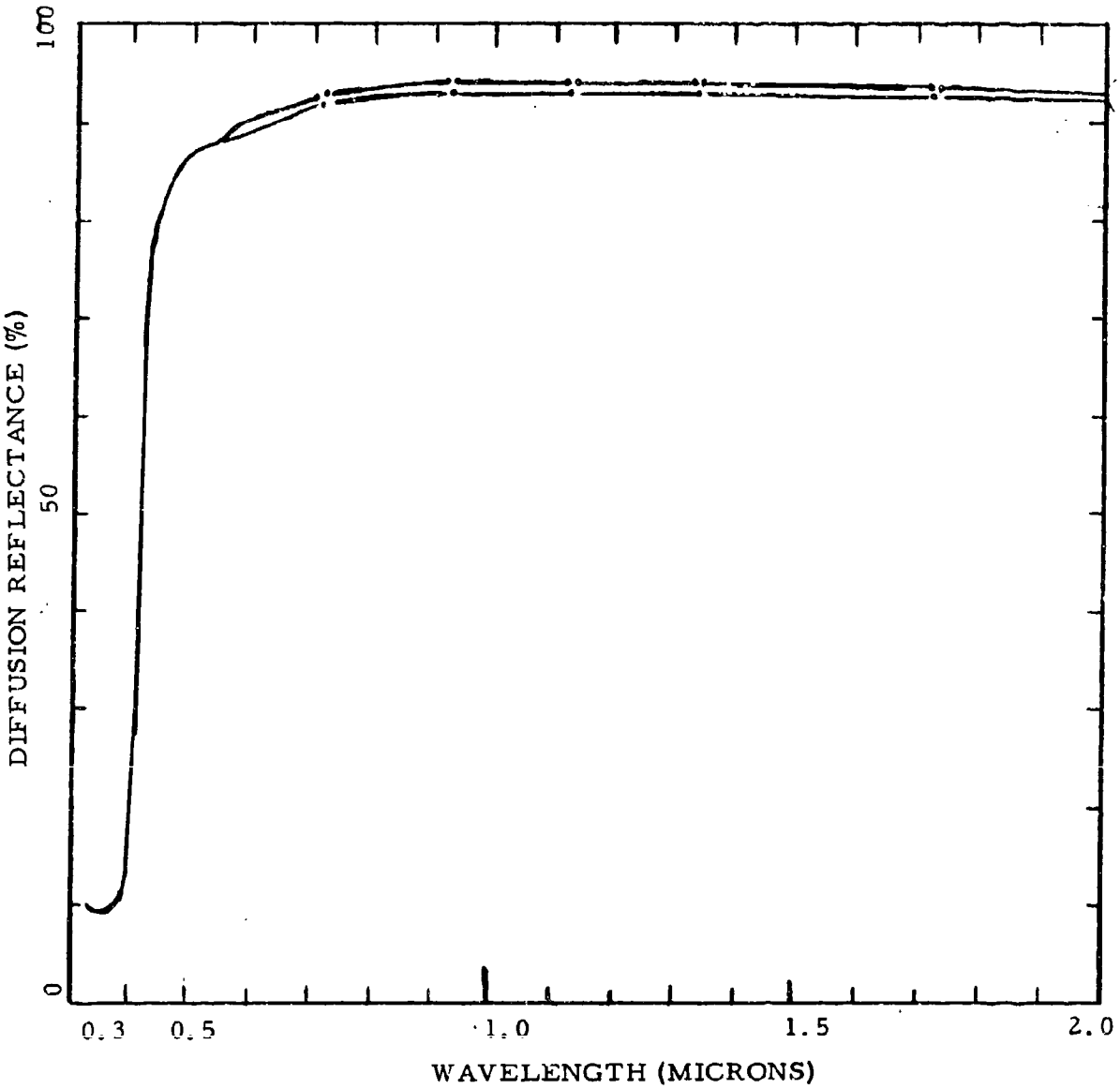

Fig. 43 - Resumption of uv Irradiation after 14 Days in Vacuum

(—·—before addtl. 1.5 esh;— - —at total of 3.75 esh)

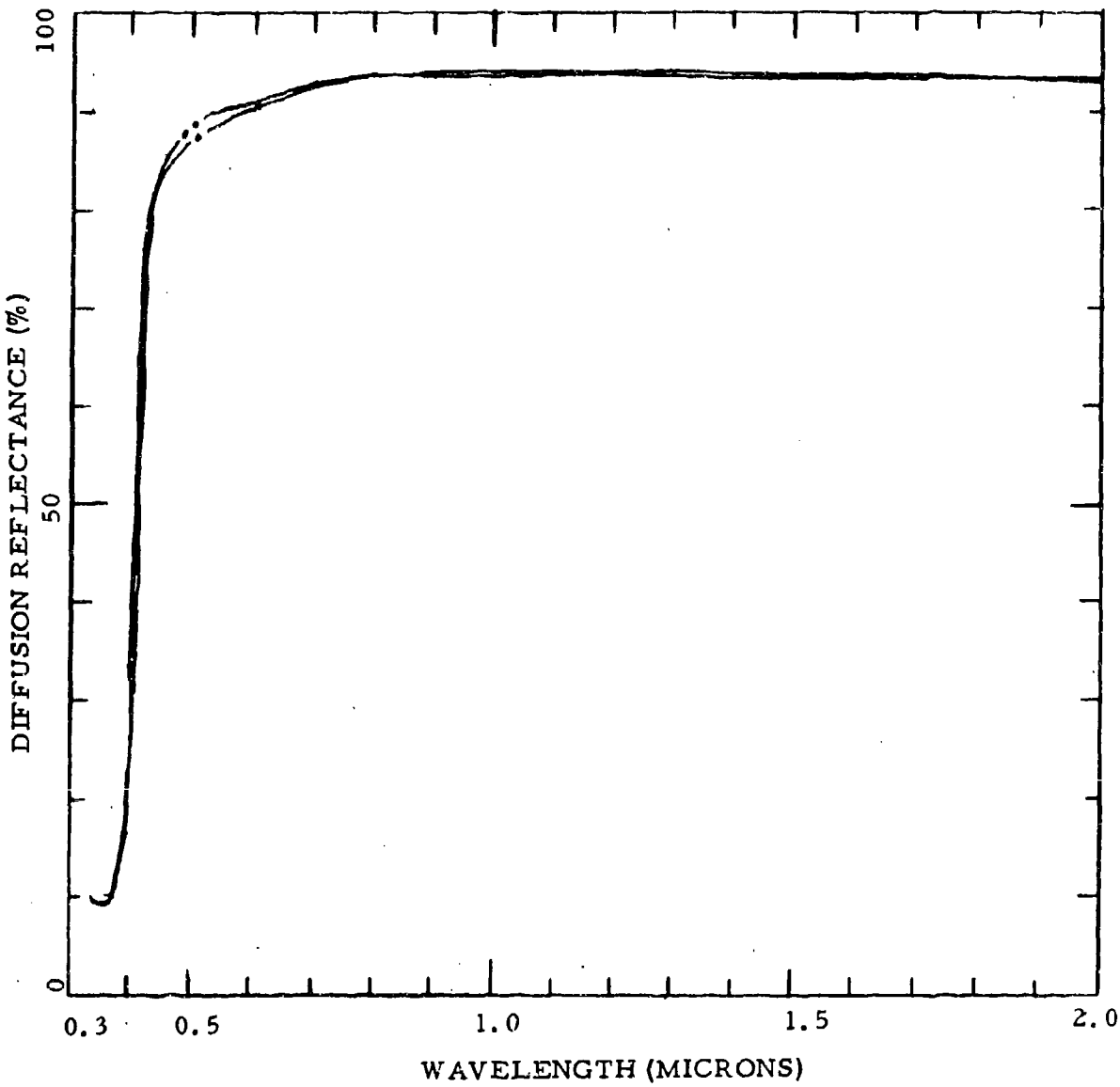

Fig. 44 - After Continued uv Irradiation

(—·— 3.75 esh; — ··— 5.25 esh)

REFERENCES

1. Greenberg, S. A., H. F. Macmilan, and A. F. Sklensky, Damage Mechanisms in Thermal Control Coating Systems, AFML-TR-67-294, Air Force Materials Laboratory, Wright-Patterson Air Force Base, Ohio, Lockheed Missiles and Space Company, September 1967.

2. Frederikse, H. P. R., W. R. Thurber, and W. R. Hosler, "Electronic Transport in Strontium Titanate," Phys. Rev. 134, A442 (1964).

3. Snowden, D. P., H. Saltsburg, and J. H. Pereue, Jr., J. Phys. Chem. Solids 25, 1099 (1964).

4. Middleton, W. E. K., and C. L. Sanders, "The Absolute Spectral Diffuse Reflectance of MgO," J. Opt. Soc. 41, 419 (1951).

5. Sanders, C. L., and W. E. K. Middleton, "The Absolute Spectral Diffuse Reflectance of MgO in the Near Infrared," J. Opt. Soc. 43, 58 (1953).

6. 1965 Book of ASTM Standards, Part 21, "Paint, Varnish, Lacquer, and Related Products-Tests for Formulated Products and Applied Coatings," American Society for Testing and Materials, Baltimore, 1965, P. 190.

7. Pollak, M., and T. H. Geballe, "Low-Frequency Conductivity Due to Hopping Processes in Silicon," Phys. Rev. 122, 1742 (1961).

APPENDIX

REDUCTION OF TiO_2 POWDERS AND RUTILE SINGLE CRYSTALS*

There are numerous discrepancies in the literature[1] on reduction of rutile, some authors claiming that a simple decrease of oxygen partial pressure is sufficient to promote reduction at elevated temperatures (near 950°C) and others that hydrogen, hydrocarbons, or other chemical reducing agents are necessary. It also appears that there may be a difference in reduction between single crystals and powders, with crystals reducing under conditions where powders will not. This would indicate an important role of the surface in the reduction process. Further, reduction in a hydrogen atmosphere is known[2] to result in introduction of hydrogen into the rutile lattice, and it is desirable to know whether reduction is possible without this introduction. The measurements reported here were made in an attempt to resolve some of these discrepancies in a qualitative fashion, and also to compare the chemical reduction of rutile with the reduction-like behavior found in rutile powder exposed to uv and possibly charged particle radiation.

The approach taken was to observe the reduction behavior of several samples of rutile of a different nature treated simultaneously in the same way in various gaseous ambients. If simply decreasing the partial pressure of oxygen at elevated temperatures is sufficient to result in reduction, then reduction should be achieved in either a clean vacuum system or in a stream of an inert gas such as pure helium.

The apparatus used was kept simple to minimize sources of potential contamination. A multicompartment quartz boat contains several specimens of various powders of single crystals and is centered in a quartz furnace, and the specimen temperature was determined by a thermocouple sealed in the furnace tube from the downstream end. A thermocouple junction is in thermal contact with the specimens but does not touch them. The heating procedure varied

* To be submitted to Journal of the Physics and Chemistry of Solids.

somewhat, depending on the particular experimental objective, but the specimen powder charges were usually purged of air at room temperature for at least 1 hr. Control temperature was reached within 60 to 90 min after starting the heating cycle. The specimens were kept at the desired temperature, usually for about 3 hrs, and then allowed to cool to room temperature by shutting off the furnace. During cool-down, the gas (or vacuum) ambient was maintained in the sample cell. The appearance of the specimen was then observed, and the occurrence of reduction was correlated with the experimental conditions.

The rutile powders and single crystals examined came from three sources:

1) Ti-Pure powder, type R-910, produced by E.I. DuPont. This material was chosen since it is fairly typical stabilized pigment. Emission spectroscopy showed: aluminum, ~4,000 ppm; silicon, 1,000 ppm; and magnesium, 10 ppm. Analysis for carbon, which is important in view of the possible role of carbonaceous impurities in the oxygen loss process, showed 87 ppm.

2) Experimental high-purity powder material* (Lot 5037-30A) from the W. R. Grace Company. Spectrographic analysis showed: silicon, 200 ppm; aluminum, 60 ppm; nickel, 100 ppm; and magnesium, 10 ppm. Carbon analysis yielded 21 ppm. The specific area is ~1 m^2/g, according to the manufacturer, as determined by the BET method. The appearance of this material is slightly off-white to the eye; this does not change even after prolonged initial heating at 200°C. X-ray diffraction analysis was carried out and showed the powder to be of rutile phase with a crystallite size greater than ~1150 Å, approaching the limit of this method using KCl for comparison.

3) A single-crystal specimen, obtained from the National Lead Company. Similar material showed: silicon, 4 ppm; aluminum, 1.8 ppm; chlorine, 1 ppm; and potassium, 0.3 ppm.

The results obtained are summarized in Table 1. Those experimental conditions under which the specimen did not reduce are presented in the upper portion of the table, while the conditions which led to total or partial reduction, expected or unexpected, are shown in the central portion. After each run which produced a reduction, reoxidation was carried out in air, as indicated at the bottom of Table 1.

* Supplied through the courtesy of Dr. R. G. Rice.

TABLE I

RESULTS OF HEATING RUTILE POWDERS AND RUTILE SINGLE CRYSTAL IN DIFFERENT AMBIENTS AND VACUUM

Specimen*	Crystal or charge designation	Control temp. (°C)	Time at temp. (hr)	Ambient		Forepump trap temp.**	Traps		Heat-up rate		Change††
				Species	P†		Molecular sieve	Charcoal	Normal	Stepped	
Single crystal	160168	950	1/2	He	1 atm		LN_2	LN_2	X		Unaffected
Single crystal	230168	950	3	Vacuum	~15 μ	LN_2	LN_2	LN_2	X		Unaffected
Single crystal	070268	950	3	Vacuum	~ 5 μ	LN_2	LN_2	LN_2		X	Unaffected
Single crystal	150268	950	2	Vacuum	~13 μ	LN_2	LN_2	LN_2	X		Unaffected
Powder A	070268	950	3	Vacuum	~ 5 μ	LN_2	LN_2	LN_2		X	Unaffected
Powder A	150268	950	2	Vacuum	~13 μ	LN_2	LN_2	LN_2	X		Unaffected
Powder B	061067	950	2	He	1 atm		LN_2	LN_2	X		Unaffected
Powder B	070268	950	3	Vacuum	~ 5 μ	LN_2	LN_2	LN_2		X	Unaffected
Powder B	150268	950	2	Vacuum	~13 μ	LN_2	LN_2	LN_2	X		Unaffected
											Reduced
Single crystal	250768	950	2	Vacuum	~ 8 μ	RT	By-passed	By-passed	X		Gray-black
Single crystal	050268	950	2	Vacuum	~ 2 μ	LN_2	LN_2	LN_2	X		Slight blue
Single crystal	130268	950	2-1/2	Vacuum	~ 8 μ	RT	By-passed	By-passed	X		Gray-black
Single crystal	200268	950	2-1/2	Vacuum	~ 8 μ	RT	By-passed	By-passed	X		Gray-black
Powder A	050268	950	2	Vacuum	~ 2 μ	LN_2	LN_2	LN_2	X		Light gray***
Powder A	130268	950	2-1/2	Vacuum	~ 8 μ	RT	By-passed	By-passed	X		Dark gray
Powder A	200168	950	2-1/2	Vacuum	~ 8 μ	RT	By-passed	By-passed	X		Dark gray
Powder B	050268	950	2	Vacuum	~ 2 μ	LN_2	LN_2	LN_2	X		Light gray***
Powder B	130268	950	2-1/2	Vacuum	~ 8 μ	RT	By-passed	By-passed	X		Blue-gray
Powder B	200268	950	2-1/2	Vacuum	~ 8 μ	RT	By-passed	By-passed	X		Blue-gray
											Oxidized
All specimens after each reduction process		800	3	Air	1 atm				X		Reverted to pre-reduction condition

*The single crystals were obtained from the National Lead Company; powder A was an experimental powder from W. R. Grace Company, and powder B was a commercial powder produced by E. I. du Pont.

†Pressure values given are for approximate monitoring only.

**LN_2 liquid nitrogen temperature; RT = room temperature.

††Leak testing was carried out principally by the Δp method.

***Heavy outgassing during initial heating: P_{max} ~1000μHg

For the experiments conducted using a vacuum ambient, the status of the various traps is indicated. A marked effect of contamination was found while leak-checking. Using methyl alcohol or acetone as a leak indicator would give a color change on subsequent specimen heating to high temperatures even if only a small leak had been present. This reduction process would take place even after attempts were made to drive off the methyl alcohol vapors at temperatures between 100° and 200°C. Other vacuum-testing methods were therefore substituted, e.g., helium gas and a mass spectrometer leak detector, or comparing the rate of pressure rise at room temperature with the sample tube closed off from the pumps. Another effect of contamination was found on initial heating of some powder specimens when the outgassing pressure rose to ~1,000 μ Hg while a heating rate of ~15°C/min was employed. This effect was associated with a slight reduction, even though the fully trapped system was used. It appears that initially the powders contain absorbed reducing agents which, during their desorption, can cause chemical reduction. A similar observation was made by Gebhardt and Herrington[3]. After repeated contamination-caused reductions and subsequent reoxidations, made to ascertain the reproducibility of the results, the furnace tube itself became a source of contaminant which apparently condensed on it during cool-down and could not completely be removed during the following air-oxidation treatment at a lower temperature. After the quartz furnace tube was slightly etched with a mild $HF-HNO_3$ acid solution, "clean" conditions were reestablished. This seems to indicate that only a low concentration of contamination is required for the reduction reaction to take place.

Generally, it was found that the single crystal was most easily reduced, the experimental W. R. Grace powder being intermediate, and the DuPont R-910 being least severely affected by those experimental conditions leading to a reducing reaction. For the powders, the relative susceptibility to chemical reduction corresponds to their relative susceptibility to damage (reflectance degradation) by uv light. This is presumably due to the protective role of "impurities." The much higher susceptibility of the single crystal to chemical reduction appears to demonstrate a protective role of the surface layer in pigments, which have a much higher fraction of their volume near the surface.

The following conclusions were reached for the powders and single crystals examined:

1) No reduction results when rutile powder is exposed to a flow of purified helium gas at 950°C. It appears that lowering the partial pressure of oxygen in the ambient

atmosphere is not sufficient to bring about reduction of TiO_2 powders.

2) No reduction results when TiO_2 rutile single crystals are exposed to a flow of purified helium gas at 950°C.

3) No reduction results for powder at 950°C when the (air) ambient pressure is reduced by a factor of 10^{-6} as long as no contaminant is generated or permitted to enter the system. This contrasts with numerous reports of reduction at 950°C or less at pressures up to severl mm Hg.

4) A trapping train of molecular sieve and activated charcoal cooled to liquid nitrogen temperatures is effective in blocking contamination from a mechanical forepump.

5) Desorption of impurities from "as received" powder can lead to reduction even in a "clean" vacuum system.

6) Condensed contamination in the system may not be removable by heat alone but may require chemical means.

7) Even small quantities of methyl alcohol, introduced in the vapor phase, cannot be removed from the powder by heating and evacuation near 200°C and lead to reduction of the rutile when the temperature is increased.

8) Single crystals are more sensitive to reduction by contamination than powders.

9) The relative susceptibility of rutile powder to reduction can be influenced by "impurities" in the powder.

10) The susceptibility of some rutile pigments to chemical reduction correlates with the extent of the reflectance degradation under irradiation.

APPENDIX

REFERENCES

1. Grant, I. A., "Properties of Rutile (Titanium Dioxide)" Rev. Mod. Phys. 31, 646 (1959).

2. Von Hippel, A., J. Kalnajs, and W. B. Westphal, "Protons, Dipoles, and Charge Carriers in Rutile," J. Phys. Chem. Solids 23, 779 (1962).

3. Gebhardt J. and K. Herrington, "Reduction of Contaminated Rutile Surfaces by Degassing," J. Phys. Chem. 62, 120 (1958).

UNCLASSIFIED
Security Classification

DOCUMENT CONTROL DATA - R & D

(Security classification of title, body of abstract and indexing annotation must be entered when the overall report is classified)

1 ORIGINATING ACTIVITY *(Corporate author)*
Gulf General Atomic Incorporated
P.O. Box 608
San Diego, California 92112

2a. REPORT SECURITY CLASSIFICATION
UNCLASSIFIED

2b. GROUP

3 REPORT TITLE
MECHANISMS OF DEGRADATION OF POLYMERIC THERMAL CONTROL COATINGS; PART I, INVESTIGATION ON DEGRADATION OF THERMAL CONTROL COATING MATERIALS

4 DESCRIPTIVE NOTES *(Type of report and inclusive dates)*
June 1967 through September 1968

5 AUTHOR(S) *(First name, middle initial, last name)*
D. M. J. Compton, T. E. Firle, and J. T. Neu

6 REPORT DATE	7a. TOTAL NO. OF PAGES	7b. NO. OF REFS
January 1969		10

8a. CONTRACT OR GRANT NO.	9a. ORIGINATOR'S REPORT NUMBER(S)
F33615-67-C-1810	GA-8885
b. PROJECT NO. 7342	
c. Task No. 734202	9b. OTHER REPORT NO(S) *(Any other numbers that may be assigned this report)* AFML-TR-68-334 Part I
d.	

10 DISTRIBUTION STATEMENT
This document has been approved for public release and sale; its distribution is unlimited.

11. SUPPLEMENTARY NOTES	12. SPONSORING MILITARY ACTIVITY
	Air Force Materials Laboratory Air Force Systems Command Wright-Patterson AFB, Ohio 45433

13. ABSTRACT

Progress of an investigation on the mechanisms of degradation of white pigments used in polymeric thermal control coatings by ultraviolet radiation is reported. The materials investigated were rutile (TiO_2) with different controlled impurity levels and surface treatments and high-purity strontium titanate ($SrTiO_3$). Apparatus combining a gas chromatograph with means for measuring optical reflectance and electrical conductivity enables samples of pigments to be investigated in a controlled environment. Changes in optical properties, produced by exposure to ultraviolet light, are correlated with gas evolution and adsorption. Some optical changes were correlated with gas evolution and electrical conductivity. The gas evolved in all cases was CO_2, with no O_2 being observed. Carbonaceous impurities found in these materials are believed to play a role in the damage process. Instrumentation and test techniques were developed, including a recently completed reflectometer of novel design.

A comparison was made between chemical reduction of various rutile pigments and the effects of uv light: Chemical reduction produces changes in optical and other properties that correlate with one of the two types of effects produced by uv light (reduction of reflectance near one micron) and the relative susceptibility of different pigments to chemical reductions similar to their relative susceptibility to uv degradation. Comparison with the effects of charged particle radiation is in progress. Also, a study of radiation effects and mechanisms of degradation of polymeric coatings pigmented with TiO_2 and $SrTiO_3$ is in progress.

DD FORM 1 NOV 68 1473

UNCLASSIFIED
Security Classification

14 KEY WORDS	LINK A		LINK B		LINK C	
	ROLE	WT	ROLE	WT	ROLE	WT
Thermal control coatings						
Ultraviolet						
Titanium dioxide						
Strontium titanate						
Optical degradation						
Electron irradiation						
Chemical reduction						
Carbon dioxide						
Adsorption						
Desorption						
Electrical conductivity						